

Diss. ETH No. 17299

**HYDRATION, DOUGH FORMATION AND STRUCTURE
DEVELOPMENT IN DURUM WHEAT PASTA
PROCESSING**

A dissertation submitted to the

SWISS FEDERAL INSTITUTE OF TECHNOLOGY ZURICH

for the degree of
Doctor of Sciences

presented by

Andreas Markus Kratzer

Dipl. Lm.-Ing. ETH
born April 2, 1979
from Austria

Accepted on the recommendation of

Prof. Dr. Felix Escher, examiner
PD Dr. Béatrice Conde-Petit, co-examiner
Dr. Bernard Cuq, co-examiner

Zurich 2007

TABLE OF CONTENTS

Summary.....	V
Zusammenfassung.....	VII
1 General introduction	1
2 Process structure relation in pasta dough extrusion	5
2.1 Introduction	6
2.2 Experimental.....	9
2.2.1 Preparation of pasta dough and pasta samples on laboratory scale	9
2.2.2 Determination of protein solubility	16
2.2.3 Differential scanning calorimetry (DSC)	18
2.2.4 Confocal laser scanning (CLSM) and light microscopy	19
2.2.5 Rheological characterization of pasta dough	20
2.2.6 Determination of breaking strength and surface characteristics of dried pasta.....	20
2.2.7 Characterization of cooking behavior and properties of cooked pasta	21
2.3 Results and discussion.....	23
2.3.1 Characteristics of the extrusion processes	23
2.3.2 Influence of extrusion conditions on the starch and protein fraction of durum wheat semolina	28
2.3.3 Influence of extrusion conditions on the microstructure of pasta dough and pasta.....	35
2.3.4 Influence of extrusion conditions on the viscoelasticity of pasta dough	38

2.3.5	Influence of extrusion conditions on the characteristics of dried and cooked pasta	42
2.4	Conclusions	51
3	Water uptake and water vapor sorption of durum wheat semolina, wheat starch and gluten	53
3.1	Introduction	54
3.2	Experimental.....	56
3.2.1	Samples... ..	56
3.2.2	Determination of water vapor sorption kinetics at high relative humidity ...	58
3.2.3	Determination of water vapor sorption isotherms.....	58
3.2.4	Determination of water holding capacity.....	59
3.2.5	Determination of water uptake by an automated Enslin method	59
3.2.6	Characterization of melting and swelling of wheat starch by differential scanning calorimetry (DSC) and hot stage microscopy.....	60
3.3	Results and discussion.....	63
3.3.1	Water vapor sorption behavior of durum wheat semolina, wheat starch and gluten.....	63
3.3.2	Water holding capacity of durum wheat semolina, wheat starch and gluten	68
3.3.3	Dynamics of water uptake of gluten and wheat starch	70
3.3.4	Dynamics of water uptake of durum wheat semolina.....	76
3.4	Conclusions	81
4	Hydration dynamics of durum wheat endosperm as studied by magnetic resonance imaging (MRI) and soaking experiments ...	83
4.1	Introduction	84
4.2	Experimental.....	86
4.2.1	Preparation of durum wheat endosperm cylinders.....	86
4.2.2	Determination of porosity and surface topography of durum wheat endosperm cylinders	87
4.2.3	MRI experiments for following the hydration of durum wheat endosperm .	89

4.2.4	Calibration of the T_2 relaxation time as function of water concentration.....	89
4.2.5	In-situ determination of durum wheat endosperm hydration at excess water conditions by MRI.....	90
4.2.6	In-situ determination of durum wheat endosperm hydration at limited water conditions by MRI.....	92
4.2.7	Gravimetric determination of water uptake upon hydration at excess water conditions	92
4.2.8	Determination of an apparent diffusion coefficient of water in durum wheat endosperm by numerical modeling	94
4.3	Results and discussion.....	95
4.3.1	Porosity and surface topography of durum wheat endosperm cylinders	95
4.3.2	Calibration curve for the calculation of water contents from T_2 relaxation time.....	97
4.3.3	Water distribution in durum wheat endosperm during hydration at excess water conditions	99
4.3.4	Water uptake of durum wheat endosperm cylinders upon hydration at excess water conditions.....	103
4.3.5	Water contents of durum wheat endosperm during hydration at excess water conditions: comparison of MRI and gravimetric experiments.....	104
4.3.6	Water distribution in durum wheat endosperm after hydration at limited water conditions	105
4.3.7	Numerically modeled apparent diffusion coefficient of water in durum wheat endosperm.....	109
4.4	Conclusions	111
5	General discussion – hydration and dough formation at intermediate water concentrations.....	113
5.1	Overall view on hydration of wheat endosperm.....	113
5.2	Hydration of wheat endosperm at intermediate water concentrations.....	116
5.3	Dough formation of wheat endosperm at intermediate water concentrations.....	119
6	References.....	123

Seite Leer /
Blank leaf

SUMMARY

Processing of dried durum wheat pasta involves conditioning and mixing of semolina with water, compacting and shaping by extrusion or sheeting, and dehydration. The present investigations first aimed at elucidating the process structure relationship in pasta dough formation and extrusion, and then on the detailed analysis of hydration kinetics of durum wheat endosperm.

Durum wheat semolina was hydrated to levels of regular pasta dough (30 - 33 g /100 g wb) and extruded in screw and plunger systems at varying mechanical and thermal energy input, and extruded pasta dough and dried pasta (spaghetti) were characterized. Increasing energy input during extrusion lead to decreasing protein solubility and partial melting of starch. The microstructure of pasta dough, which can be viewed as composite with protein as continuous phase and starch granules as fillers, became more homogeneous with increasing energy input. Excessive energy input lead to phase separation between starch and protein and to a coarser protein network. Decreasing storage and loss modulus of extruded pasta dough confirmed the impact of high energy input on structure. While appearance of dried spaghetti improved with increasing energy input, cooking properties were affected negatively if the energy input became excessive.

Hydration of durum wheat semolina, wheat starch and gluten with liquid water and water vapor was measured under dynamic and equilibrium conditions. After liquid water uptake, the finer particle size fraction of semolina had higher water contents than the coarser fractions. When dry semolina was exposed to water vapor, no significant differences were found in equilibrium moisture contents between the particle size fractions, while semi-dry semolina reached higher equilibrium moisture contents at finer particle size. When exposing semolina and wheat starch to liquid water at increasing

temperatures, a pronounced increase of liquid water uptake was observed at 47.5 °C. This increase was due to the beginning of the melting and swelling of starch which started at 47.5 °C, provided that heating rates were low and water was available in excess. The results indicate that typical water contents of pasta dough (30 – 33 g/100 g wb) are below the swelling capacity of durum wheat semolina but are sufficient to meet the capacity of water vapor sorption.

The kinetics of liquid water uptake was further investigated on geometrically exactly defined endosperm cylinders (diameter 1 mm, length 4-5 mm) that were cut out from durum wheat kernels. The total water uptake measured gravimetrically after different length of soaking the cylinders in water showed a limit of water uptake corresponding to a moisture content of around 40 g/100 g wb after 60 min soaking time. From these water uptake data, an apparent diffusion coefficient of water into durum wheat endosperm was estimated by numerical simulation to be around $0.76 \times 10^{-10} \text{ m}^2/\text{sec}$. Magnetic resonance imaging (MRI) was then used to quantify water distribution in the endosperm cylinders during soaking at both excess and limited water availability. The calibration of MRI signals for water content was achieved by correlating the spin-spin relaxation times T_2 obtained from cylinders that were adjusted to intermediate moisture levels of 19 to 45 g/100 g wb. Maps of water distribution over the cross section of endosperm cylinders at different soaking times up to equilibrium conditions were generated. The data for the dynamics of water uptake measured by MRI fitted well to the data measured gravimetrically.

It is concluded that an ideal conditioning and mixing operation in pasta processing should aim at conditions that allow a homogeneous plasticization of semolina with water. Thereafter, an optimal extrusion process should introduce just enough mechanical energy to open the cellular organization of endosperm tissue so that a homogeneous pasta dough is formed in which a fine network of still little aggregated endosperm protein embeds the starch granules as evenly as possible. In this manner pasta exhibits optimal cohesion and textural properties upon cooking, in particular if the protein network is fixed by drying at high temperatures.

ZUSAMMENFASSUNG

Das Verfahren zur Herstellung von getrockneten Teigwaren aus Hartweizengriess umfasst die Prozesse zur Befeuchtung und Mischung des Griesses mit Wasser, das Kompaktieren und Formen des Teiges durch Extrusion oder Walzen und das Trocknen. Die vorliegende Arbeit befasste sich mit der Beschreibung der Zusammenhänge zwischen Prozess und Struktur bei der Teigbildung und –extrusion und mit der genauen Bestimmung der Kinetik der Wasseraufnahme von Hartweizenendosperm.

Hartweizengriess wurde auf übliche Wassergehalte von Teigwarenteig (30-33 g /100 g FG) aufgefeuchtet und in Schnecken- und Kolbenextrusionssystemen unter Variation des mechanischen und thermischen Energieeintrages extrudiert. Der extrudierte Teig sowie die getrockneten Teigwaren (Spaghetti) wurden charakterisiert. Ein erhöhter Energieeintrag während der Extrusion führte zu geringerer Löslichkeit der Proteine und zu partiellem Schmelzen der Stärke. Die Mikrostruktur von Teigwarenteig, die als ein Komposit, zusammengesetzt aus einer kontinuierlichen Proteinphase mit den Stärkekörnern als Füller, angesehen werden kann, wurde durch steigenden Energieeintrag während der Extrusion homogener. Sehr hohe Energieeinträge führten allerdings zur Phasenseparierung zwischen Stärke und Protein und zur Ausbildung einer gröber strukturierten Proteinphase. Die Abnahmen von Speicher- sowie Verlustmodul bestätigten die Auswirkungen eines hohen Energieeintrages auf die Struktur von extrudiertem Teigwarenteig. Während das Aussehen getrockneter Spaghetti von zunehmendem Energieeintrag positiv beeinflusst wurde, wurden die Kocheigenschaften negativ beeinflusst, wenn der Energieeintrag sehr hoch war.

Die Kinetik der Wasser- und Wasserdampfaufnahme von Hartweizengriess, Weizenstärke und Gluten wurde im Gleichgewicht und unter dynamischen Bedingungen

gemessen. Feinere Partikelgrössenfraktionen hatten nach der Wasseraufnahme höhere Wassergehalte als gröbere. Wenn Partikelgrössenfraktionen von trockenem Griess Wasserdampf ausgesetzt wurden, wurden keine signifikanten Unterschiede bezüglich der Wassergehalte im Gleichgewicht gefunden. Bei der Verwendung von halb-trockenem Griess erreichten jedoch die feineren Partikelgrössenfraktionen höhere Wassergehalte im Gleichgewicht. Wenn Griess und Weizenstärke flüssigem Wasser bei zunehmender Temperatur ausgesetzt wurden, so wurde eine deutliche Zunahme der Wasseraufnahme bei 47.5 °C festgestellt. Diese Zunahme war durch das einsetzende Schmelzen und Quellen der Stärke bei 47.5 °C bedingt, vorausgesetzt dass die Aufheizgeschwindigkeit klein und Wasser im Überschuss verfügbar waren. Die Resultate weisen darauf hin, dass die üblichen Wassergehalte von Teigwarenteig (30-33 g/100 g FG) tiefer sind als die Wasseraufnahmekapazität von Hartweizengriess, aber höher als jene der Kapazität zur Sorption von Wasserdampf.

Die Kinetik der Wasseraufnahme wurde ferner an geometrisch exakten Zylindern (Durchmesser ~1 mm, Länge ~4-5 mm), die aus ganzen Hartweizenkörnern gedreht wurden, untersucht. Die gravimetrisch ermittelte, totale Wasseraufnahme der Zylinder nach unterschiedlichen Tauchzeiten der Zylinder in Wasser zeigte einen Sättigungswert der Zylinder von etwa 40 g/100 g FG nach 60 min. Über numerische Simulation konnte mit diesen Daten zur Wasseraufnahme ein scheinbarer Diffusionskoeffizient von Wasser in Hartweizenendosperm ermittelt werden ($0.76 \times 10^{-10} \text{ m}^2/\text{sec}$). Zusätzlich wurde Kernspinresonanz-Tomographie (MRI) verwendet, um quantitativ die Wasserverteilung in den Zylindern sowohl bei der Wasseraufnahme im Wasserüberschuss als auch bei limitierter Wasserverfügbarkeit zu bestimmen. Die Kalibrierung der MRI-Signale hinsichtlich des Wassergehaltes wurde über die Messung der spin-spin Relaxationszeit T_2 von definiert aufgefuehteten Zylindern (19-45 g/100 g FG) erreicht. Die Messung der Wasserverteilung über den Querschnitt der Zylinder wurde sodann zu verschiedenen Wasseraufnahmezeiten bis zum Erreichen von Gleichgewichtsbedingungen durchgeführt. Die so mittels MRI dynamisch ermittelten Daten zur Wasseraufnahme stimmten gut mit den gravimetrisch ermittelten Daten überein.

Es wird postuliert, dass im Verfahren der Teigwarenherstellung ein idealer Konditionier- und Mischprozess die homogene Plastifizierung (Erweichung) des Griesses mit Wasser zum Ziel haben sollte. Darauf folgend sollte ein idealer Extrusionsprozess gerade soviel mechanische Energie in das entstehende Teigsystem eintragen, um die zelluläre Struktur des nativen Endosperms aufzuschliessen und um einen homogenen Teigwarenteig zu formen, in welchem eine fein strukturierte und nur wenig aggregierte Proteinphase die Stärkekörner so gleichmässig wie möglich eingebettet. Unter dieser strukturellen Voraussetzung weisen Teigwaren optimalen Zusammenhalt und optimale Textureigenschaften nach dem Kochen auf, insbesondere wenn die gleichmässig ausgeformte Proteinphase während einer Hoch-Temperaturtrocknung gefestigt wird.

1 General introduction

According to a generally accepted definition, pasta can be described as a ready-to-cook food, prepared from milling products of cereal endosperm which are molded into the desired shape after the addition of water by means of cold extrusion or sheeting. Additional ingredients may comprise egg and coloring agents, based on vegetables or sepia extract. Pasta can be consumed upon production or stabilized by means of dehydration, refrigeration, sterilization or freezing. However, for the most part, the term pasta refers to dried pasta that is produced from durum wheat (*Triticum durum*) semolina without any further ingredients or additives. Dried pasta products of this kind enjoy widespread popularity due to their almost unlimited shelf life, positive nutritional profile, well accepted texture and taste and not least, their moderate cost.

Common processing of dried durum wheat pasta principally comprises three steps, i.e. conditioning and mixing of semolina with water, extrusion or sheeting aiming at the compaction and shaping of the plasticized semolina and dehydration. Over the years optimization of the drying step has been of particular interest and extensive research led to the introduction of much higher drying temperatures than in the traditional process. As a consequence, not only shorter drying times and improved hygienic standards were achieved, but the higher temperatures were also beneficial for the overall cooking quality of the final product, with higher firmness, less stickiness and lower cooking loss (Aktan and Khan 1992, Manser 1981, Novaro et al. 1993, Zweifel et al. 2003). In contrast, comparatively little research has been initiated on the physicochemical mechanisms of the transformation of semolina during conditioning, mixing, and extrusion or sheeting. Most studies were of empiric nature and focused on the relation between process parameters and pasta quality (Abecassis et al. 1994, Debbouz and Doetkott 1996, Manser

1981). These investigations and practical experience over many years show that optimal water content of pasta dough to ensure a sufficiently homogeneous distribution of water among the semolina particles lies between 30 and 33 g/100 g wb. It is also well known that critical temperatures for pasta extrusion exist above which negative effects on pasta quality occur, generally attributed to undesired modifications of the protein fraction. Although it is rather difficult to specify an exact temperature limit, the critical range is nevertheless regarded to start between 50 and 60 °C. So far, optimization of pasta processing has also been dependent on the fact that conditioning with water and mixing are slow operations so that ample time is available for the full hydration of semolina. However, with the introduction of accelerated processes for the conditioning and mixing, hydration and dough formation may be impaired and the quality of the final product deficient. It is quite clear that the optimization of these fast processes requires more information on the basic principles of hydration of semolina and pasta dough formation. This information is also of general interest in many aspects of cereal technology.

In terms of material science, pasta processing may be viewed as the transformation of durum wheat endosperm, which is a cell structured natural composite of the major components starch and protein and minor constituents like hemicelluloses and pentosane, into a biopolymer composite material consisting of a continuous protein phase with starch granules as a filler. The first aim of the present investigation was to study the structural and physicochemical changes of endosperm material during pasta dough mixing and extrusion of pasta dough (chapter 2). Pasta dough and pasta were prepared at pilot plant scale at varying conditions and characterized at different levels of structural organization. The changes in the starch and protein fractions were assessed by means of differential scanning calorimetry and protein solubility. Microscopic techniques were used to characterize the changes at a microstructural level and rheological tests were performed to assess the influence of processing conditions on the viscoelasticity of extruded pasta dough. Furthermore, the influence of processing on the mechanical properties, appearance and cooking behavior of the dried pasta was determined.

The second objective was to analyze the interaction of durum wheat endosperm with water. For this purpose, uptake of liquid water and water vapor by semolina and by wheat starch and endosperm protein was followed with various experimental techniques at equilibrium and dynamic conditions (chapter 3). The kinetics of liquid water uptake was further investigated on geometrically exactly defined endosperm cylinders (diameter 1 mm, length 4-5 mm) that were cut out from durum wheat kernels. With the use of these samples it was possible to measure the water transport into and the water concentrations inside durum wheat endosperm by magnetic resonance imaging combined with gravimetric analyses and to determine an apparent diffusion coefficient for water in durum wheat endosperm by numerical simulation (chapter 4).

A concluding discussion (chapter 5) interprets the material transformations in conditioning, mixing and extrusion on the basis of a state diagram for durum wheat endosperm.

2 *Process structure relation in pasta dough extrusion**

Durum wheat semolina was hydrated to levels of pasta dough water content and extruded by a single screw extruder, a twin-screw extruder and a cylinder-plunger system at varying mechanical and thermal energy input. The effect of extrusion processes and conditions on pasta dough was characterized by protein solubility, differential scanning calorimetry, microscopy and oscillatory shear measurements. Of dried, spaghetti-shaped pasta appearance, breaking strength and cooking properties by classical cooking and instrumental texture tests were determined. Increasing mechanical and thermal energy input during extrusion lead to decreasing protein solubility and partial melting of starch. The microstructure of pasta dough which can be viewed as a composite with the proteins as the continuous phase and the starch granules as filler, became more homogeneous with increasing energy input. But on the other hand, excessive energy input lead to phase separation between starch and protein and to a coarser protein network. Decreasing storage and loss moduli and phase angle of pasta dough confirm the impact of high energy input on structure. Higher energy input in extrusion improved appearance of dried pasta, whereas simple compressing of semolina in the cylinder-plunger system resulted in rough pasta with white spots. Cooking properties of the pasta upon drying were affected negatively by higher energy input during extrusion.

* This chapter has been prepared for publication as:

Kratzer, A., Niklaus, C., Escher, F., Conde-Petit, B. Influence of different extrusion processes and conditions on pasta dough properties and pasta quality.

2.1 Introduction

The production of dried durum wheat pasta basically involves three steps: (1) the conditioning and mixing process aiming at the homogeneous plasticization of the semolina, (2) the compacting and shaping step by means of extrusion or sheeting and (3) the drying step to stabilize the pasta regarding its cohesion and shelf life.

It is generally accepted that the texture of pasta largely depends on the high protein content and adequate protein quality of durum wheat semolina (Dexter and Matsuo 1978, Sissons et al. 2005). The wheat endosperm proteins are able to form a continuous and interconnected protein phase, and by this to entrap the starch granules and to provide the necessary cohesion of pasta. In bread dough, the fully hydrated native endosperm proteins of wheat form a polymeric three-dimensional network known as gluten. In pasta dough, hydration is limited and gluten formation takes place at the utmost partially. By using microscopy Matuso et al. (1978) showed that after the mixing step no gluten development was detectable at all, and after compaction of the hydrated semolina in the extruder, only partial gluten formation was observed. The authors concluded that hydration levels in pasta dough would always be insufficient to form the same type of gluten network as it is found in bread dough. They described the protein matrix of pasta dough as “jagged” in contrast to “smooth” and “continuous” in bread dough.

Nevertheless, the formation of a sufficiently homogeneous and cohesive protein network remains the key to an ideal microstructure of pasta (Pagani et al. 1989, Resmini and Pagani 1983, Zweifel et al. 2003). As protein is the minor component of durum wheat semolina compared to starch (10-14 compared to 74-90 g/100 g db, respectively), homogeneous phase distribution of the proteins in pasta dough is challenging to achieve. Improper processing conditions easily prevent the formation of a sufficiently cohesive pasta dough. Abecassis et al. (1994) found elevated extrusion temperature (35-70 °C) to be the main parameter affecting pasta cooking properties, with increased cooking loss being the consequence of higher dough temperatures. Debbouz and Doetkott (1996)

studied the influence of the process parameters extruder barrel temperature and screw speed on pasta properties. Barrel temperature was shown to have a significant impact on all the quality attributes tested and therefore was defined as the most important process parameter during pasta extrusion. Higher barrel temperature at constant water content (31 g/100 g wb) enhanced the yellow-index of pasta, but decreased its cooking quality with higher water uptake during cooking and a lower firmness. According to these authors, optimal pasta quality is obtained by applying water contents of 30-31 g/100 g wb in combination with barrel temperatures of 45-52 °C. This temperature range also corresponds to the observations by Manser (1981) who suggests dough temperatures below 45-47 °C.

There is evidence that denaturation and aggregation of protein occur when dough temperatures exceed the critical values mentioned above. The determination of protein solubility presents a suitable method for characterizing these transformations taking place in pasta dough during pasta processing. Dexter et al. (1977) studied the evolution of protein solubility over the whole process of pasta production and found a decrease in solubility as a consequence of the extrusion step, but no further decrease during low-temperature drying. For pasta dough mixing, a decrease in the protein solubility was found to occur at higher mixing temperatures, i.e. 50 compared to 30 °C, and in developed “bread dough-like” pasta dough. At water contents above 30 g/100 g wb during mixing an increase in the protein solubility was found and referred to as gluten breakdown. The same phenomenon was observed in “overmixed” bread dough (Dexter and Matsuo 1979, Icard-Verniere and Feillet 1999). As a consequence of high-temperature drying, a marked decrease in protein solubility was detected (Aktan and Khan 1992, Zweifel et al. 2003). Besides the protein solubility the amount of the insoluble glutenin macro polymer (GMP) is used to characterize the influence of processing conditions on the protein fraction of wheat dough. According to the studies of Don et al. (2003a), GMP is the part of the glutenins that is insoluble in sodium dodecyl sulphate (SDS) solution and forms a gel after a flour sample is suspended in SDS and ultracentrifuged. Don et al. (2003b) investigated the mixing process of bread dough and

found that increasing mixing time generally reduced the amount of GMP. No GMP at all was found after the mixing of dough for 5-27 min, depending on the protein strength of the wheat cultivar. Hence, elevated mechanical forces during dough mixing lead to GMP breakdown at the high water content of bread dough. Peighambardoust et al. (2005) investigated the effect of elongational and shear energy input on durum wheat dough systems during mixing at a water content of 40 g/100 wb. They found that the amount of GMP was greatly reduced by dough mixing in a Z-blade mixer, in which both, elongational and shear flow, contributed to the mechanical energy input. In contrast, mixing of dough in a simple shear mode did affect the GMP content to a lesser degree. Additionally, micrographs of the dough structure revealed a more homogeneous starch-protein distribution in the dough mixed at simple shear. The microstructure of pasta dough was also investigated by Pagani et al. (1989) who compared extruded, sheeted and hand-sheeted pasta dough and analyzed the cooking quality of the pasta produced by these different shaping processes. Extrusion was found to yield the lowest cooking quality due to a “breakdown” of the protein network structure. Additionally, extruded pasta also showed the lowest porosity what correlated inversely with cooking quality. However, in the latter study, a blend of soft and durum wheat flour was used and according to the authors this rather unsuited mix of raw materials would have allowed to assess the different impacts of the investigated processes on pasta quality more easily.

The aim of the present investigation was to study the process structure relation between extrusion and the properties of pasta and pasta dough. Three different extrusion processes by single-screw and twin-screw extrusion and by a cylinder-plunger system allowed to vary the mechanical and thermal energy input in a wide range. The materials were characterized on the molecular and supramolecular level regarding protein solubility and thermal properties of starch, while the microstructure of pasta and pasta dough was assessed by microscopic techniques. At macroscale, the rheological properties of pasta dough and the textural attributes and cooking properties of dried pasta were measured.

2.2 Experimental

2.2.1 Preparation of pasta dough and pasta samples on laboratory scale

Conditioning and mixing

According to the supplier's specifications, the durum wheat semolina (HWG-M, Swissmill, Zurich, Switzerland) used for the experiments consisted of a mixture of Canadian western amber durum wheat, U.S. amber durum wheat (45 % each) and European durum wheat (10 %). The semolina was of a medium granulation ranging from 0-500 μm and the main mass fraction was between 250 and 315 μm (36.7 g/100 g). The protein content of the semolina was analyzed by using a standard Kjeldahl-method (protein content = $\text{N} \times 5.7$) and was $14.4 \pm 0.6\text{g}/100\text{ g db}$. For all experiments, the water content of the durum wheat semolina was analyzed by drying approximately 2 g of semolina at 120 °C for 10 min in an infrared heated balance (Mettler-Toledo, Typ LP 16, Greifensee, Switzerland).

All mixing experiments were performed with tap water at room temperature to obtain a moisture content of 31 g/100 g wb in the mixed dough, unless otherwise noted. A laboratory batch mixer (Bühler AG, Uzwil, Switzerland), described by Frey and Neukom (1967), was used. The mixer operates with a horizontal axle, on which the mixing paddles are attached, and the water is sprayed onto the fluidized semolina from above (Figure 2.1). The mixer was filled with 2.5 kg of semolina and the adequate amount of water was sprayed while mixing the material at 65 rpm. The spraying pressure was 3.5 bar and the spraying time was 8.5 min. After water addition, the mixing speed was reduced to 40 rpm and mixing proceeded up to a total mixing time of 10 min. The exact amount of water that remained in the spraying system was determined gravimetrically ($5.5 \pm 0.9\text{ g}$). Hence, 5.5 g of water were filled into the spraying device in addition to the water necessary for the semolina hydration itself.

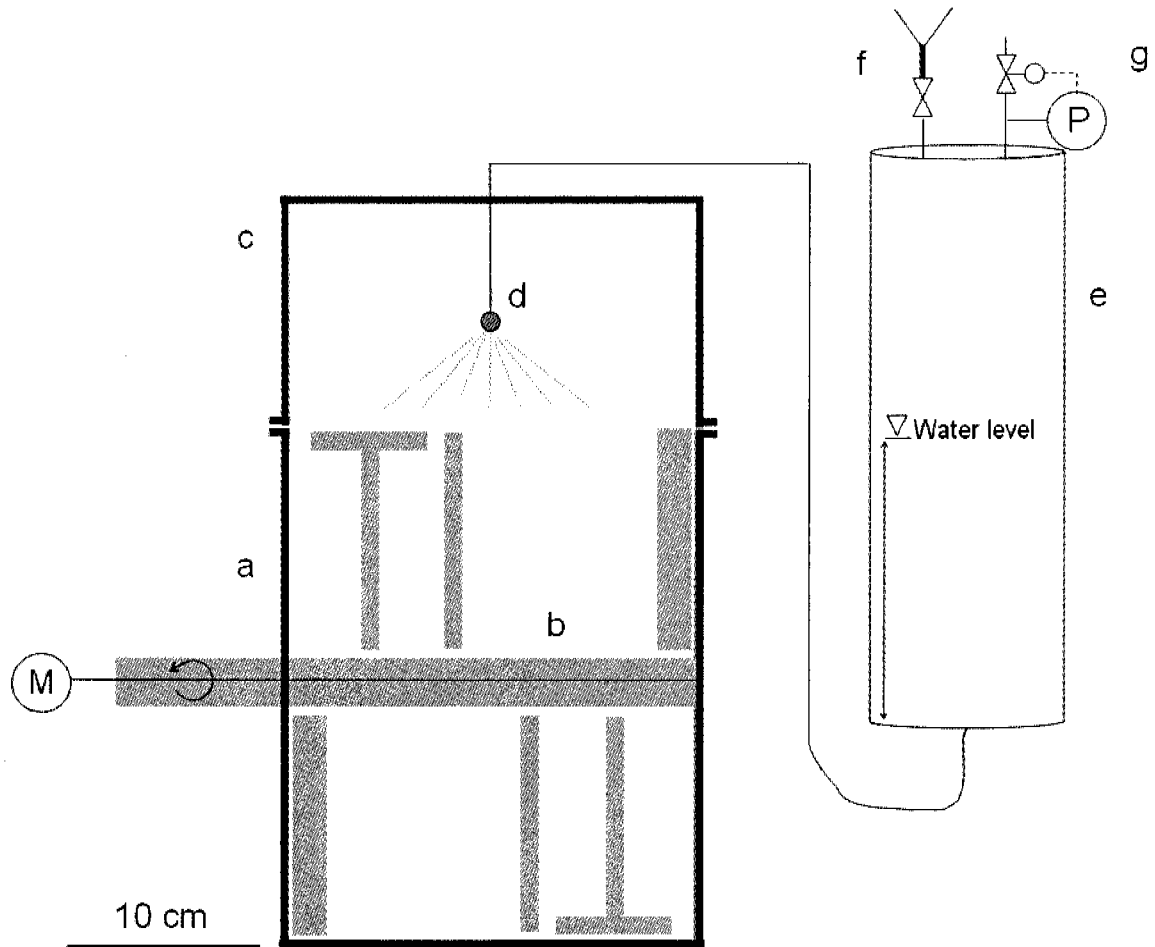


Figure 2.1: Schematic view of the mixer used for the hydration of semolina. The mixing chamber (a) was filled with 2.5 kg of semolina. The rotating axle (b) is equipped with paddles and fluidizes the semolina inside the mixing chamber. The removable lid (c) serves as a holder for the spray nozzle (d) which is connected to the pressure proof water reservoir (e) through a flexible hose. The water reservoir is filled with a funnel (f) and the water is set under pressure with compressed air, regulated by a manual pressure control valve (g).

Extrusion

For the extrusion of hydrated semolina at laboratory scale a *standard single-screw pasta extruder* and a *twin-screw extruder* were used. Additionally, a *cylinder-plunger system* based on a capillary rheometer was used to simulate the compression and extrusion of hydrated semolina to pasta dough without the typical mechanical work input of an extruder.

The *single-screw pasta extruder* (Bühler FLK-81296, length : diameter ratio = 35 : 5 cm, Uzwil, Switzerland) was operated at a screw speed of 25 rpm, a mass flow of approximately 30 kg/hr and a barrel temperature of 40 °C. Extrusion took place under vacuum (200 mbar) and the pasta dough was extruded through a PTFE-coated spaghetti die (Osterwalder AG, St. Gallen, Switzerland).

A schematic side view and description of the *twin-screw extruder* (DSE-20/20, Brabender OHG, Duisburg, Germany) are given in Figure 2.2. Along the barrel length (length : diameter ratio = 48 : 2 cm), there were three individually controlled temperature zones. At the end of the barrel, there was a measuring ring where a pressure transducer and a thermocouple were installed. The measuring ring and the die-zone were temperature controlled by an external heating/cooling water bath. The hydrated semolina was transferred into the loss in weight feeder (K-CL-KT20, K-tron Ltd., Niederlenz, Switzerland) and extrusion took place under vacuum (200 mbar) at varying process conditions regarding screw speed and screw configuration (Table 2.1). The screw configurations consisted of conveying elements, a back extrusion element in front of the vacuum outlet position and shear elements at the end of the screw for some experiments. The feed rate was kept constant at 3 kg/hr. The dough was formed through PTFE-coated dies (Osterwalder AG, St. Gallen, Switzerland) into a plate shaped geometry (cross-section of 25 x 2 mm, slit length 60 mm) or into spaghetti shape (5 strands, diameter 1.85 mm). Specific mechanical energy input during extrusion was calculated according to equation 2.1 (Abecassis et al. 1994).

$$\text{SME [J / kg]} = \frac{M \cdot \omega}{\dot{m}} \quad (\text{equation 2.1})$$

where SME is the specific mechanical energy input, M the torque [Nm], ω the screw speed [rad/sec] and \dot{m} the throughput of the extruder [kg/sec]. The torque for operating the empty extruder was subtracted from the measured torque values during pasta extrusion.

Table 2.1: Extrusion conditions for the production of pasta dough in the shape of plates or spaghetti in the twin-screw extruder.

Shear elements (SE) [-]	Screw speed [rpm]	Barrel temperatures in zone 1/2/3/die [°C]	Feed rate [kg/hr]
0	50	25/30/30/30	3
0	125	25/30/30/30	3
0	200	25/30/30/30	3
1	50	25/30/30/30	3
1	125	25/30/30/30	3
1	200	25/30/30/30	3
2	50	25/30/30/30	3
2	125	25/30/30/30	3
2	200	25/30/30/30	3

For the compression of the hydrated semolina in the *cylinder-plunger system*, the moistened semolina was filled into the brass pipes (volume 50 cm³) of the capillary rheometer (Göttfert Rheograph 2002, Göttfert GmbH, Buchen/Odenwald, Germany) and pre-compacted manually. The filled pipes were then mounted in the rheometer and the plunger was operated at a speed of 1.5 mm/sec. The device was kept at a temperature of 40 °C and the dough was pressed through a PTFE-coated spaghetti die (5 strands, diameter 1.85 mm). The pressure of the dough was detected during the experiment at the die. The extruded pasta-strands were collected in plastic bags to prevent moisture loss and transferred to the dryer within 20 min.

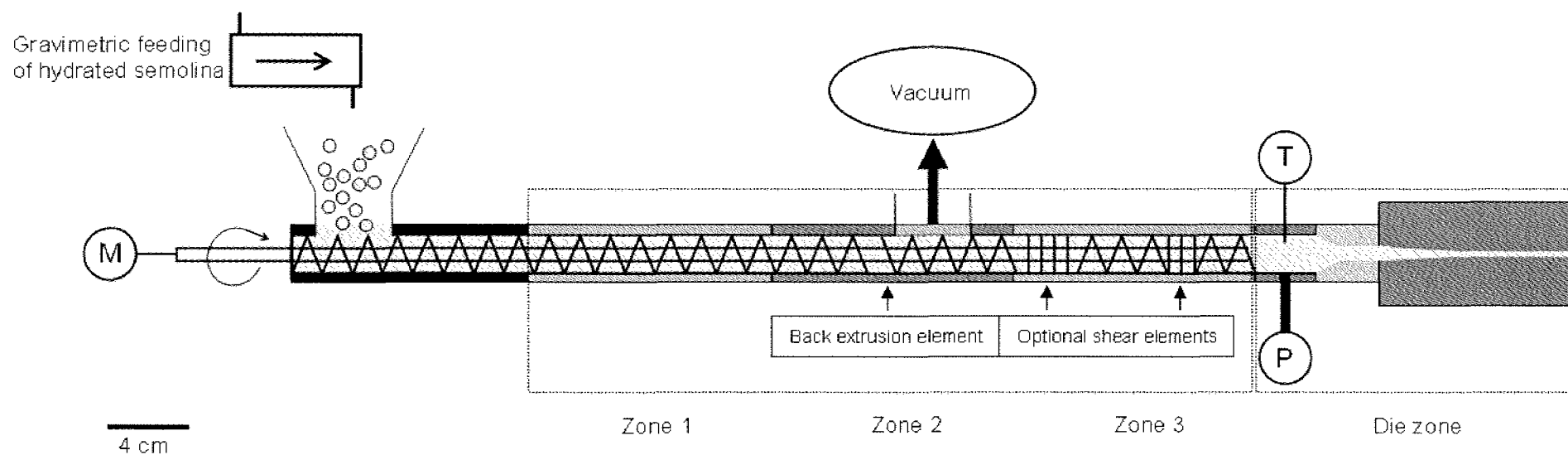


Figure 2.2: Schematic side view of the twin-screw extruder used for the preparation of pasta dough on laboratory scale.

The three zones 1, 2, and 3 are temperature controlled individually and the die zone is heated and cooled by a water flow in a jacket.

Drying

Upon extrusion, the spaghetti strands were dried in a laboratory dryer (Afrem Ltd., Lyon, France) by using a high-temperature drying cycle that lasted 8 hr and reached a maximum temperature of 88 °C. Figure 2.3 presents the temperature-humidity-time profile of the set and measured conditions of the drying cycle.

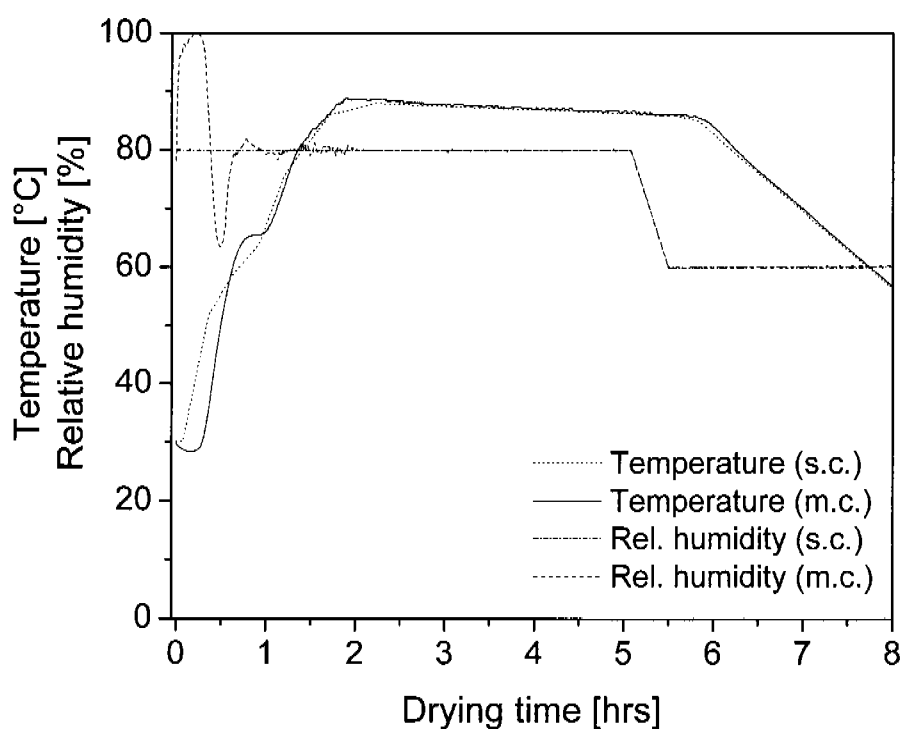


Figure 2.3: Set (s.c.) and measured (m.c.) temperature and relative humidity during the high-temperature drying cycle used for the drying of pasta samples.

2.2.2 Determination of protein solubility

Preparation of samples

The samples for the determinations of the protein solubility were taken at various stages during pasta processing. The samples were immediately frozen and stored in liquid nitrogen. The samples were freeze dried for approximately 16 hr (SWWL Secfroid, Lausanne, Switzerland). And then ground in a laboratory mill (Retsch-ZW1, Retsch GmbH, Haan, Germany) using a 0.5 mm mesh size screen. For further analyses, the samples were stored in sealed plastic bags at room temperature. The water content of the milled samples was determined by drying approximately 1 g for 90 min at 133 °C in a drying oven.

Protein solubility in diluted acetic acid

2 ± 0.005 g of the sample were weighed into centrifuge tubes (40 mL) and extracted for 2 hr in 40 mL of diluted acetic acid ($c = 0.5$ mol/L) at room temperature under slow rotation. After extraction, the samples were centrifuged at $7000 \times g$ at 5 °C for 45 min (Laboratory centrifuge 3K30, Sigma GmbH, Osterode am Harz, Germany). An aliquot of the supernatant (10 mL) was pipetted into a Kjeldahl-flask and analyzed for its nitrogen content with a standard Kjeldahl procedure. The factor for calculating the protein content from the nitrogen content was 5.7. The results of the protein solubility were expressed as g/100 g protein. In order to calculate this quotient, also the protein content of the semolina was determined with a standard Kjeldahl method (protein = $N \times 5.7$).

Protein insolubility in sodiumdodecylsulfat (SDS) solution

For the determination of the protein insolubility in SDS-solution, a slightly modified method of Peighambardoust et al. (2005) was used. The samples were defatted by mixing approximately 2 g with 15 mL of petroleum ether (low boiling, Fluka AG, Buchs, Switzerland) for 15 min in 50 mL centrifuge tubes. The mixture was centrifuged at 1000 x g at 25 °C for 10 min, the supernatant was discarded and the defatted sample was dried at room temperature. From the defatted sample, 0.658 ± 0.02 g were weighed into 15 mL ultracentrifuge tubes and a small magnetic stirrer was added. During stirring, 15 mL of SDS-solution ($c_{\text{SDS}} = 15$ g/l, Fluka AG, Buchs, Switzerland) were added and during a total mixing time of 15 min, the suspension became free of lumps and manual stirring with a small spatula was performed to disintegrate persistent lumps. The centrifuge tubes were equilibrated regarding their mass and ultracentrifuged at 80000 x g at 25 °C for 30 min (L 60 Ultracentrifuge, Beckman instruments, Palo Alto, USA). Upon centrifugation, the glutenin macro polymer (GMP) was found as a gel layer between a starchy pellet and the SDS supernatant (Figure 2.4). After discarding the supernatant, the GMP was removed with a spatula and its mass was recorded as GMP wet weight. Determinations of the protein content (Kjeldahl-method) of the GMP gel showed that it consisted of 11.7 ± 2 g protein/100 g GMP wb.

Thermal incubation of hydrated semolina

Incubation tests with hydrated semolina were performed to analyze the impact of heat on the protein solubility. Approximately 50 g of hydrated semolina (31 g/100 g wb) were filled into sealed plastic bags and then incubated in water baths at temperatures between 40 and 60 °C for times between 5 and 60 min. The samples were then frozen in liquid nitrogen and freeze dried. Protein solubility in acetic acid and insolubility in SDS-solution (GMP wet weight) were determined as described above.

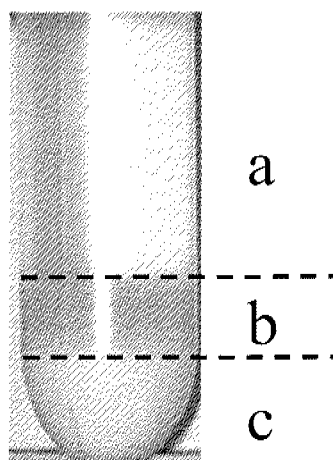


Figure 2.4: Separation of the samples after ultracentrifugation into (a) SDS-soluble fraction, (b) glutenin macro polymer (GMP) and (c) other SDS-insolubles.

2.2.3 Differential scanning calorimetry (DSC)

Samples were freeze dried and ground as described in section 2.2.2 and suspended in water at a water content of 80 g/100 g wb. From these suspensions, approximately 15-20 mg were weighed into aluminum DSC pans (Perkin Elmer Ltd., Norwalk, USA). The DSC measurements were carried out on a 2920-DSC (TA Instruments Ltd., New Castle, USA) which had been calibrated with indium and an empty pan served as reference. The pans were heated at 5 °C/min from 20 to 95 °C under nitrogen flush (40 cm³/min). The recorded endothermic transition was evaluated for the melting range, peak temperature (T_{M1}) and melting enthalpy by using the TA Instruments analysis software. The measurement was carried out in duplicate.

2.2.4 Confocal laser scanning (CLSM) and light microscopy

Pasta dough structure after extrusion was characterized by confocal laser scanning microscopy (CLSM). Fluorescence of the pasta dough samples was obtained by addition of a fluorescence dye (rhodamine B, Fluka AG, Buchs, Switzerland) to the water used to moisten the semolina ($c_{\text{rhodamine}} = 0.0001 \text{ g/L}$). After extrusion, the pasta dough samples were transferred to the microscope in sealed plastic bags and observation was performed within 60 min after extrusion. Without any further preparation, the dough samples were placed on a glass slide and covered with a cover glass and a droplet of water-glycerol solution. Images were recorded in the epi-fluorescence mode on a Leica TCS-SP spectrometer-equipped CLSM, mounted on an upright DM IRBE fluorescence light microscope (Leica Lasertechnik GmbH, Heidelberg, Germany). Illumination was performed with an Ar-ion laser at a wavelength of 586 nm and emission was recorded from 575 to 620 nm. Digitized images were taken at a resolution of 512 x 512 pixels.

Sections of durum wheat endosperm and dried pasta were obtained by soaking the dry samples in deionized water at room temperature for 1 hr. Upon soaking, the samples were covered with a cryoprotecting agent (Tissue-Tek OCT, Miles, Kankakee, USA) and frozen in isopentane. After cryosectioning (Jung CM 3000, Leica, Nussloch, Germany), the sections were stained with ruthenium-red to enhance the contrast of cellular structures. Micrographs were taken at the Axioskop 2-mot microscope (Zeiss Ltd., Oberkochen, Germany) and pictures were recorded with a 3CCD-camera (Hamamatsu C5810, Hamamatsu Photonics, Hamamatsu-City, Japan).

2.2.5 Rheological characterization of pasta dough

The determination of the viscoelastic properties of fresh pasta dough sheets was carried out immediately after extrusion (3-5 min) with a stress sweep test. In order to prevent drying of the samples prior to analysis, they were transported to the rheometer in sealed plastic bags. From the extruded pasta sheet, a circular sample (diameter 21 mm) was cut out and placed on the AR-2000 rheometer (TA Instruments Ltd., New Castle, USA). The gap was set to 2 mm and was normal force controlled (5 N) during the test. After setting the gap, the sample was allowed to equilibrate for 1 min. The stress sweep test was performed in oscillatory mode with a plate-plate geometry (diameter 20 mm) at 25 °C and a frequency of 1 Hz. During the measurements, a solvent trap filled with distilled water prevented drying of the sample edges. Storage and loss moduli were recorded and the end of the linear viscoelastic domain was calculated from the yield point of the storage modulus. Results were expressed as mean and standard deviation of at least three experiments.

2.2.6 Determination of breaking strength and surface characteristics of dried pasta

The breaking strength of dried pasta was measured with a three point bending test according to Zweifel et al. (2003), using a universal testing machine (Zwick Z010, Ulm, Germany) equipped with a 10 N load cell. The force-deformation curves were evaluated for the maximum resistance force at the breaking point. The test was performed exactly seven days after the production of the samples. Results were expressed as mean and standard deviation of ten measurements.

Surface characteristics of dried pasta were determined optically by observing the dried pasta under a stereo microscope (SZ-PT, Olympus Corp., Tokyo, Japan). Pictures were recorded with the Hamamatsu C5810 camera.

2.2.7 Characterization of cooking behavior and properties of cooked pasta

Optimal cooking time, water uptake and cooking loss

The optimal cooking time of the dried spaghetti was determined according to Dürr and Neukom (1973). Spaghetti were broken into a length of approximately 10 cm and ten strands were cooked in boiling tap water (800 mL in a 1000 mL beaker). Samples were taken after 8 min every 15 sec and were pressed between two glass slides and optimal cooking time was defined as the time, when the white core of ungelatinized starch in the center just had disappeared. The determination was performed 2-4 times for each sample.

Cooking loss and water uptake were determined in duplicate by cooking 5 ± 0.001 g of spaghetti to their optimal cooking time. After cooling the pasta by immersion in water at room temperature for 60 sec, the mass of the cooked pasta was weighed and the dry matter of the cooked and uncooked samples was determined after drying in a drying oven at 105 °C for 14 hr. Cooking loss (CL) and water uptake (WU) were calculated according equation 2.2 and 2.3.

$$CL [g/100 g db] = \frac{g dm_{uncooked} - g dm_{cooked}}{g dm_{uncooked}} \cdot 100 \quad (\text{equation 2.2})$$

$$WU [g/100 g db] = \frac{g mass_{cooked} - g dm_{cooked}}{g dm_{cooked}} \cdot 100 \quad (\text{equation 2.3})$$

where $g dm_{uncooked}$ and $g dm_{cooked}$ are the masses of the sample before and after cooking [g] and $g mass_{cooked}$ is the total mass of the pasta after optimal cooking [g].

Diameter, firmness and penetration depth

Spaghetti samples (12 strands with a length of 10 cm) were cooked optimally and subsequently cooled by immersion in tap water at room temperature for 60 sec. Excess water was removed by shaking the samples in a sieve for 15 sec. Force deformation curves were recorded with the Zwick universal testing machine by cutting one cooked spaghetti strand with a special tooth-tool (thickness of 1 mm), attached to the 10 N load cell. The diameter of the spaghetti was calculated from the tool position, when a touching force of 0.01 N was reached. The penetration depth at a force of 0.1 N was recorded to characterize the intermediate layer of the cooked spaghetti and finally the maximum force was recorded as an indicator of firmness in the center of the spaghetti strand. The relative depth of penetration was calculated as percentage of the penetration depth at 0.1 N in relation to the diameter of the cooked spaghetti. Results were expressed as mean and standard deviation of 20 measurements (two cooking series with 10 measurements each).

Stickiness of cooked pasta

The stickiness was measured on optimally cooked spaghetti. After cooking the spaghetti were shaken in a sieve for 15 sec to remove excess surface water. Approximately 45 spaghetti strands were placed in parallel on a ribbed base plate. Exactly 3 min after cooking, the tensile test on the Zwick universal testing machine was started: A circular brass plate (diameter 97 mm) was lowered onto the spaghetti layer, pressed them with a force of 80 N and lifted again after a holding time of 2 sec. The negative force during the upward movement due to adhesion of the pasta to the brass plate was recorded. The area of the force-time curve below the ordinate was numerically integrated and defined as a measure for spaghetti stickiness. Results are presented as mean and standard deviation of three measurements.

2.3 Results and discussion

2.3.1 Characteristics of the extrusion processes

Dough temperature, mechanical energy input, pressure and torque resulting in the twin-screw extruder are presented in Figure 2.5 and Figure 2.6. Extrusion with the sheet type and the spaghetti type die gave comparable values. At increasing screw speed from 50 to 200 rpm dough temperature and specific mechanical energy input (SME) generally increased from 50 to 76 °C and from 200 to 550 kJ/kg, respectively (Figure 2.5). In contrast, extrusion pressure and torque decreased at higher screw speed from 110 to 50 bar and from 38 to 18 Nm, respectively (Figure 2.6).

SME values obtained in the present extrusion trials were quite high compared to pasta extrusion systems at industrial scale (~70 kJ/kg) or data published by Abecassis et al. (1994) (for a single-screw laboratory extruder 66-122 kJ/kg). The high values were a consequence of the high L/D ratio and the twin-screw configuration. They were intended in order to be able to determine the impact of high SME on the structural properties of pasta dough. As a further consequence of high SME the dough reached temperatures which were at or beyond the critical level cited in the introduction. However, unpublished own measurements in pasta production units at industrial scale revealed that dough temperatures in continuous pasta extrusion systems may well reach up to 55-60 °C.

The influence of the shear element configuration on the physical response during pasta extrusion was lower than to the effect of screw speed. At equal screw speed, SME and dough temperature at the die were in the same range irrespective of the number of shear elements in the screw configuration. This might be due to the high cooling capacity of the extruder barrel at a high surface to throughput ratio. Nevertheless, the extrusion pressure decreased significantly when more shear elements were present in the screw configuration. As dough temperatures were similar, the lower extrusion pressures

indicate different structural and therefore rheological properties of pasta dough as a consequence of the introduction of shear elements.

For the extrusion in the single-screw pasta extruder, an extrusion pressure of 110-120 bar and dough temperatures of 40 ± 2 °C were recorded.

The compacting and extrusion pressure recorded in the cylinder-plunger system is shown in Figure 2.7. For pasta dough at a water content of 31 g/100 g wb, pressure was between 85 and 110 bar, while dough temperatures were at approximately 40 °C. As expected, at lower water content (29.5 g/100 g wb) pressure increased to 125-145 bar, whereas it decreased at the slightly higher water content of 32.5 g/100 g wb to 60-75 bar. The strong influence of water content on extrusion pressure reflects the sensitivity of pasta dough viscosity on slight changes in water content. LeRoux et al. (1995) also reported the strong dependence of extrusion pressure on semolina hydration.

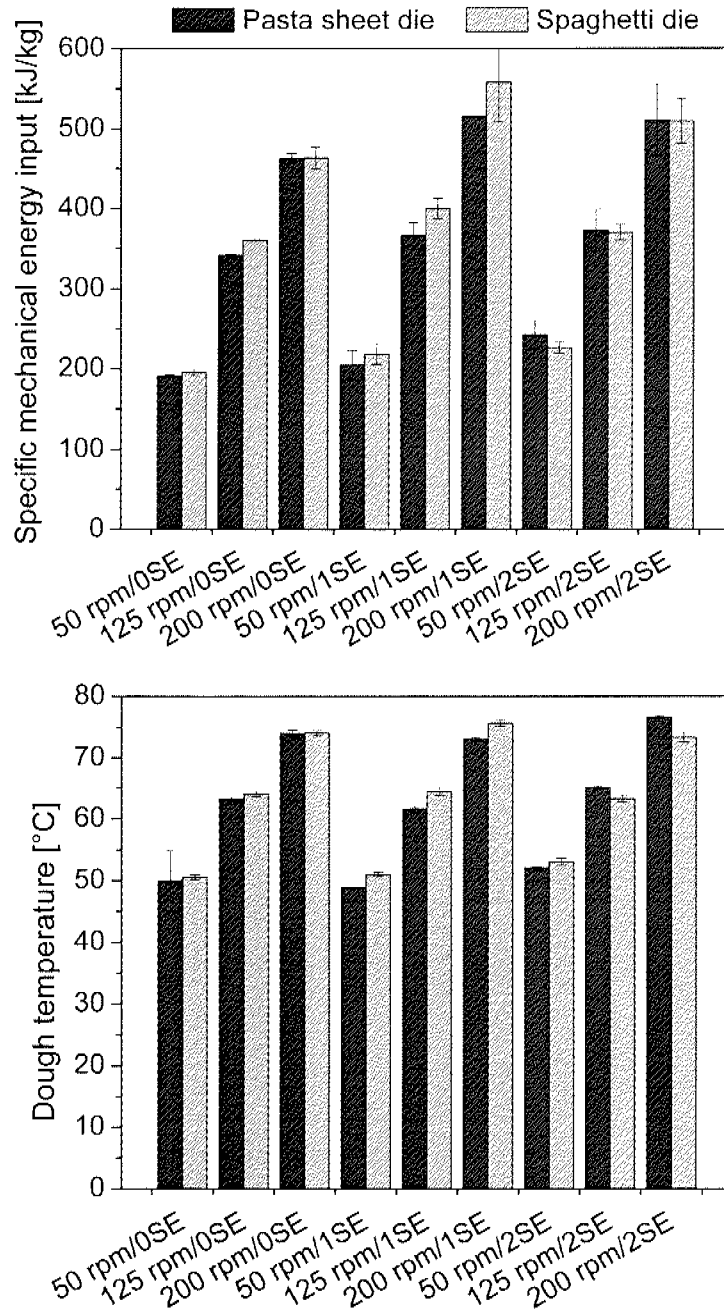


Figure 2.5: Specific mechanical energy input and dough temperature at the die in the extrusion of pasta dough into sheets and spaghetti shape in the twin-screw extruder at different screw speeds and configurations (Explanation of abbreviations in Table 2.1).

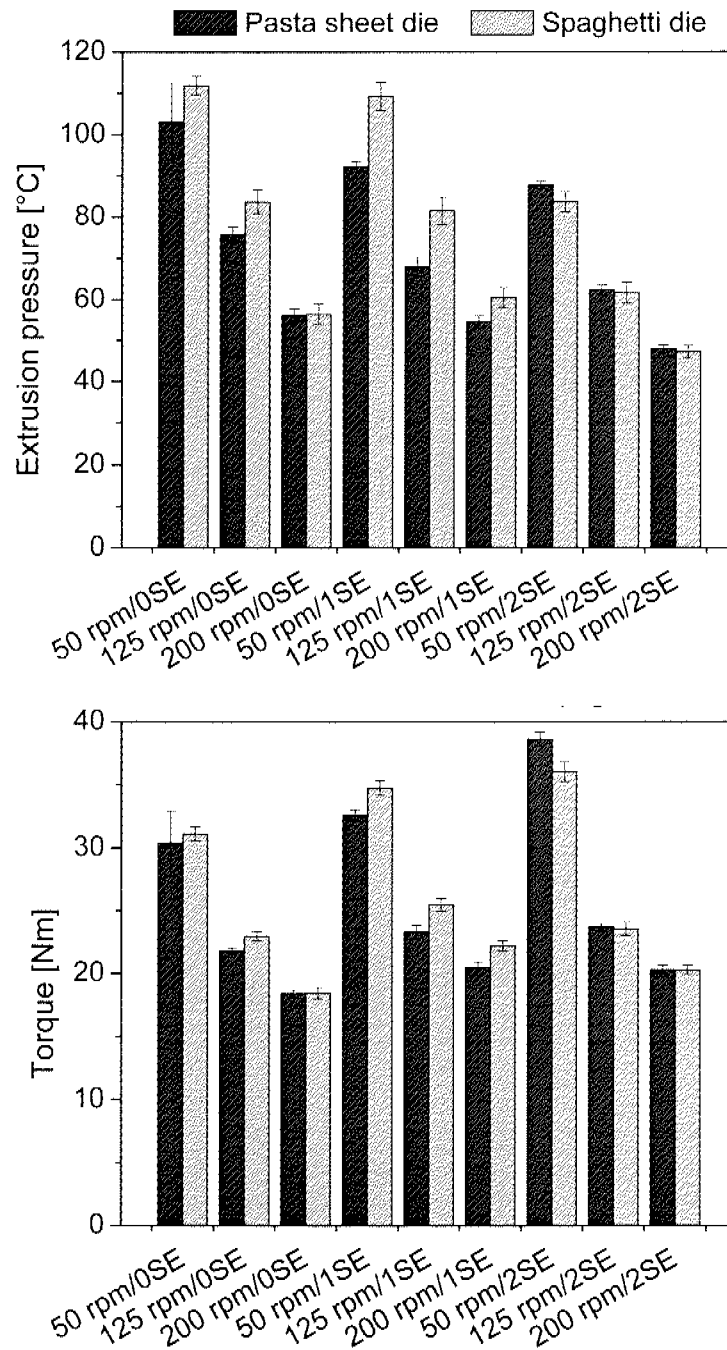


Figure 2.6: Pressure and torque in the extrusion of pasta dough into sheets and spaghetti shape in the twin-screw extruder at different screw speeds and configurations (Explanation of abbreviations in Table 2.1).

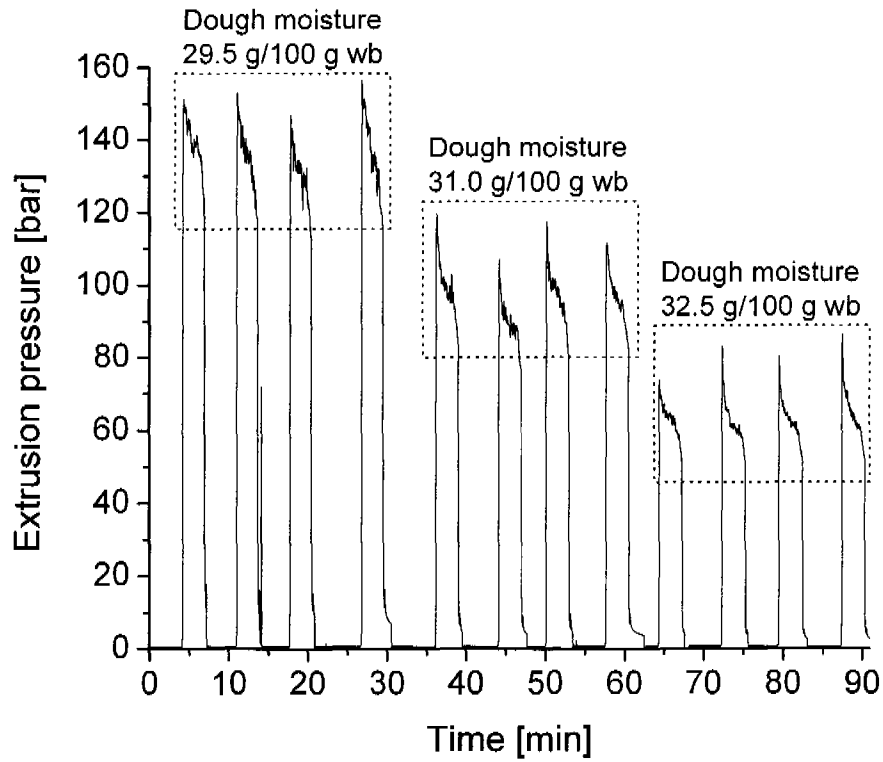


Figure 2.7: Pressure during the compaction and extrusion of moistened semolina in the cylinder-plunger system at three different dough moisture levels. The sharp drop of extrusion pressure to zero corresponds to the exchange of the brass pipes containing the moistened semolina.

2.3.2 Influence of extrusion conditions on the starch and protein fraction of durum wheat semolina

Changes in the thermal behavior of the starch fraction

The influence of process conditions, in particular the thermal energy input, on the starch fraction in pasta dough was characterized by DSC. Table 2.2 lists the DSC results for the pasta dough sheets that were extruded at different screw speed in the twin-screw extruder. The starch melting enthalpy for the samples extruded at 50 rpm was in the range of 3 J/g and decreased to approximately 2.2 J/g for the pasta extruded at 200 rpm, indicating that partial melting occurred during the latter extrusion conditions. Additional microscopic observations (not shown) confirmed the partial melting of the sample extruded at 200 rpm as the native birefringence of the starch granules was lost partially in this sample.

Table 2.2: Influence of screw speed and resulting SME and temperature in twin-screw extrusion of pasta dough on the melting temperature T_{M1} and melting enthalpy of starch, measured by DSC at excess water conditions (80 g/100 g wb).

Screw speed / SME / temp. [1/min] / [kJ/kg] / [°C]	Starch melting		
	T_{M1} [°C]	Range [°C]	Enthalpy [J/g]
50 / 195 / 50	59.8	52.4 – 68.2	3.0
125 / 350 / 65	60.1	53.1 – 69.1	2.6
200 / 460 / 74	60.8	53.3 – 68.5	2.1

Changes in the solubility of the protein fraction

Figure 2.8 presents the protein solubility (AASP) of dough and pasta samples. The AASP of unprocessed freeze dried milled semolina in diluted acetic acid amounted to 65 g/100 g protein. This value was lower than the value of 71.4 g/100 g published by Dexter and Matsuo (1977). These authors performed two extraction runs what may have shifted the extractabilities to higher values. The mixing process to a water content of 31 g/100 g wb raised the AASP to 68 g/100 g protein. An increase of the AASP due to the mixing step was also observed by Dexter and Matuso (1977) and Icard-Vernière and Feillet (1999). It can be attributed to the hydration of endosperm proteins which are plasticized, gain mobility and change their native globular to a fibrillar conformation which in turn promotes extractability.

The glutenin macropolymer (GMP) wet weights of dough and pasta samples are summarized in Figure 2.9. The GMP wet weight of unprocessed semolina was 1.03 g, but with 0.22 g significantly lower in the freeze dried and milled semolina. Peighambardoust et al. (2005) also determined the GMP amount of hard wheat flour and found a value of 1.3 g. However, they did not freeze dry and mill the sample prior to determination. The reason why hardly any GMP was found in semolina after freeze drying and milling is unclear. After mixing the semolina to a water content of 31 g/100 g wb, the GMP wet weight was 0.83 g. Don et al. (2003b) observed a decrease in GMP during the mixing process of bread dough and attributed it to the disintegration of the native and globular endosperm protein structure by work input during mixing.

As a consequence of the extrusion process of hydrated semolina, a clear trend towards decreased protein solubility in acetic acid was found (Figure 2.8). The decrease in protein solubility was smallest for the hydrated semolina compressed in the cylinder-plunger system (~67 g/100 g) followed by the pasta extruded in the single-screw extruder (~65 g/100 g) and the pasta after twin-screw extrusion (~60 g/100 g). Additionally, increasing screw speed and by this higher work input and dough temperatures during

twin-screw extrusion lowered AASP. However, at the same screw speed, pasta dough extruded with screw configurations containing shear elements exhibited no changes in the AASP. The GMP wet weight increased as a consequence of higher screw speed during extrusion in the twin-screw extruder (Figure 2.9).

In order to distinguish between the temperature influence on one hand and the combined effect of work input and heat on the other hand on protein solubility, incubation tests on hydrated semolina were performed to study the effect of heat exclusively. Figure 2.10 shows AASP and GMP wet weight of the hydrated and thermally treated semolina. The thermal influence on the protein denaturation and aggregation of semolina is detectable only at a temperature of 60 °C and at incubation times longer than 10 min. These simple tests state that the thermal effect on its own is not capable of inducing the changes in the protein solubility because the residence time in the extruder was shorter than 2 min. This means that heat is critical for the protein denaturation during pasta processing only in combination with mechanical work input caused by shear and elongational stresses during extrusion.

Lower AASP values and higher GMP wet weight are a measure for the extent of protein denaturation and aggregation of pasta dough proteins at increased levels of energy input during extrusion. No comparable literature was found for the evolution of protein solubility or GMP formation during pasta dough extrusion at different SME or temperature levels. For semolina treated in a twin-screw cooking extruder at a much lower water content of approximately 18 g/100 g wb, Ummadi et al. (1995) also observed a marked increase of insoluble proteins when barrel temperatures were raised from 50 to 96 °C. For bread dough, Weegels et al. (1994) showed that heat denaturation and aggregation of gluten at temperatures of 80 °C was pronounced at moisture contents higher than 20 g/100 g wb. They also detected this aggregation by the decreased SDS-extractability of the gluten proteins (higher GMP-amount). As the classical concept for GMP is based on the native endosperm protein structure in wheat its increase in extruded pasta dough can be interpreted as newly generated SDS-insoluble protein due to aggregation reactions of the endosperm proteins as a consequence of mechanical and thermal energy input during extrusion.

Compared to the drastic decrease of AASP during high-temperature drying of pasta (Figure 2.8), the degree of protein denaturation during extrusion is of a minor extent. During drying at 88 °C AASP dropped to a level of 25 g/100 g. Zweifel et al. (2003) showed that the decrease in AASP as a consequence of high-temperature drying was correlated positively with a more aggregated state of the protein matrix which promoted the cohesion in cooked pasta. In this context it has to be considered that low protein solubility in the dried pasta only contributes to the cohesion of pasta if the phase distribution of protein is homogeneous. Therefore, it is conceivable that a reduction of protein solubility already during mixing and extrusion at higher work input also goes along with phase separation of starch and protein.

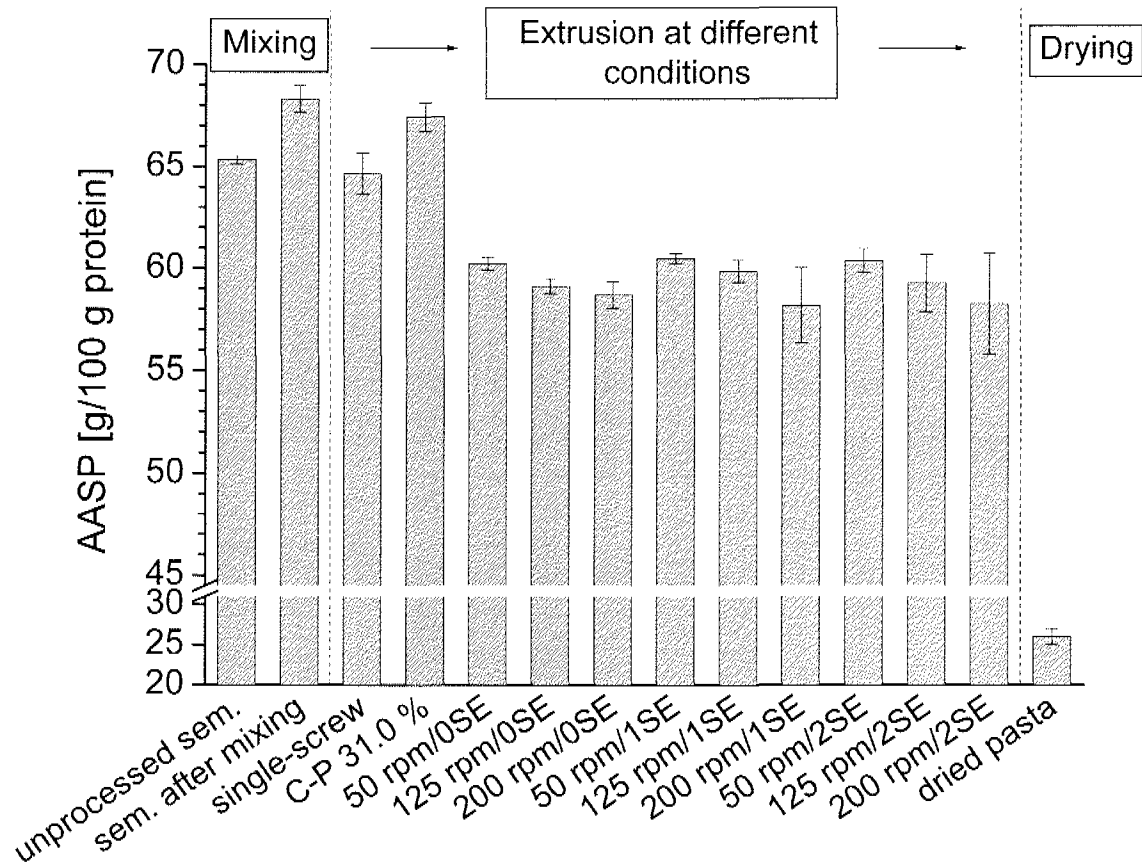


Figure 2.8: Evolution of the protein solubility in acetic acid (AASP) during pasta dough mixing, extrusion and drying (Explanation of the abbreviations in section 2.2.1).

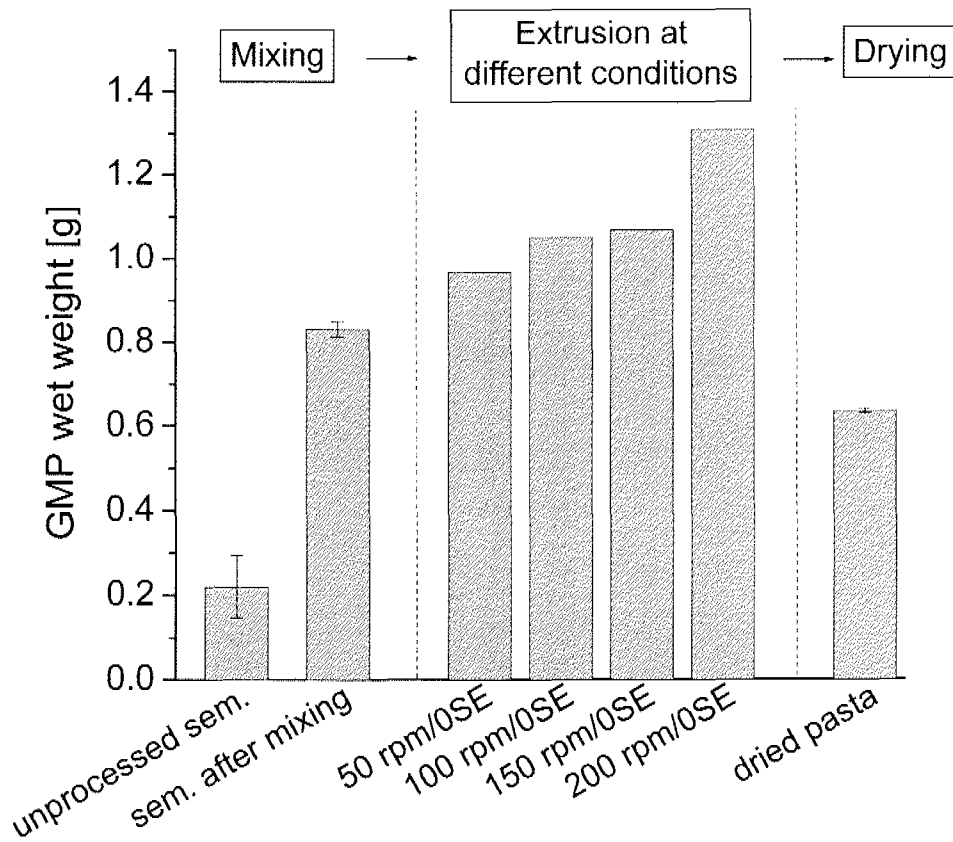


Figure 2.9: Evolution of the GMP wet weight as influenced by pasta dough mixing, extrusion and drying (Explanation of the abbreviations in section 2.2.1).

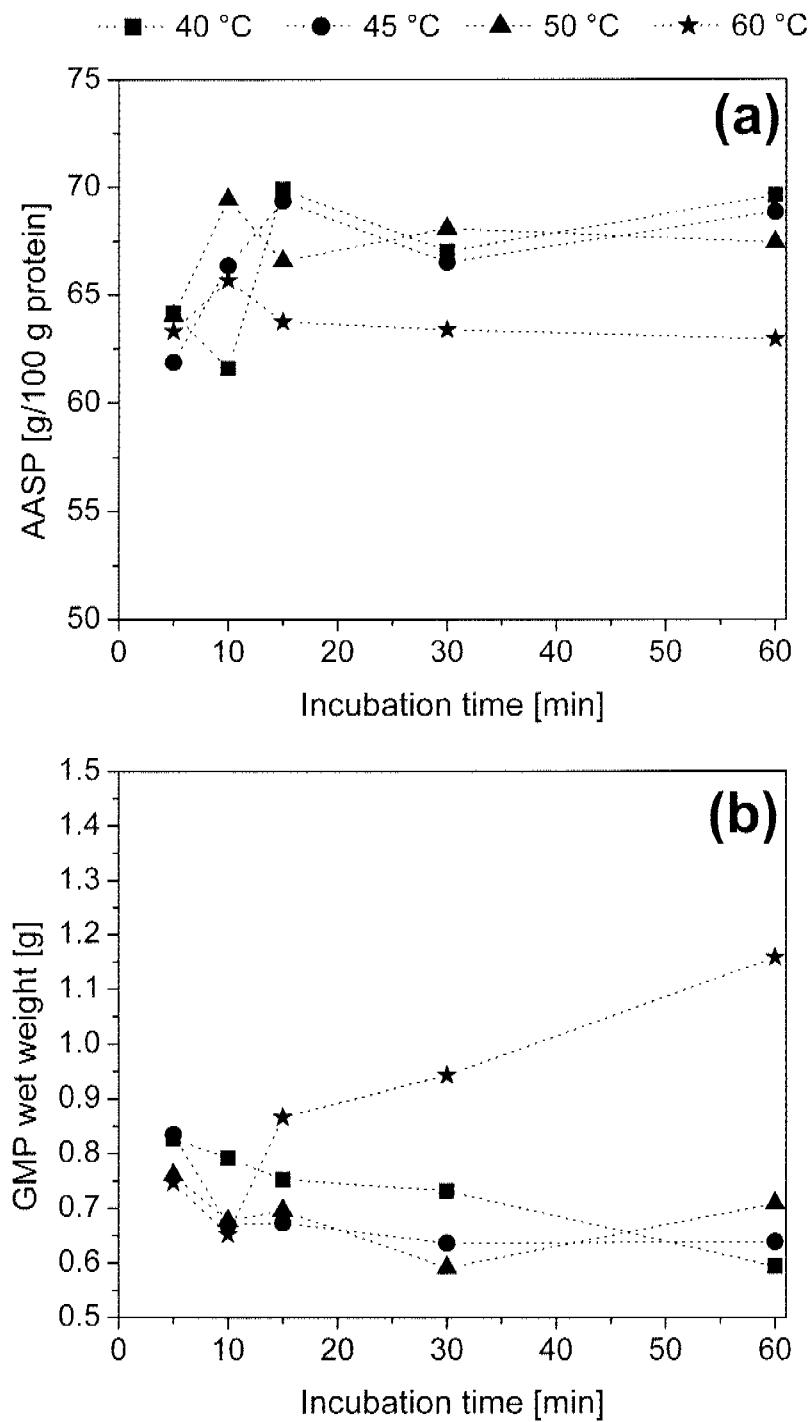


Figure 2.10: Influence of incubation time and temperature on the protein solubility (a) in acetic acid (AASP) and GMP wet weight (b) in hydrated semolina.

2.3.3 Influence of extrusion conditions on the microstructure of pasta dough and pasta

Figure 2.11 shows the microstructure of pasta dough extruded at different process conditions. Staining with rhodamine during the mixing process enabled the visualization of the protein matrix which appears in red. The protein network as continuous phase in which the starch granules act as a filler can be clearly seen. The pictures of extruded pasta dough also indicate that aggregation of the continuous protein phase of pasta occurs on the micrometer scale when extrusion conditions become more severe. The distribution of the protein matrix tends to be less homogenous in dough extruded at 150 rpm than in dough extruded at 75 rpm. The image of the sample extruded at 150 rpm suggests further increased aggregation of the proteins due to the higher mechanical and thermal energy input during extrusion.

The micrographs in Figure 2.12 point to the transformation of the microstructure of durum wheat endosperm resulting from different extrusion processes. Figure 2.12a shows the cellular organization of native durum wheat endosperm which is totally lost after the transformation to pasta as a result of the mechanical work input during the extrusion process in the single- and twin-screw extruder (Figure 2.12c and d). Figure 2.12b shows the microstructure of spaghetti that were compacted by the cylinder-plunger system. In contrast to the extruded spaghetti, the cellular structure of wheat endosperm was retained partially because of the lower mechanical stress during simple compressing and shaping of spaghetti in the cylinder-plunger system.

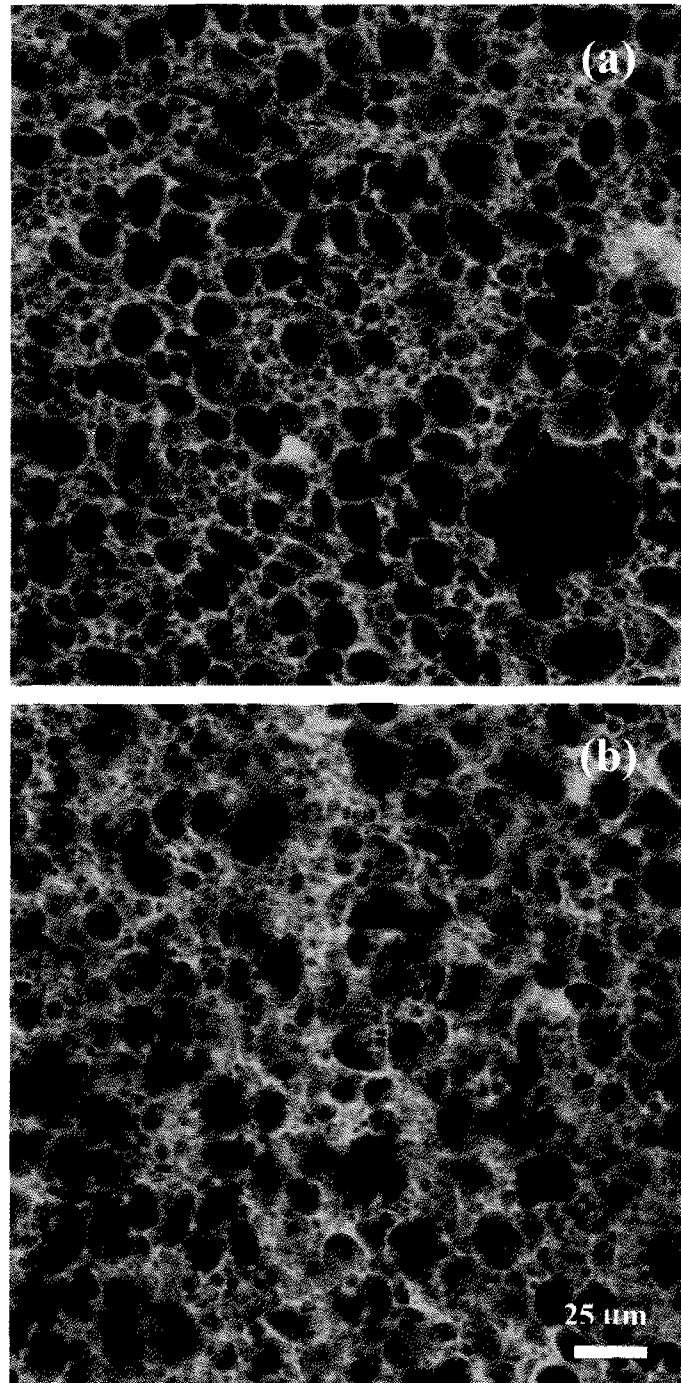


Figure 2.11: CSLM micrographs of the microstructure of extruded pasta resulting from different extrusion conditions. The protein phase is stained with rhodamine that had been added to the water used during mixing and is shown in red. (a) Dough extruded at 75 rpm (SME 109 kJ/kg and dough temp. 49.9 °C). (b) Dough extruded at 150 rpm (SME 179 kJ/kg and dough temp. 55.0 °C).

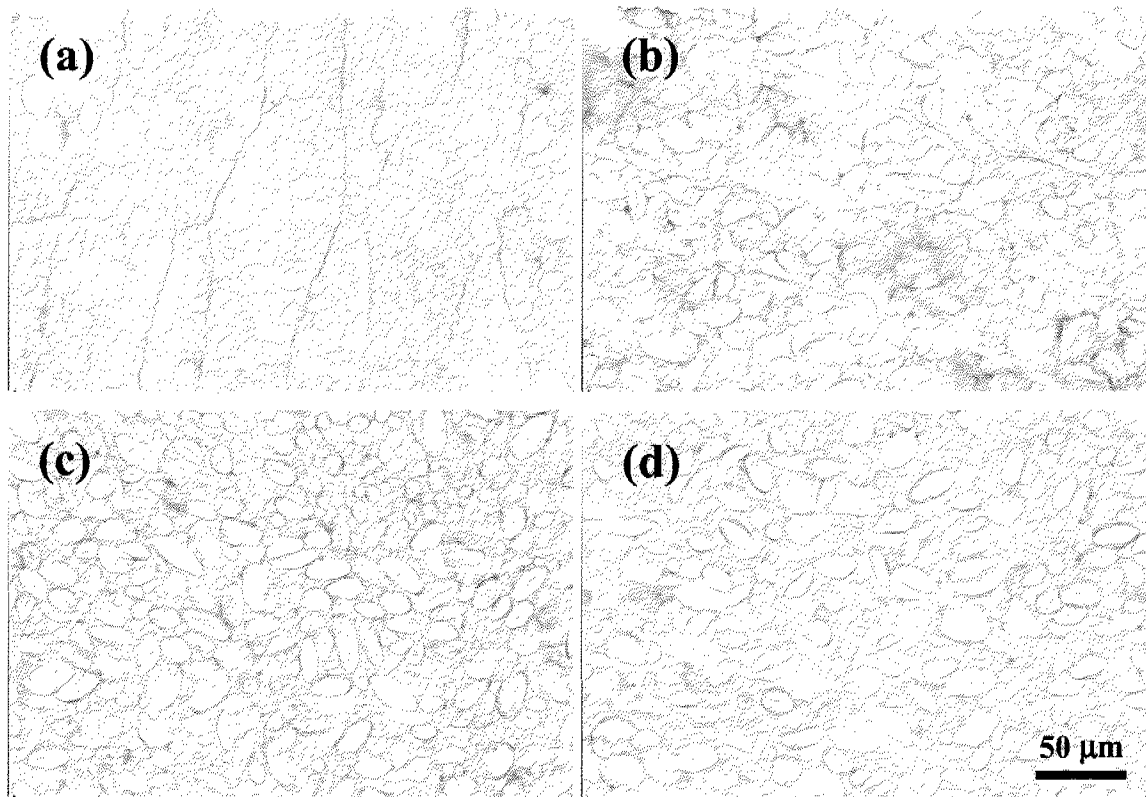


Figure 2.12: Bright-field micrographs showing the microstructure of durum wheat endosperm and of dried spaghetti produced at different extrusion processes. Sections were stained with ruthenium-red.

- (a) Microstructure of unprocessed durum wheat endosperm.
- (b) Sample extruded in the cylinder-plunger system at a dough water content of 31 g/100 g wb.
- (c) Spaghetti extruded in the single-screw extruder.
- (d) Representative spaghetti extruded in the twin-screw extruder.

2.3.4 Influence of extrusion conditions on the viscoelasticity of pasta dough

The response of the rheological properties of pasta dough to conditions during extrusion is shown in Table 2.3 and Figure 2.13 and Figure 2.14. Pasta dough extruded in the single-screw extruder was characterized by higher storage and loss moduli and higher $\tan \delta$ compared to pasta dough extruded in the twin-screw extruder. For the twin-screw extruder, increasing screw speed correlated with a decrease of storage modulus G' , a decrease in the phase angle $\tan \delta$ but an increase of the yield point. The yield point is a rheological property of pasta dough pointing to the shear stress at the end of linear viscoelastic behavior of the material. At constant screw speed G' , G'' and $\tan \delta$ also decreased with the introduction of shear elements into the screw configuration. Interestingly, the yield point of pasta dough was not affected by the use of one shear element in the screw but dropped significantly when two shear elements were used.

Rheological measurements are a valid tool to characterize the structure of pasta dough as affected by thermal and mechanical conditions during extrusion. According to Perressini et al. (2000), low G' values of pasta dough can be explained with fewer elastically effective cross links or entanglements. The more heat or SME was transferred into the dough during extrusion the more the elasticity (G') of the extruded dough decreased. Since the two parameters SME and dough temperature are both a function of screw speed it was not possible to separate the effects of thermal and mechanical energy input on dough properties.

As both, storage and loss moduli of pasta dough decreased with increasing screw speed and from single- to twin-screw extrusion the concurrent decrease in $\tan \delta$ corresponds to a more pronounced decrease of the loss modulus. This means that the viscous properties of pasta dough were affected to a higher extent by more severe extrusion conditions than the elastic properties. The gliadins are known to be responsible for the viscous flow properties of durum wheat dough (Edwards et al. 2003, Edwards et al. 2001) and it is conceivable that the gliadins were particularly affected in their structure by extrusion conditions at higher energy input.

Table 2.3: Rheological properties of pasta dough extruded in the single- and twin-screw extruder at different conditions.

Scr. speed / SME / temp. [1/min] / [kJ/kg] / [°C]	G' [Pa x 10 ⁵]	G'' [Pa x 10 ⁵]	tan δ [-]	Yield point [Pa]
single-screw:				
25 / n.d. / 40	10.7 ± 0.3	4.52 ± 0.1	0.422 ± 0.0092	430
twin-screw:				
50 / 191 / 50	8.6 ± 0.2	2.76 ± 0.1	0.323 ± 0.0018	501
125 / 342 / 63	7.9 ± 0.2	2.48 ± 0.1	0.313 ± 0.0017	631
200 / 463 / 74	5.2 ± 0.2	1.60 ± 0.1	0.310 ± 0.0008	1259
50 / 205 / 49	7.4 ± 0.3	2.35 ± 0.1	0.319 ± 0.0015	501
125 / 366 / 63	5.9 ± 0.2	1.78 ± 0.1	0.301 ± 0.0018	631
200 / 515 / 72	5.0 ± 0.1	1.51 ± 0.1	0.304 ± 0.0011	1260
50 / 243 / 52	6.2 ± 0.2	1.98 ± 0.2	0.317 ± 0.0031	251
125 / 373 / 65	5.2 ± 0.2	1.57 ± 0.2	0.300 ± 0.0017	501
200 / 510 / 77	4.2 ± 0.2	1.31 ± 0.4	0.308 ± 0.0076	631

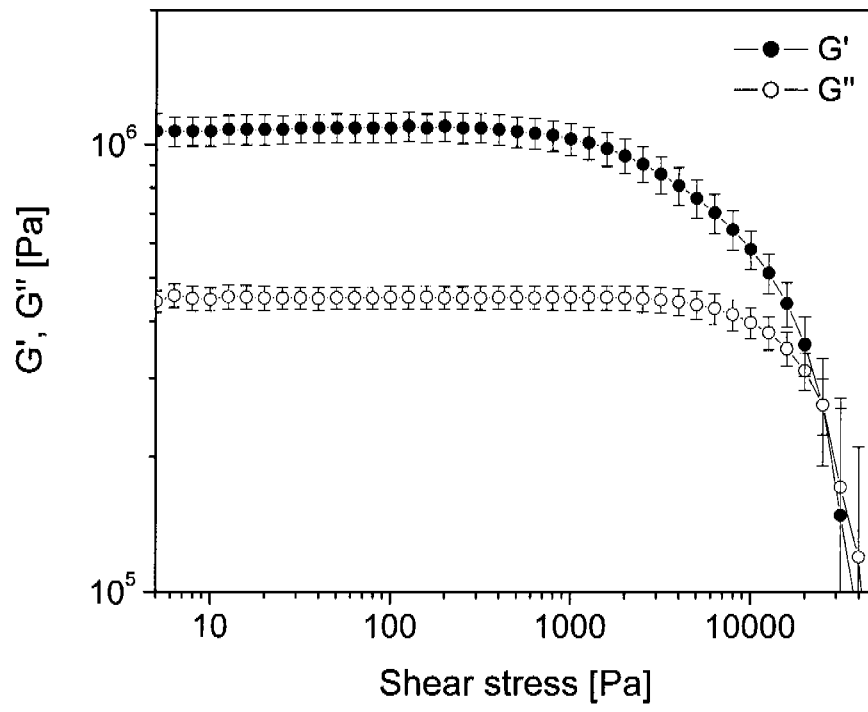


Figure 2.13: G' and G'' of pasta dough extruded in the single-screw extruder as measured in a stress sweep test at 25 °C.

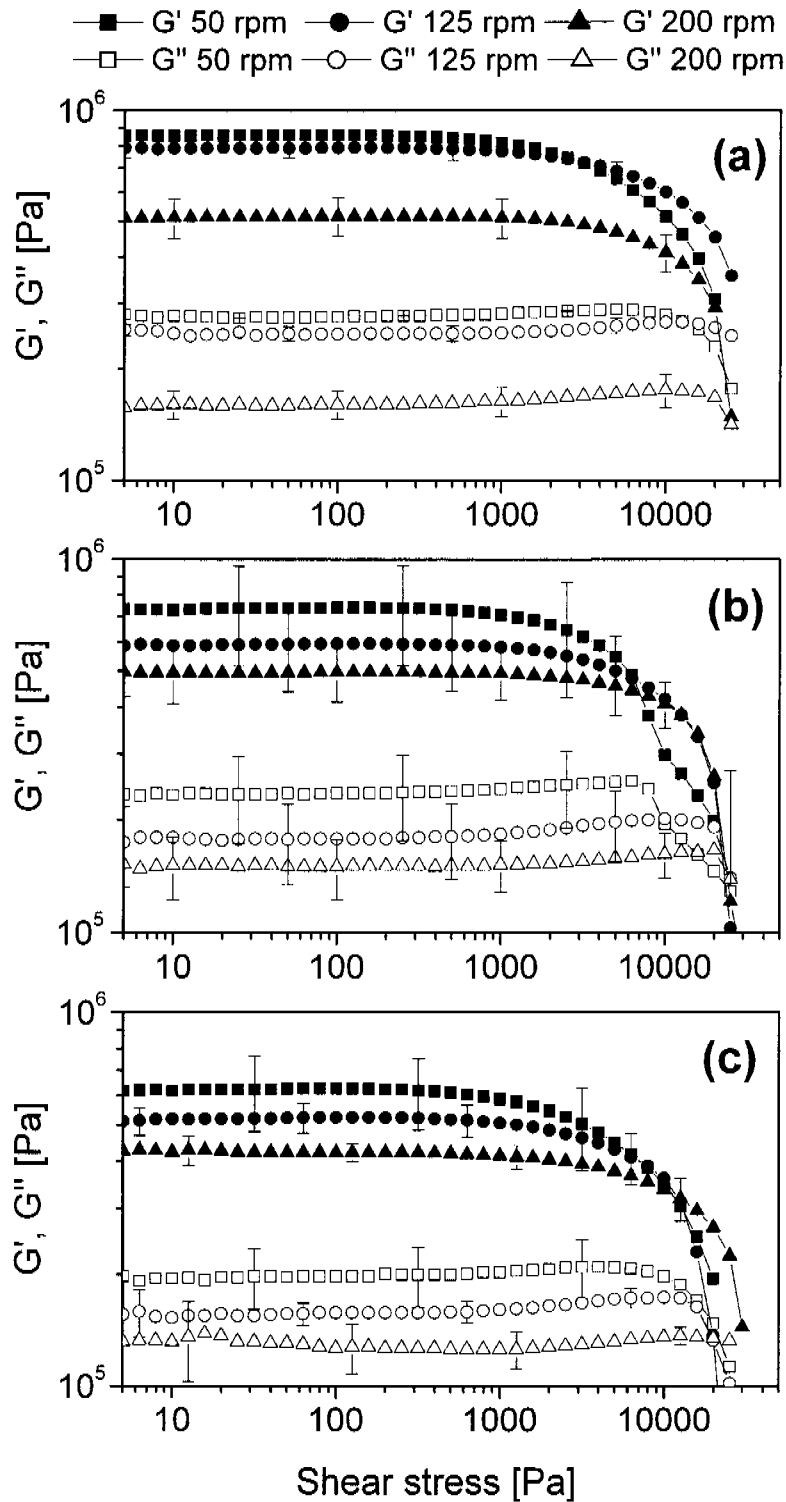


Figure 2.14: G' and G'' of pasta dough extruded in the twin-screw extruder as measured in a stress sweep test at 25 °C. Screw configuration during extrusion contained (a) no, (b) one, and (c) two shear elements.

2.3.5 Influence of extrusion conditions on the characteristics of dried and cooked pasta

Surface characteristics and breaking strength

The surface photographs of the dried pasta revealed distinct differences between the differently extruded samples (Figure 2.15). While the spaghetti produced in the single- and twin-screw extruder had a smooth surface and were free of white spots and strains (Figure 2.15a and b), the spaghetti that were pressed in the cylinder-plunger system had a lot of white spots and a rather rough surface which also felt rough upon touching it with fingers (Figure 2.15c, d and e). With increasing water content of the semolina, the number of white spots decreased slightly, but white spots were persistent even at a water content of 32.5 g/100 g wb.

The breaking strength of dried spaghetti was analyzed seven days after production (Figure 2.16). The breaking strength of the spaghetti produced in the single-screw pasta extruder was 3 N. All samples produced in the twin-screw extruder at different extrusion conditions had a breaking strength significantly higher between 3.2 and 3.9 N. There was the clear trend that pasta produced at 125 and 200 rpm had higher breaking strength than the spaghetti extruded at 50 rpm, but no influence of the shear elements was detected. The spaghetti that were extruded in the cylinder plunger system exhibited lowest breaking strength in the range of 2.5 N for all dough moistures tested.

The breaking strength is a measure for the homogeneity of the material and for the density and continuity of the protein network which gives pasta its cohesiveness (Zweifel 2001). The spaghetti compressed and extruded in the cylinder-plunger system presented white spots, strains and structural inhomogeneities and therefore the breaking resistance was lower, as the inhomogeneities might have acted like predetermined breaking points in the spaghetti structure. The higher breaking strength of the pasta produced by twin-screw extrusion may be due to the higher structural homogeneity (visible inhomogeneities were not absent). The higher energy input most probably contributed to

the disintegration of the cellular structure of the endosperm and to the formation of a more homogeneous and denser structure that maybe was also enhanced by the changed starch properties due to the partial melting of the starch at the high energy input levels.

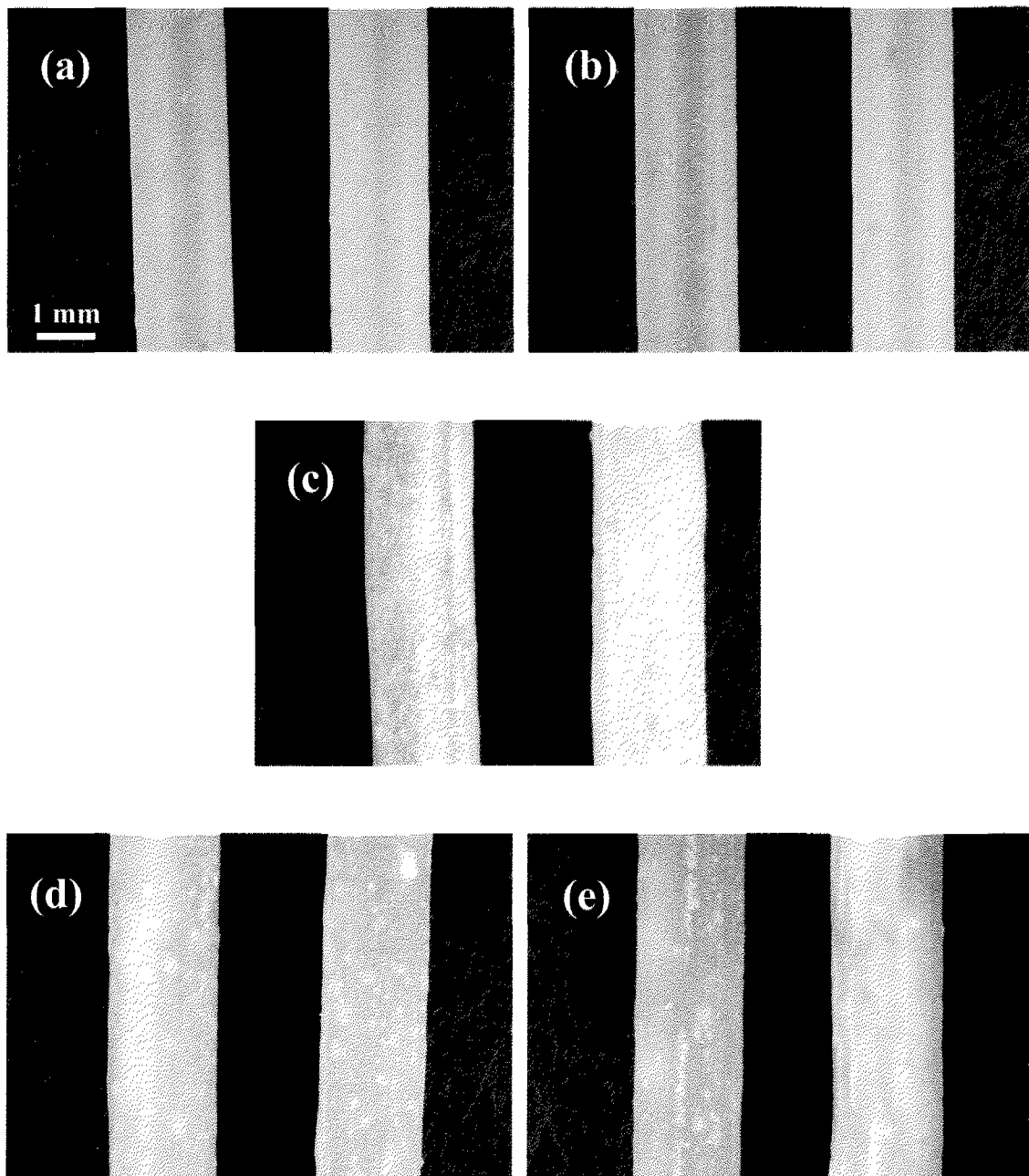


Figure 2.15: Surface photographs of differently extruded spaghetti after drying.

- (a) Spaghetti extruded in the single-screw extruder.
- (b) Representative spaghetti extruded in the twin-screw extruder.
- (c,d,e) Samples extruded in the cylinder-plunger system at pasta dough water contents of 29.5, 31.0, and 32.5 g/100 g wb, respectively.

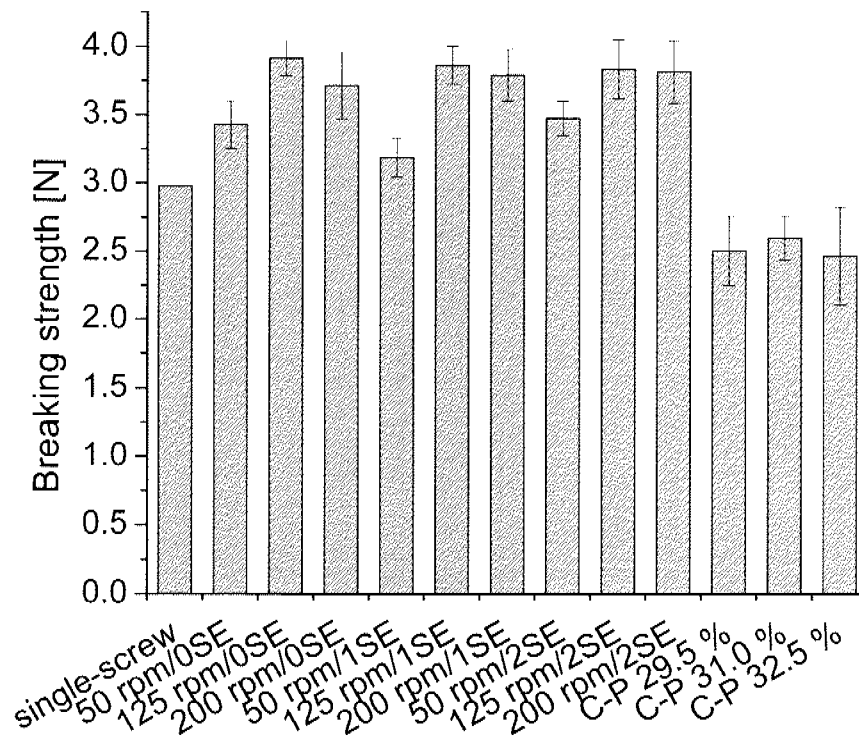


Figure 2.16: Breaking strength of differently extruded and dried spaghetti (Explanation of the abbreviations in section 2.2.1).

Cooking properties

The cooking behavior of pasta is directly linked to the structural properties of the pasta matrix and therefore also characterizing the impact of different extrusion conditions on pasta dough structure. Furthermore, the cooking behavior is an important criterion for the quality of pasta. The cooking properties of differently extruded and dried spaghetti were instrumentally assessed and the results are given in Figure 2.17. To ensure adequate comparability of the measured attributes, the optimal cooking time was analyzed and individually applied to each sample. The pasta extruded in the single-screw extruder, the spaghetti compacted in the cylinder-plunger system and the twin-screw extruded pasta at 50 rpm had optimal cooking times in a very narrow range between 10.6 and 11.5 min (Figure 2.17a). For the samples extruded in the twin-screw extruder the general trend was that cooking time decreased at higher screw speeds and with the use of shear elements. At 200 rpm and with two shear elements cooking time dropped to 9 min.

The diameter of cooked spaghetti is a measure for the swelling degree upon cooking (Figure 2.17b). The diameter of the dried pasta was in a narrow range between 1.59 (after single-screw extrusion), 1.73 (twin-screw extrusion) and 1.76-1.78 mm (cylinder-plunger extrusion). Despite these similar initial diameters, after cooking significantly higher diameters were detected for the spaghetti extruded in the cylinder-plunger system. The spaghetti that had been extruded in the twin-screw extruder had lower diameters, decreasing with higher screw speed. The results for the diameter correspond well to the results for the water uptake (Figure 2.17d); higher diameter concurred with higher water uptake. Especially the sample that was extruded in the single-screw extruder had a very high water uptake of approximately 245 g water/100 g db. Water uptake of the pasta extruded in the twin-screw extruder decreased at higher screw speed from approximately 205 to 175 g water/100 g db.

The cooking loss of pasta during cooking is shown in Figure 2.17c. Cooking loss was lowest for the sample after single-screw extrusion (approximately 5 g/100 g db) and slightly higher for the spaghetti that were extruded in the cylinder-plunger system (in the range of 6 g/100 g db). The spaghetti extruded in the twin-screw extruder exhibited the highest cooking losses between 7.5 and 15 g/100 g db, with the samples extruded at higher screw speed having the higher cooking loss.

Cooking loss during the cooking of pasta can arise from two sources. The leaching of polymeric material into the cooking water and the disintegration of the pasta strand during cooking, what results in the release of particles such as starch granules or integral pasta pieces into the cooking water. Due to the less homogeneous structure, the latter might have been the case for the pasta that was extruded in the cylinder-plunger system. For extruded pasta, several studies explained lower cooking losses of pasta after high-temperature drying as a result of a stronger protein network that gives higher cohesion to the pasta strand (Aktan and Khan 1992, Novaro et al. 1993, Zweifel et al. 2003). It is obvious that especially the samples that were extruded in the twin-screw extruder at higher energy input lack these cohesion properties due to a low continuity protein network. As parts of the proteins already have aggregated during the extrusion step, only a coarse protein network was formed and therefore was not available to give enough cohesion to the pasta during cooking. There is general agreement that denaturation reactions of the proteins occur when dough temperatures exceed critical values. Several authors also found dough temperature to be the most critical variable regarding the cooking loss of the end product. Abecassis et al. (1994) found dough temperatures of 71 °C at the die to cause very high cooking loss of the pasta sample (51.5 g/100 g db). Debbouz and Doetkott (1996) did not measure dough temperature directly but also concluded that barrel temperature had a very high influence on cooking loss and recommended a value of 45-53 °C which might correspond to dough temperatures below 60 °C.

Stickiness (Figure 2.17f) was closely related to cooking loss. Lowest stickiness was detected for the spaghetti that were extruded in the cylinder-plunger system (2-2.6 Ns). The spaghetti that were extruded by single-screw extrusion and those produced in the twin-screw extruder at a screw speed of 50 rpm had stickiness values around 3.5 Ns, while those extruded at increased screw speed (125 and 200 rpm) were the stickiest with values up to 8.5 Ns. According to Zweifel et al. (2001), stickiness arises from strongly swollen starch granules at the spaghetti surface, which are not sufficiently entrapped inside the pasta matrix. This was attributed to be a consequence of a missing or weak protein matrix. This finding is also applicable as explanation for the relatively high stickiness of the samples that were extruded at the high energy input levels during extrusion at 125 and 200 rpm. In contrast, the pasta that was compacted in the cylinder-plunger system had lower stickiness, as the partially conserved cellular organization might have impeded excessive leaching of starch at the surface of pasta. Furthermore, the starch fraction of the spaghetti that were extruded at elevated screw speed in the twin-screw extruder already showed partial melting after extrusion (Table 2.2). This disintegration of the starch granules and the concurrent phase separation of amylose and amylopectin already during extrusion might also have contributed to the higher stickiness and cooking losses of these samples.

The firmness of cooked spaghetti was assessed by a texture test performed with a tooth-like tool (Figure 2.17e). As there exists a marked moisture gradient in cooked pasta (Irie et al. 2004), the resulting force-deformation curves were evaluated for their maximum force as a measure for the internal firmness of the pasta strand. The relative depth of penetration at a force of 0.1 N was evaluated as a textural measure for the intermediate region between surface and center of the spaghetti strand. The firmness of the pasta produced in the single-screw extruder was 0.9 N. The spaghetti processed in the twin-screw extruder exhibited firmness values between 0.7 and 1.1 N, with the clear trend that samples that were extruded at higher screw speed had lower firmness. The spaghetti that were compressed in the cylinder-plunger system had firmness values between 0.8 and 0.95 N; higher firmness values were found for the spaghetti produced at lower water

content of the semolina. The relative depth of penetration was inversely correlated with the firmness of the spaghetti in the center; samples having high firmness values showed higher relative penetration depth (15-24 %). In other words, the texture of these samples was less firm in the region between the center and the surface of the pasta.

Firmness and relative depth of penetration are dependent to a great deal on the swelling degree and the water uptake of the pasta, but are also directly correlated to the structural cohesion properties of the pasta matrix. The cohesion of the pasta matrix is a function of starch swelling which is in turn dependent on the density and elastic strength of the protein matrix, able to withstand starch swelling. It is therefore consistent with all other cooking parameters tested that the samples that were extruded at higher work input, what resulted in less homogeneous protein matrices, had the lowest firmness values.

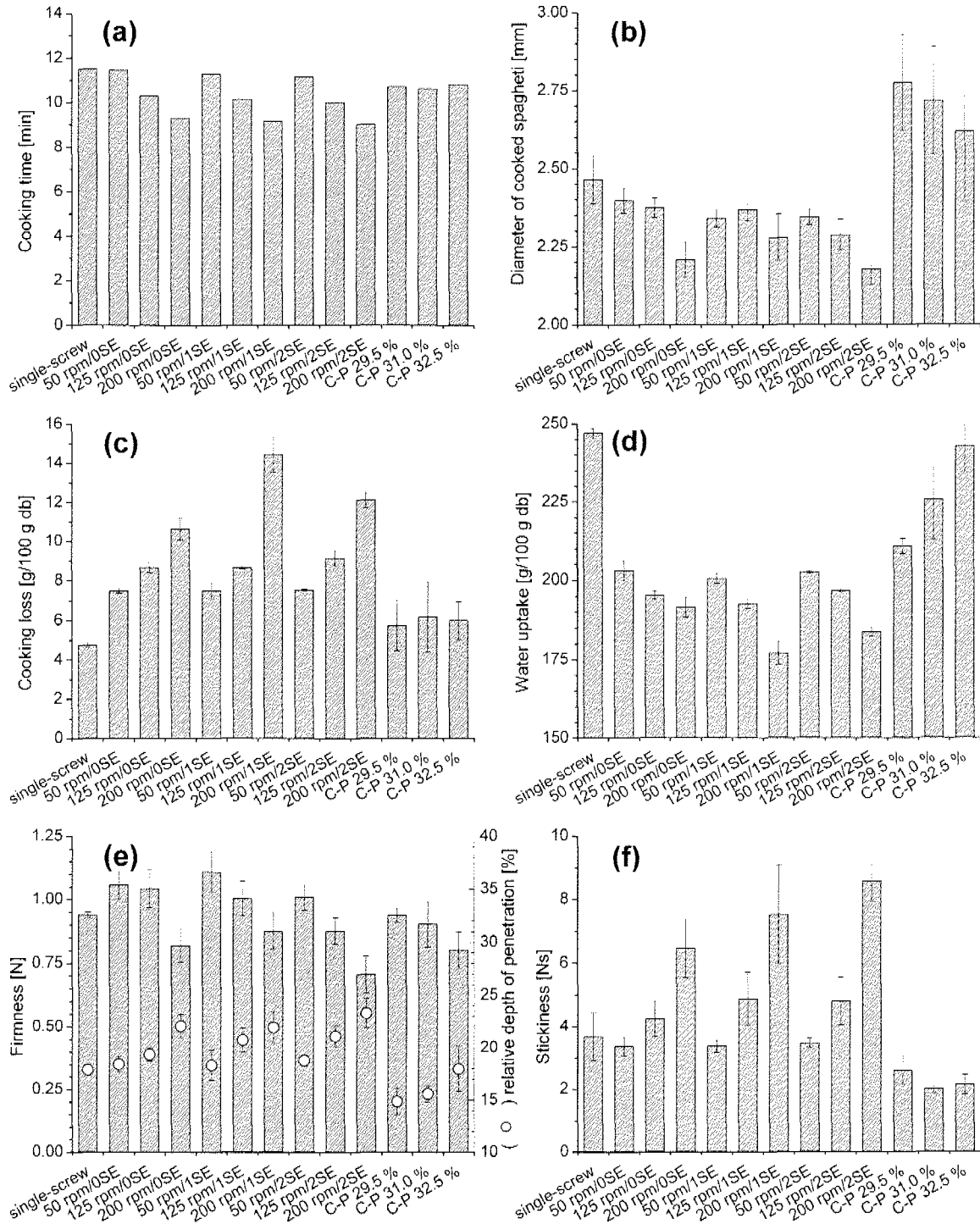


Figure 2.17: Cooking properties of differently extruded spaghetti after drying: (a) optimal cooking time, (b) diameter of the cooked spaghetti, (c) cooking loss, (d) water uptake, (e) firmness and relative depth of penetration and (f) stickiness (Explanation of the abbreviations in section 2.2.1).

2.4 Conclusions

The aim of the investigations described in this chapter was to study the impact of different extrusion methods and conditions on pasta dough properties and final pasta quality. The extrusion conditions as observed in the single- and twin-screw extruder and in the cylinder-plunger system differed mainly in the extent of mechanical energy (SME) transferred to the pasta dough during extrusion. As a consequence of higher SME up to 550 kJ/kg, dough temperatures were increased up to 76 °C with the following consequences.

At the molecular and supramolecular level, the extrusion of the hydrated semolina caused a decrease in the protein solubility in acetic acid and thus an increase of the insoluble glutenin macro polymer (GMP) fraction, depending on the mechanical work input. Incubation experiments revealed that not only the thermal effect was responsible for these denaturation/aggregation reactions of the proteins, but the combination of mechanical work input with the generated heat during extrusion lead to the observed changes in protein solubility. At severe extrusion conditions during twin-screw extrusion, the thermal behavior of the starch fraction was influenced as indicated by partial melting of the native crystalline structure of starch.

As shown at the microstructural level, a consequence of excessive work input during extrusion was phase separation of protein and starch resulting in a protein network of less continuity. On the other hand, simple compression of plasticized semolina in a cylinder-plunger model was shown to exert insufficient mechanical work input to homogenize the native cellular structure of durum wheat endosperm.

At the macroscopic or continuum level, the rheological properties of pasta dough after extrusion were directly linked to the work input during extrusion. Higher work input resulted in decreased storage- and loss moduli and lower phase angle of extruded pasta dough. These differences in the rheological properties indicate structural “softening” of pasta dough as a result of higher work input during extrusion.

Macroscopically, higher work input during extrusion caused the final pasta products to have different cooking properties. Higher stickiness and cooking loss but lower firmness were detected for pasta that was extruded at higher mechanical and thermal energy input. However, as a result of the higher work input during extrusion also the breaking strength was increased and the number of white spots and strains in the dried pasta was decreased. Simple compression of hydrated semolina in a cylinder-plunger model did not provide sufficient homogenization of the pasta dough matrix due to the low or missing mechanical stresses as present in an extruder. The consequences were white spots and strains and a rather rough pasta surface.

An optimal extrusion process for pasta dough should aim at the homogeneous compression of plasticized semolina without excessive work input so that protein solubility and viscoelastic properties are not reduced. But a minimal work input into the hydrated semolina is necessary in order to obtain an evenly developed pasta dough matrix with the proteins forming the continuous phase and a fine structured network. This in turn provides the proteins with a high “cross linking potential” during the successive high-temperature drying step resulting in durum wheat pasta with optimal cohesion upon cooking.

3 Water uptake and water vapor sorption of durum wheat semolina, wheat starch and gluten*

The hydration of durum wheat semolina, wheat starch and gluten with liquid water and water vapor was studied under dynamic and equilibrium conditions. After liquid water uptake, the finer particle size fractions of semolina generally had higher water contents than the coarser fractions due to their higher specific surface and different protein starch ratio which might have promoted swelling. When dry semolina was exposed to water vapor, no significant differences were found in equilibrium moisture contents between the particle size fractions, while semi-dry semolina reached higher equilibrium moisture contents at finer particle size. When exposing semolina and wheat starch to water at increasing temperatures a pronounced increase of liquid water uptake was observed at 47.5 °C. Hot stage microscopy and DSC experiments confirmed that this increase was due to the beginning of starch melting and swelling which started at 47.5 °C, provided that heating rates were low and water was available in excess. The results indicate that typical water contents of pasta dough (30-33 g/100 g wb) are below the swelling capacity of durum wheat semolina but are sufficient to meet the water vapor sorption capacity of semolina.

* This chapter has been prepared for publication as:

Kratzer, A., Escher, F., Conde-Petit, B. Liquid water uptake and water vapor sorption of durum wheat semolina, wheat starch and gluten.

3.1 Introduction

In durum wheat pasta processing, detailed knowledge on the kinetics of water uptake by semolina during conditioning, mixing and dough formation is of great importance. The hydration process typically aims at overall dough moisture contents of 30-33 g/100 g wb, to be achieved at process temperatures of approximately 25-40 °C (Antognelli 1980, Debbouz and Doetkott 1996, Manser 1981). The incorporated water acts as a plasticizer on the polymeric system of semolina and transforms it into a rubbery state (Cuq and Icard-Verniere 2001, Zeleznak and Hoseney 1987). Furthermore, water acts as a swelling agent for the biopolymers present in semolina while it is only a weak solvent for these polymers. There is general agreement that an even distribution of water throughout the semolina is a prerequisite for the production of sufficiently homogeneous pasta dough which then can be shaped by means of extrusion or sheeting. Additionally, evenly hydrated semolina particles are beneficial for the overall appearance of the dried pasta and especially for the prevention of excessive roughness and white spots and strains (Manser 1985).

In principle, hydration may take place via water vapor sorption or via liquid water. As for water vapor sorption there exist numerous studies on water vapor sorption of wheat products in general and durum wheat semolina in particular. However, none of the published work describes the experimental characterization of the water vapor sorption of durum wheat semolina at saturation, i.e. at water activity 1 or 100 % relative humidity which relates to the common water content of pasta dough. Bushuk and Winkler (1957) investigated the moisture sorption behavior of wheat flour, gluten and wheat starch at a water activity between 0.89 and 0.92 and temperatures between 20 and 50 °C and did not find a strong influence of temperature on the equilibrium moisture content (flour: 19.3-20.0, gluten: 20.0-20.5 and starch: 19.5-20.7 g/100 g wb). Shotton and Harb (1965) analyzed wheat starch at a water activity of 1 and found a water content of 21.9 g/100 g wb at 25 °C, and an increase to 23.7 g/100 g wb at 50 °C. Roman-Gutierrez et al. (2002) measured a higher water content for gluten than for starch at a water activity

of 0.95, i.e. 20.8 and 19.0 g/100 g wb, respectively. At the same water activity, these authors calculated the moisture distribution between the components of hard wheat flour and showed that gluten can incorporate a higher amount of water (14.2 % of total adsorbed water) than calculated on the basis of its mass proportion (12.9 g/100 g db of flour). Hébrard et al. (2003) investigated the water vapor sorption of different particle size fractions of durum wheat semolina and found equilibrium moisture contents in the range of 22 g/100 g wb at a water activity of 0.95. They reported higher equilibrium moisture contents for finer fractions (0-200 μm) than for coarser fractions ($> 200 \mu\text{m}$) and attributed this difference to geometric (higher specific surface) and biochemical (higher protein, pentosan and damaged starch content) properties of the finer fractions.

Virtually no data on the dynamics of uptake of liquid water are available for durum wheat semolina. One investigation compares the hydration kinetics of corn and durum wheat semolina by the use of a Baumann method (Mestres et al. 1990).

The objective of the present investigation was to determine and compare the liquid water and the water vapor uptake of durum wheat semolina, wheat starch and gluten, and to measure the influence of particle size and temperature on hydration kinetics. A classical desiccator method was used for water vapor sorption tests. Liquid water uptake was determined with a soaking/centrifugation method at excess water conditions and the dynamic Enslin method. The Enslin apparatus used is named after Otto Enslin who investigated the water uptake by capillary suction of non swellable clay fractions like silica or galena (Enslin 1933). The setup was used originally by Freundlich et al. (1931) who studied the swelling properties of bentonite, thus a swellable substance. Enslin (1933) proposed to use this apparatus to determine the swelling properties of swellable powders, the pore volume of non swellable powders, and the wettability of powders. Several researchers modified the Enslin apparatus. Among the modifications the Baumann apparatus is commonly known and was used for the determination of hydration rates of food powders (Elizalde et al. 1996).

3.2 Experimental

3.2.1 Samples

For all experiments, commercial durum wheat semolina was used (HWG-M, Swissmill, Zurich, Switzerland). According to the supplier's specifications, the durum wheat semolina consisted of a mixture of Canadian western amber durum wheat, U.S. amber durum wheat (45 % each) and European durum wheat (10 %). The protein content of the semolina analyzed by a standard Kjeldahl-method (protein content = $N \times 5.7$) amounted to $14.4 \pm 0.6\text{g}/100\text{ g db}$. The particle size distribution was measured by a sieve analysis on a sieve cascade (Retsch Vibrosieb, Retsch GmbH, Haan, Germany). The cascade was loaded with 100 g of semolina and sieving was carried out for 5 min at a shaking amplitude of 0.75 and the remainders on each of the sieves were determined gravimetrically. The used sieves test sieves according to ISO 565 (Haver & Boecker, Oelde, Germany) had mesh size openings of 600, 500, 400, 355, 315, 250, 200, 150, 125 and 100 μm and were not equipped with any sieving help device. The semolina was of a medium granulation (Figure 3.1) ranging from 0-500 μm and the main mass fraction was found to be between 250 and 315 μm (36.7 %).

In order to produce fractions of defined particle size, the durum wheat semolina was fractionated by using the sieve cascade with the same settings. The fractions were collected and stored in sealed plastic bags for further experiments.

The gluten sample used was "Aleuronat" (Blattmann Cerestar AG, Wädenswil, Switzerland) and had a protein content of 75 g/100 g db according to the supplier's specification. The wheat starch used was native wheat starch "C*Gel 20006" (Blattmann Cerestar AG).

The moisture content of samples was analyzed gravimetrically by drying 1-3 g of the samples in a drying oven (WTB Binder Labortechnik GmbH, Tuttlingen, Germany) at 133 °C for 90 min, at least in duplicate.

The protein content of samples was measured with a standard nitrogen analysis device (Dumas-method, protein content = $N \times 5.7$).

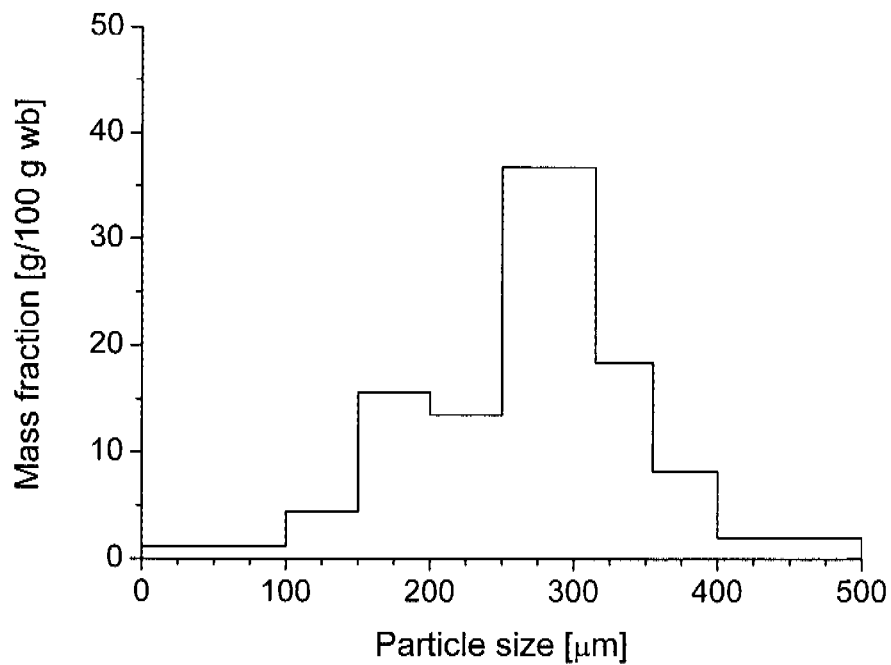


Figure 3.1: Particle size distribution of the durum wheat semolina as determined by sieve analysis.

3.2.2 Determination of water vapor sorption kinetics at high relative humidity

Water vapor sorption at high relative humidity was measured with the gravimetric desiccator method for four particle size fractions of durum wheat semolina, i.e. 100-150 μm and 400-500 μm as the two extremes and 250-315 μm and 315-355 μm as the main particle size of the semolina. The samples were adjusted above saturated NaCl solution (water activity ~ 0.75) for one week to a water content of approximately 15 g/100 g wb. 0.15 to 0.3 g (± 0.002 mg) of these samples were weighed into small weighing bottles and placed in desiccators above saturated salt solutions and pure water, respectively, in a temperature controlled cabinet at $25 \pm 0.5^\circ\text{C}$. The saturated salt solutions and their water activities at 25°C were KCl with 0.844, BaCl with 0.903 and K_2SO_4 with 0.973 (all salts at least analytical grade, Fluka, Buchs, Switzerland). Mass increase corresponding to the water vapor sorption was determined by weighing the weighing bottles periodically between 4 and 144 hr. Results are given as mean of two measurements.

3.2.3 Determination of water vapor sorption isotherms

Water vapor sorption was determined with a gravimetric desiccator method as described by Spiess and Wolf (1987). The samples were pre-dried in a vacuum chamber at room temperature for 16 hr. Approximately 0.25 g (± 0.002 mg) of the pre-dried samples were weighed into small glass weighing bottles and stored over P_2O_5 (Fluka, Buchs, Switzerland) for 24 hr in order to dry the material as extensively as possible. Thereafter, the weighing bottles containing the dry samples were placed in sorption glass jars (volume 1 L) above different saturated salt solutions in a temperature controlled cabinet at $25 \pm 0.5^\circ\text{C}$. The saturated salt solutions and their theoretical water activity at 25°C were LiCl with 0.113, MgCl_2 with 0.328, NaBr with 0.576, NaCl with 0.753, KCl with 0.844, BaCl with 0.903 and K_2SO_4 with 0.973 (all salts were at least of analytical grade, Fluka, Buchs, Switzerland). Additionally, samples were placed above pure water,

representing a water activity of 1. After an equilibration period of 72 hr, mass increase corresponding to the water vapor sorption was determined by weighing the bottles. The resulting water content was expressed as g/100 g wb and was determined at least in triplicate.

3.2.4 Determination of water holding capacity

The water holding capacity was determined by a modified Solvent Retention Capacity Method (SRC-Method, AACC-Method 56-11) for semi-dry material with a water content of 13.1, 5.5 and 11.9-13 g/100 g db of wheat starch, gluten and the semolina particle size fractions, respectively. 5 g (± 0.002 g) of the sample were suspended in 25 mL of distilled water in a pre-weighed 50 mL centrifuge tube and incubated for 20 min at controlled temperature between 25 and 60 °C in a water bath. The tubes were shaken vigorously every 5 min. Then the suspension was centrifuged at 1000 x g for 15 min and after discarding the supernatant and draining the tube for 10 min in upside down position, the remaining pellet was weighed and the mass increase was considered as the water uptake of the sample. Experiments were carried out in triplicate and the results were expressed as water content of the soaked sample (g/100 g wb).

3.2.5 Determination of water uptake by an automated Enslin method

An automated Enslin device as adapted by Arrigoni et al. (1987) and equipped with a heating/cooling jacket for temperature control was (Figure 3.2). Prior to any experiment, the water level in the reservoir (C) was leveled to the same height of the glass filter by opening the valve (B) and adding distilled water to the reservoir (C). When the first water droplets were visible on the glass filter, enough water was in the system. Then, the water flow was monitored by the balance and as soon as there was no further mass change, the valve was closed, and excess droplets on the glass filter were removed

carefully with tissue paper. With this equilibrated set up, the water uptake of semolina particle size fractions, wheat starch and gluten at semi-dry state (water content of 13.1, 5.5 and 11.9-13 g/100 g db for wheat starch, gluten and the semolina particle size fractions, respectively) was determined at temperatures between 20 and 50 °C. For each experiment 200 ± 3 mg (gluten) or 500 ± 3 mg (all other samples) were placed on the glass filter by using a glass funnel and spread to a layer with the help of a small plastic spatula. The measurement was started by opening the valve and the water uptake of the sample was recorded as weight loss in the water reservoir on the balance every 2 sec over a period of 15-20 min. The water uptake of the sample was expressed as g/100 g db of the sample and was determined at least in triplicate.

The bulk density of the semolina particle size fractions was determined gravimetrically by filling and weighing a small volume (5.81 cm^3) with loosely packed semolina (determination in triplicate).

3.2.6 Characterization of melting and swelling of wheat starch by differential scanning calorimetry (DSC) and hot stage microscopy

The native wheat starch was suspended in water at a water content of 70 g/100 g wb and from this suspension, approximately 20 mg were weighed into aluminum DSC pans (Perkin Elmer Ltd., Norwalk, USA). The DSC measurements were carried out on a 2920-DSC (TA Instruments Ltd., New Castle, USA) which had been calibrated with indium and an empty pan served as reference. The pans were heated at $1 \text{ }^\circ\text{C}/\text{min}$ from 20 to $70 \text{ }^\circ\text{C}$ with nitrogen flush ($40 \text{ cm}^3/\text{min}$). The recorded endothermic transition was evaluated for the onset (T_{OI}) and peak temperature (T_{M1}) by using the TA Instruments analysis software. The measurement was carried out in triplicate.

For the characterization of swelling and melting of wheat starch by hot stage microscopy, native wheat starch was suspended in water at a water content of

99.6 g/100 g wb. A droplet of this suspension was placed on a microscope slide and covered with a cover slip. The slide was mounted on a hot stage (Linkam LTS 350, Linkam, Waterford, UK), operated at a heating rate of 1 °C/min and observed under polarized light in an Axioplan photo microscope (Zeiss Ltd., Oberkochen, Germany). Video data was recorded by a 3CCD-Camera (Hamamatsu C5810, Hamamatsu Photonics, Hamamatsu-City, Japan). The effective temperature of the sample between the slide and the cover slip was measured by using a thin thermocouple.

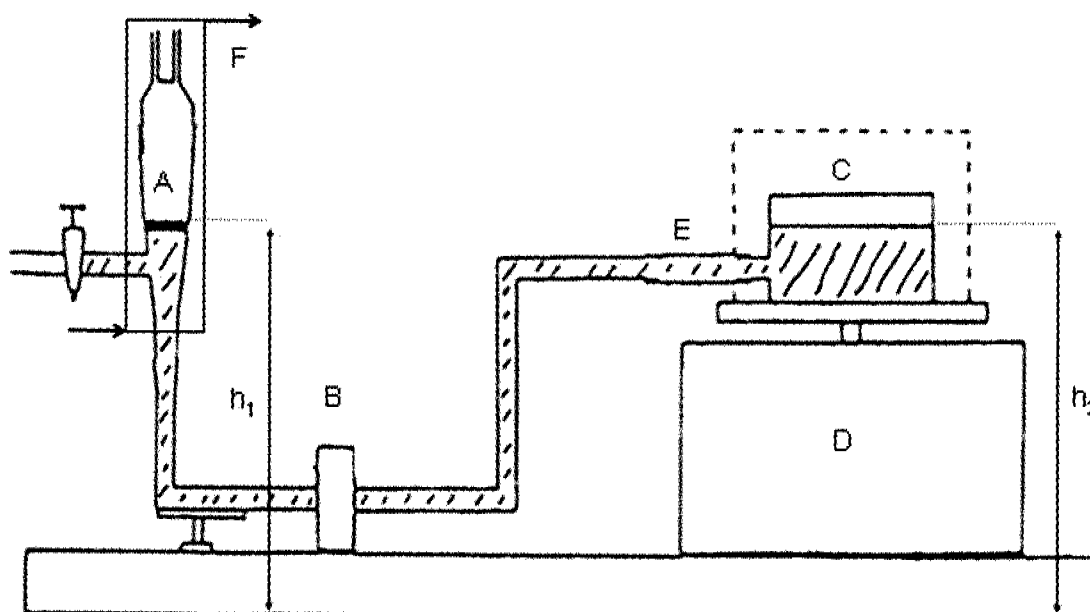


Figure 3.2: Automated Enslin setup for the determination of the water uptake (modified from Arrigoni et al. (1987)). A sintered glass filter (A) serves as the sample holder. The water reservoir (C) is positioned on a balance (D) (± 1 mg) and a flexible hose (E) ensures unimpaired functioning of the balance. The sintered glass filter (A) is temperature controlled by a heating/cooling jacket (F) that is connected to an external water bath. (A) and (C) are connected through a continuous water column, that may be disconnected by a magnetic valve (B). Calculations showed that the drop of the water level in the reservoir on the balance during the experiment is approximately 0.23 mm, when a sample size of 0.5 g of semolina is used. The height of the water level in the reservoir (h_2) was adjusted to the same height as the height of the glass filter (h_1) prior to every experiment.

3.3 Results and discussion

3.3.1 Water vapor sorption behavior of durum wheat semolina, wheat starch and gluten

The kinetics of the water vapor sorption of semi-moist durum wheat semolina fractions at high relative humidities were determined at water activities between 0.844 and 1 (Figure 3.3). The initial water content of the semolina fractions after preconditioning at a water activity of 0.75 was between 14.71 and 14.97 g/100 g wb. At all water activities and sorption times, the finer semolina fractions showed higher water contents than the coarser fractions, the difference being pronounced with increasing water activity. Equilibrium moisture contents were reached after 72 hr and did not change anymore significantly when the samples were stored up to 144 hr. At a water activity of 0.844, the semolina fractions reached equilibrium water contents between 19.5 and 20.4 g/100 g wb and at a water activity of 0.97 between 25.5 and 26.9 g/100 g wb. The equilibrium water contents of the samples at a water activity of 1 were the highest and ranged between 26.2 and 29.4 g/100 g wb. Only the finest fraction, 100-150 μm , showed a mass loss after 144 hr which was attributed to visible mould growth at this long sorption period.

Sorption isotherms of semolina, wheat starch and gluten are presented in Figure 3.4a and of different semolina particle size fractions in Figure 3.4b. All sorption isotherms showed a sigmoidal shape, typical for food products consisting to a large extent of biopolymers like starch and protein. While semolina and its particle size fractions exhibited a similar water sorption behavior over the whole range of water activities, wheat starch and gluten differed significantly from semolina. Up to a water activity of approximately 0.85, gluten reached lower equilibrium moisture contents than semolina. Wheat starch showed a more hygroscopic behavior than semolina as reflected in the higher moisture contents. But at higher water activity (> 0.85), gluten and to a lesser extent also semolina incorporated more water than wheat starch. At a water activity of 1, an equilibrium water content of 31.2 ± 0.7 g/100 g wb was detected for gluten whereas

semolina and wheat starch contained less water (28.3 ± 0.5 and 26.0 ± 1.3 g/100 g wb, respectively).

The water vapor sorption experiments revealed that the equilibrium moisture content of semolina at a water activity of 1 was between 26.2 and 29.4 g/100 g wb, depending on particle size and initial water content. These values indicate that the saturation water content of semolina with water vapor is just slightly lower than the common water content in pasta processing (30-33 g/100 g wb). This means that the water concentration in pasta dough is sufficient to saturate the dough with water if it is assumed that the water is distributed evenly among and inside all semolina particles. In contrast to the sorption experiments with initially semi-dry material (Figure 3.3), for initially dry material (Figure 3.4b), no significant influence of the semolina particle size on the equilibrium moisture content was detected although the protein content of the semolina particle size fractions was higher for the finer granulated semolina and ranged between 12.9 and 16.5 g/100 g db (Figure 3.5). However, Hébrard et al. (2003) also measured sorption isotherms for initially dry semolina particle size fractions and detected faster water vapor uptake and higher equilibrium moisture contents for the finer granulated semolina. While higher equilibrium moisture content was attributed to compositional differences, geometric effects (higher specific surface) were regarded as responsible for the faster kinetics.

At high water activity, where water might be incorporated into intermolecular free spaces by capillary condensation, it is conceivable that phenomena like partial swelling of the material become predominant. This seems to be the case for gluten, for which at high water activities a marked increase of water vapor sorption capacity as compared to native wheat starch or semolina was found. This is also in accordance with the measurements of Roman-Gutierrez et al. (2002), who detected higher water contents for gluten than for starch at a water activity of 0.95 (20.8 and 19.0 g/100 g wb, respectively). At the same water activity, these authors calculated the moisture distribution between the hard wheat flour components and showed that gluten adsorbed a higher amount of water (14.2 % of total adsorbed water) compared to its mass proportion (12.9 g/100 g db of flour).

Durum wheat semolina generally showed a water vapor sorption pattern between gluten and wheat starch. The calculated combination of water vapor sorption of starch and protein according to their mass fraction agrees well with the sorption behavior of semolina (Figure 3.6). This indicates that these two fractions are mainly determining the sorption behavior of the material. It also shows that as long as the material is only brought into contact with water vapor, the isolation processes for starch and the native wheat proteins (transformation to gluten) does not alter the water vapor sorption properties to a large extent. The results also indicate that the microstructural organization of starch and protein in plant cells (semolina) or in a free form (isolated starch and gluten) has only little impact on the interaction of the material with water vapor in equilibrium.

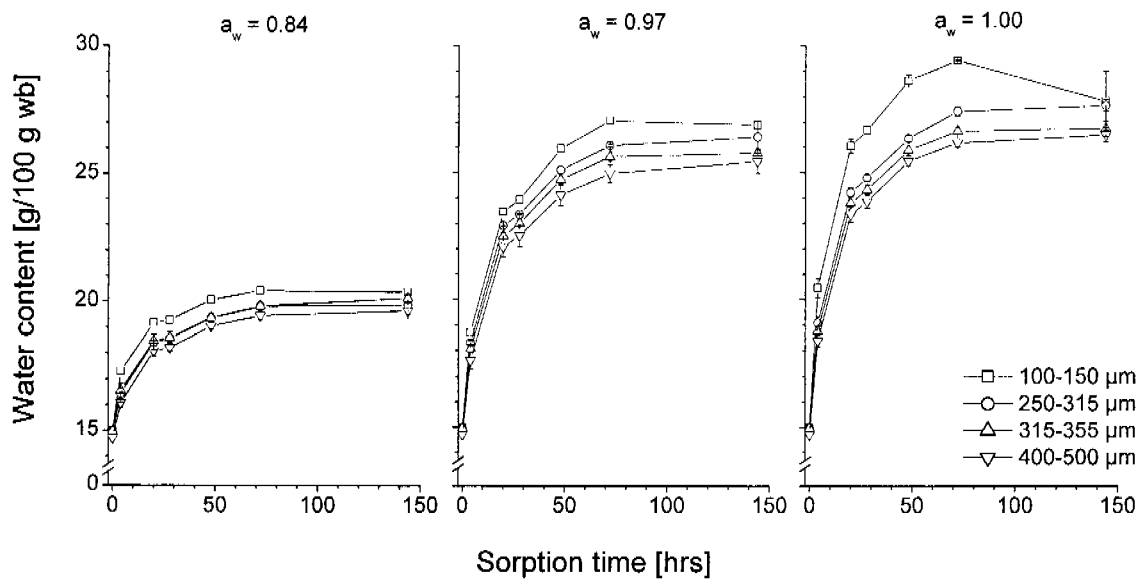


Figure 3.3: Water vapor sorption kinetics of semolina particle size fractions at different water activities at 25 °C (initially semi-dry material).

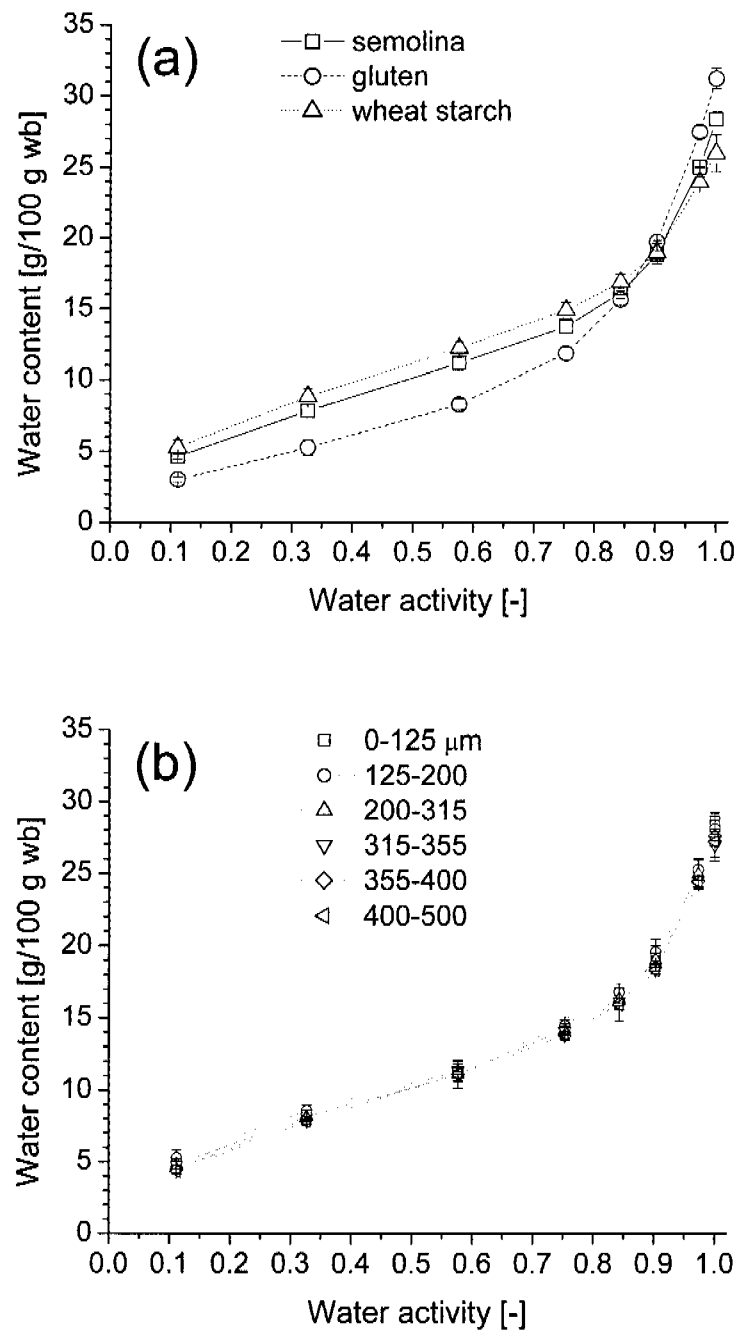


Figure 3.4: Sorption isotherms of durum wheat semolina gluten and native wheat starch, all initially semi-dry (a) and initially dry semolina particle size fractions (b) at 25 °C.

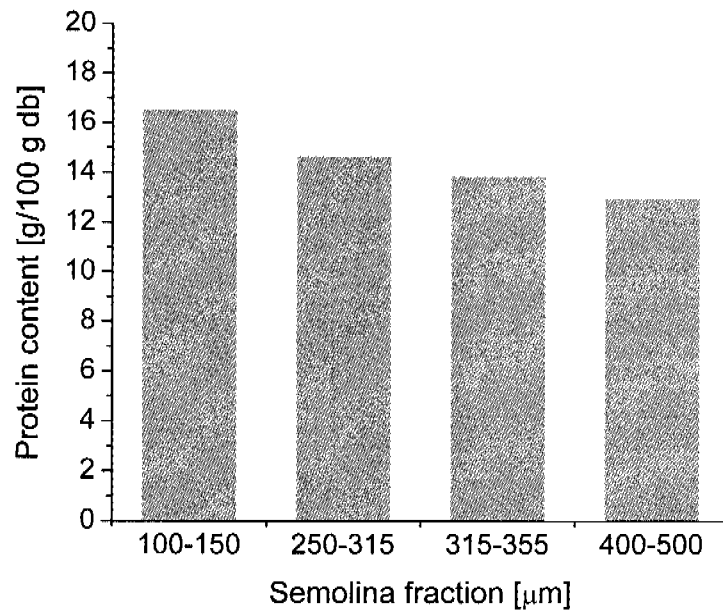


Figure 3.5: Protein content of semolina particle size fractions.

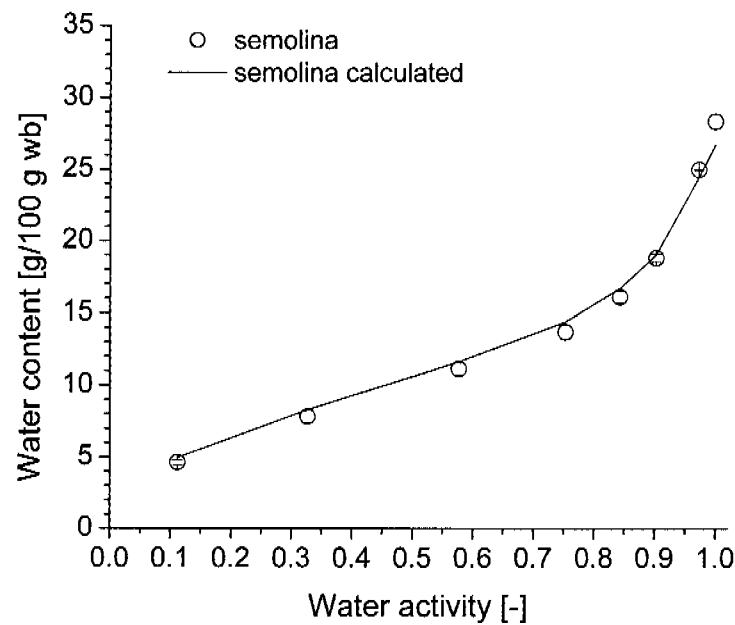


Figure 3.6: Sorption isotherm of durum wheat semolina and the sorption isotherm of durum wheat semolina as calculated from the sorption of gluten and native wheat starch (calculation basis: 14.4 % db gluten and 83 % db starch) at 25 °C.

3.3.2 Water holding capacity of durum wheat semolina, wheat starch and gluten

Figure 3.7a shows the water holding capacity of semolina, wheat starch and gluten at temperatures between 25 and 60 °C. Between 25 and 40 °C, starch was able to hold approximately 48 g/100 g wb. At 45 °C, a slight increase to 51 g/100 g wb was detected. Further temperature rise to 50 and 55 °C resulted in a marked increase of the water uptake (57 and 75 g/100 g wb, respectively). The highest water uptake of wheat starch was detected at a temperature of 60 °C (82 g/100 g wb). Compared to wheat starch, gluten showed a different water uptake pattern, characterized by relatively low temperature dependence and a rather high water uptake capacity between 65 and 71 g/100 g wb. Up to temperatures of 50 °C, gluten exhibited higher water uptake than starch but between 50 and 55 °C, the situation changed due to the excessive swelling of starch. Interestingly, the water uptake behavior of semolina was similar to wheat starch up to temperatures of 50 °C. Above 50 °C, semolina did not exhibit the excessive swelling as detected for isolated wheat starch. This might be due to the native microstructure of semolina, where the starch granules are still embedded in the native and dense structure of the endosperm cells and therefore do not have that much free volume for swelling compared to isolated starch granules.

The water uptake of the semolina particle size fractions at temperatures between 25 and 60 °C as determined by the centrifugation method is shown in Figure 3.7b. Generally, the finer particle size fractions showed higher water uptake than the coarser granulated fractions. The lower water uptake of the coarser fractions compared to the fine semolina might be a consequence of the higher specific surface area of the smaller semolina particles. This higher specific surface is likely to promote swelling phenomena of starch and protein as there is more free volume for swelling of the material at its surface. Besides this geometric effect there are biochemical differences between the semolina fractions too. According to Hébrard et al. (2003), finer granulated semolina fractions have higher protein, pentosan and damaged starch contents which also contribute to a higher water uptake.

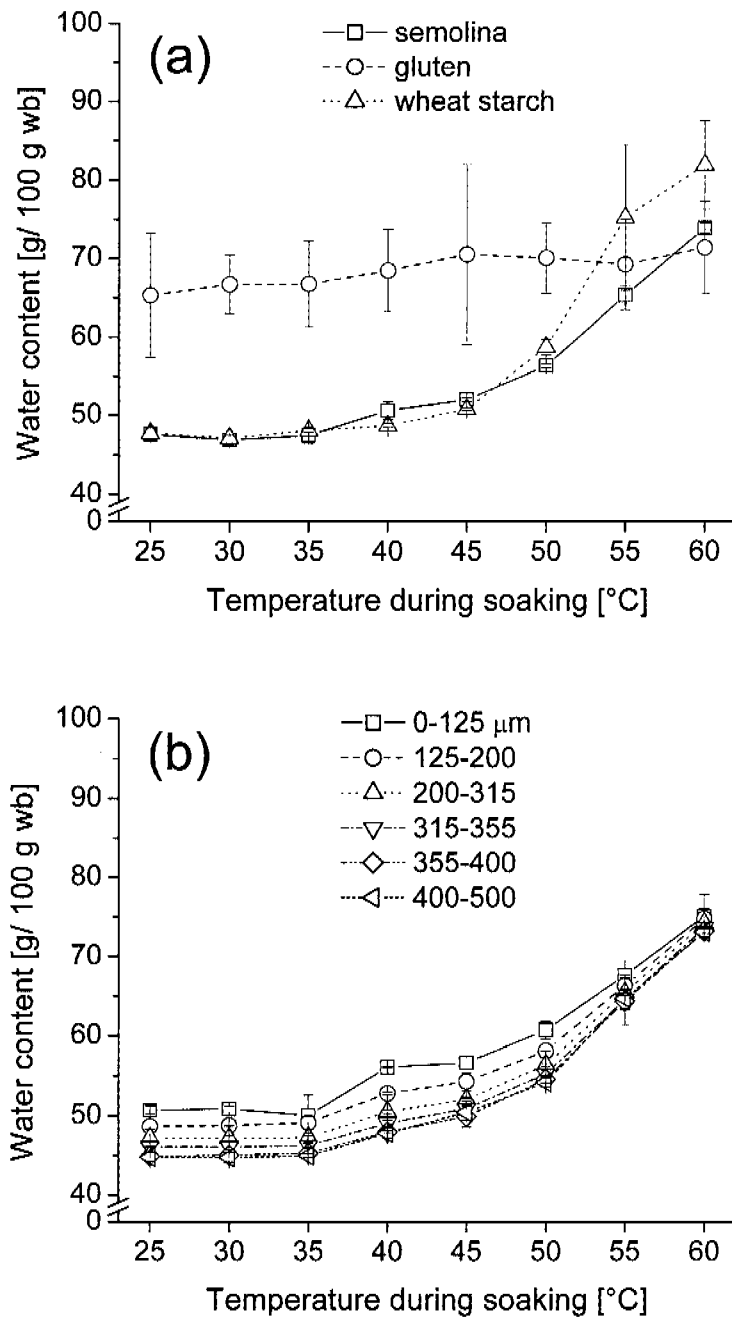


Figure 3.7: Liquid water holding capacities of durum wheat semolina, gluten and wheat starch (a) and semolina particle size fractions (b) at temperatures between 25 and 60 °C.

3.3.3 Dynamics of water uptake of gluten and wheat starch

Figure 3.8a shows the dynamics of liquid water uptake of micropiles of wheat starch and gluten as assessed by the Enslin at temperatures between 20 and 50 °C. At 20 °C, the water uptake of wheat starch reached approximately 70 g/100 g db within the first 3 min of the experiment. An increase of temperature to 30 °C also shifted the water uptake in equilibrium to approximately 80 g/100 g db, but the water uptake at equilibrium conditions was not affected significantly by further temperature increase up to 45 °C. At temperatures of 47.5 and especially at 50 °C, a marked increase in the water uptake was detected (~110 and 140 g/100 g db). Besides this increase, also the time for reaching equilibrium conditions was in the range of 20 min, compared to approximately less than 3 min for temperatures lower than 47.5 °C.

Figure 3.8b presents the results for the water uptake of gluten. In general, the reproducibility of these determinations was very poor and the water uptake in equilibrium was between 70 and 120 g/100 g db at the investigated temperatures. The highest water uptake was detected at 50 °C but the results for the lower temperatures were inconsistent; for instance the amount of imbibed water at 20 °C was higher than at 30 or 40 °C. The poor reproducibility was attributed to the formation of a gluten-gel, which acted as a barrier for further water transport. This gluten-gel was formed immediately on the sintered glass filter by the gluten powder that was in direct contact with the glass filter. Even after 20 min, the top layer of the gluten micropile was not hydrated due to this effect. According to this observation, a gel of moistened gluten can be considered as an effective water barrier, despite the high water vapor sorption affinity of gluten at high water activities.

Figure 3.9 compares the water uptake of wheat starch determined by the centrifugation method to the values obtained by the Enslin method. Generally, the values are in good agreement. However, higher water uptake of wheat starch (~10 g/100 g db) was detected with the centrifugation method at 45 °C, which could be explained by the longer contact

of water and starch during the centrifugation method (35 min incl. centrifugation compared to 20 min during the Enslin method). At 50 °C the situation was different, then the water uptake amount as determined with the Enslin method was higher (~10 g/100 g db) but in general the differences between the two methods were small. This means that the bulk density of the hydrated starch in the Enslin set up was very similar to the density after centrifugating the hydrated starch at 1000 x g for 15 min.

The pronounced increase of the water uptake of wheat starch at temperatures of 47.5 °C and above was attributed to the beginning melting and swelling of starch. In order to find out whether melting in the starch granules occurs at temperatures below 50 °C, DSC and hot stage microscopy of wheat starch dispersions were performed at a low heating rate of 1 °C/min, as the Enslin experiment is a slow process too. The DSC thermogram showed an onset temperature (T_{O1}) for the beginning of starch melting at 47.5 ± 0.5 °C and a peak maximum (T_{M1}) at 52.5 ± 0.8 °C (Figure 3.10). Therefore, the onset of starch melting at 47.5 °C is in good accordance with the results of the measurements of the water uptake as analyzed with the Enslin method. These temperatures are fairly lower than those measured by other authors. Zweifel et al. (2000) reported a T_{O1} of approximately 50 °C and a T_{M1} of approximately 60 °C of durum wheat semolina (heating rate of 4 °C/min). This shows that starch melting is a time dependent transition. To answer the question whether the onset temperature of 47.5 °C for the swelling of wheat starch is detectable in the micrometer range, the heating of a starch dispersion was observed under polarized light on a hot stage microscope. The micrographs in Figure 3.10 show that no loss in birefringence is detectable at temperatures between 30 and 45 °C but at 47.5 and especially at 50 °C the first loss in birefringence is already visible. A slight swelling can also be observed, characterized by the small increase in size of some starch granules. At 55 °C, nearly all granules loose their birefringence and swelling advances until 60 °C, where all granules have lost their birefringence. To conclude, the beginning of starch melting and swelling at high water availability and during long time (low heating rate of 1 °C/min for DSC and microscopy, 20 min for water uptake measurements) already occurs at a temperature of 47.5 °C. At this temperature, wheat

starch was able to take up 30 g more water per 100 g db than at 30-45 °C. This pronounced increase in water uptake at 47.5 °C was also accompanied with a partial loss of birefringence and the beginning of starch melting was also detected by DSC (T_{01} 47.5 °C).

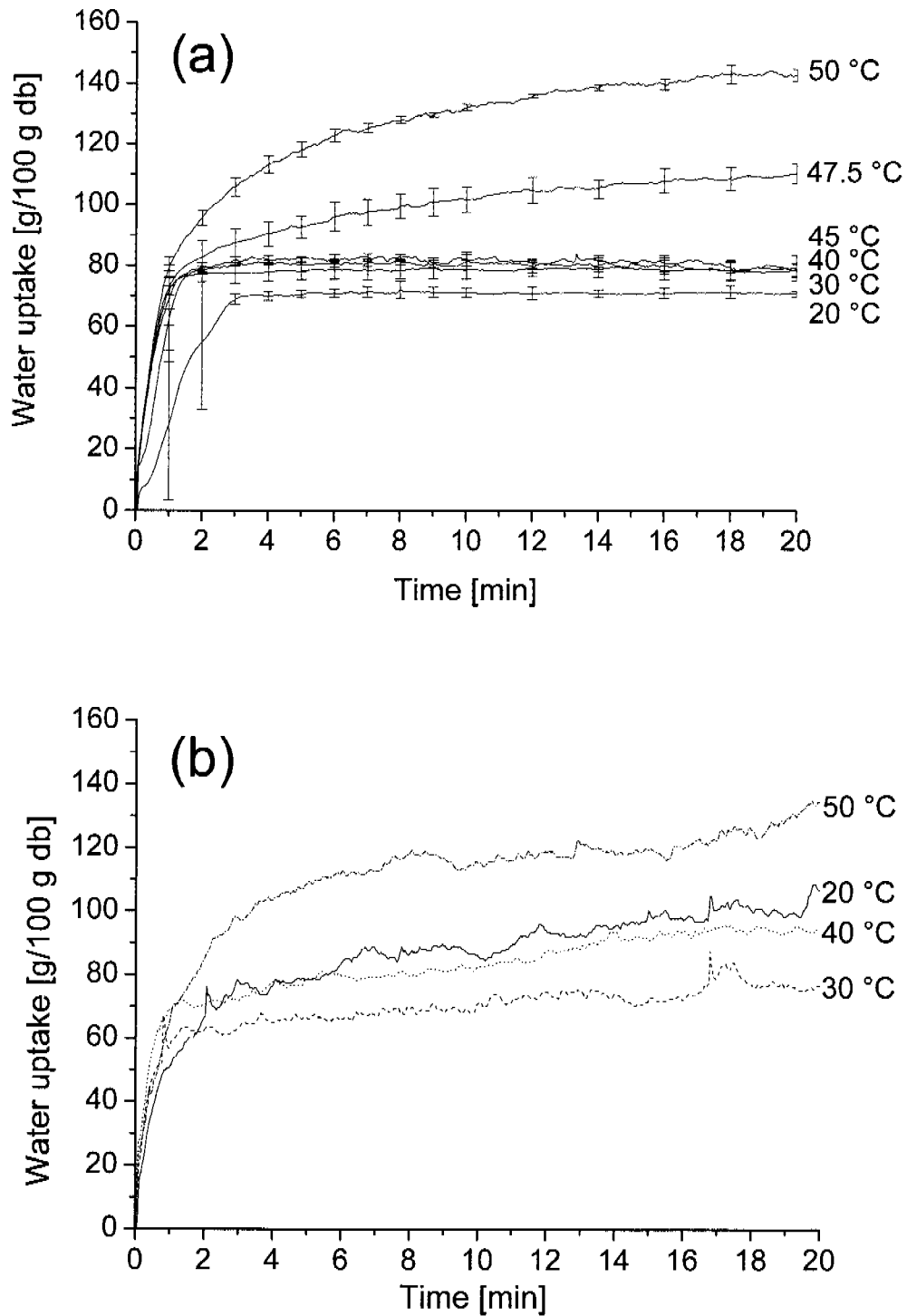


Figure 3.8: Water uptake dynamics of micropiles of wheat starch (a) and gluten (b) at temperatures between 20 and 50 °C.

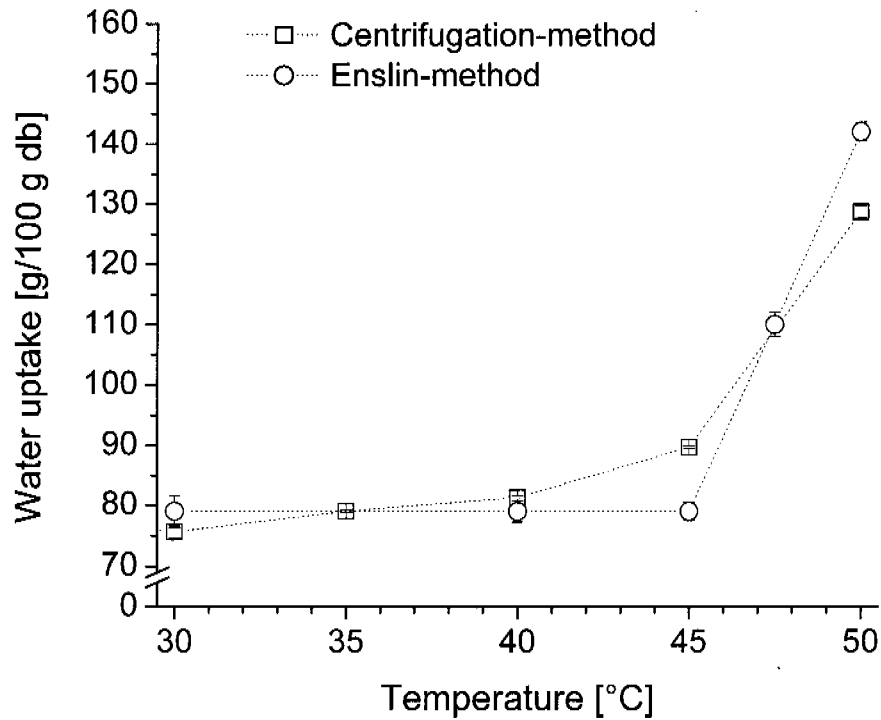
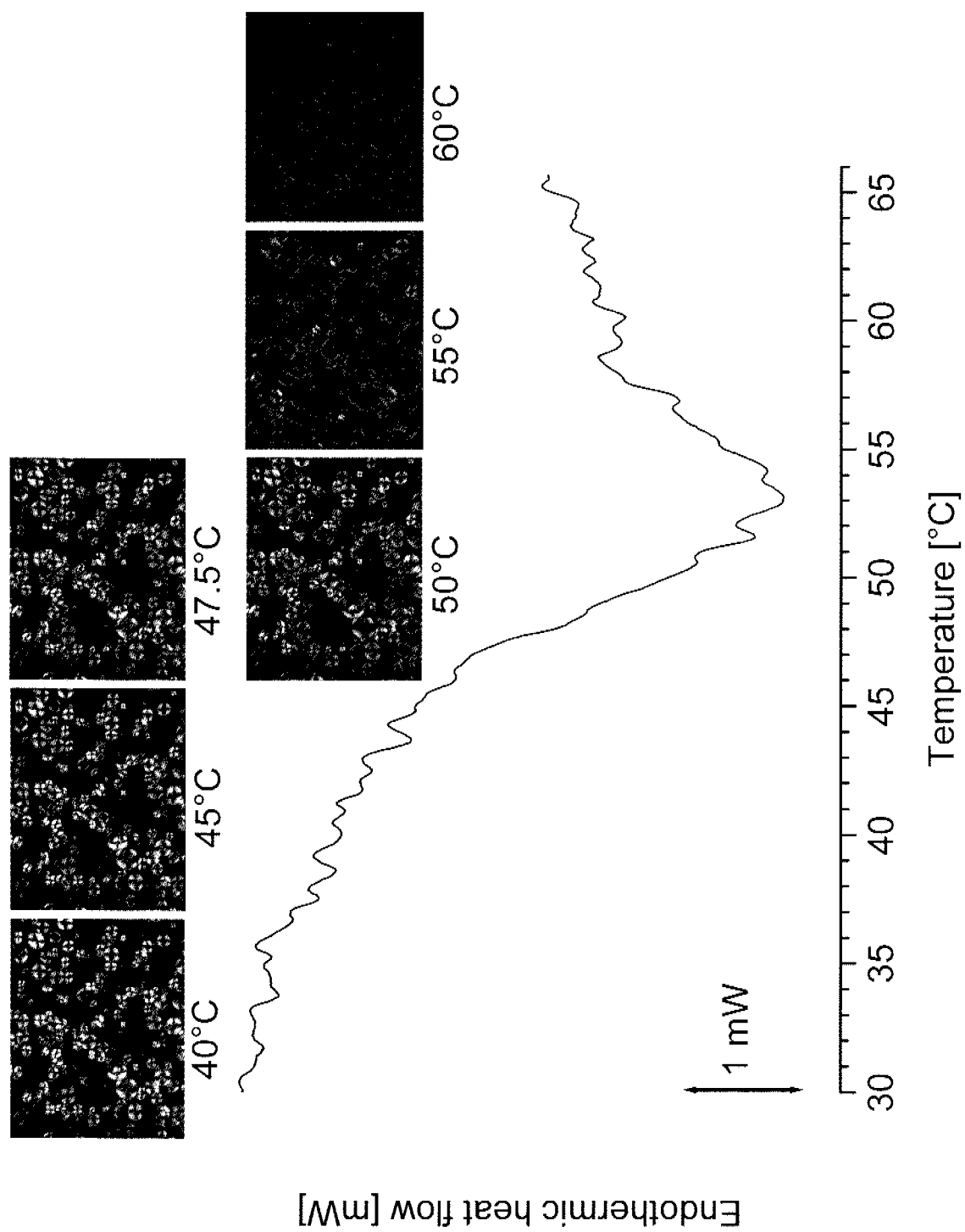


Figure 3.9: Equilibrium water uptake of micropiles of wheat starch (Enslin method) compared to water holding capacity (Centrifugation method) of wheat starch at temperatures between 30 and 50 °C.

Figure 3.10: Melting behavior of wheat starch dispersions as viewed in hot stage polarized light microscopy and as measured with DSC (heating rate for both methods: 1 °C/min).



3.3.4 Dynamics of water uptake of durum wheat semolina

The dynamic water uptake curves of micropiles of semolina particle size fractions at temperatures between 20 and 50 °C are presented in Figure 3.11. Regarding the influence of particles size, it was found that micropiles of larger particles generally exhibited slower water uptake rates at all temperatures. The very fine fractions (< 200 µm) also showed a different water uptake pattern, characterized by longer times for reaching equilibrium conditions and distinctly higher equilibrium water uptake. This might be attributed to the low bulk densities of the micropiles of the finest fractions (Figure 3.12) which affected the capillary structure of the micropiles and therefore caused the different water uptake behavior. The water uptake rates (Figure 3.13) for the semolina fractions during the first minute of the experiments were between 30 and 80 g/100 g db, increasing with temperature. A marked drop in the water uptake rate was detected for particles larger than 355 µm. Equilibrium conditions for the water uptake were reached earlier for the finer than for the coarser granulated fractions (> 355 µm). The maximum water uptake in equilibrium was between 130 and 230 g/100g db, depending on temperature and particle size (Figure 3.14). Like for isolated wheat starch, the temperature dependence of the water uptake was low between 20 and 40 °C but at 50 °C a marked increase in the water uptake of 20-40 g water/100 g db was detected.

The difficulty to discriminate between the water uptake into the endosperm material and the water that just fills the pore volume of the micropiles is an instrumental disadvantage of the Enslin set up. The water content analyzed with the Enslin method was in the range of 58-71 g/100 g wb, depending on particle size and temperature. The comparison with the water contents measured by centrifugation (45-61 g/100 g wb) reveals that approximately half of the water content measured with the Enslin method is interstitial water of the pore volume of the micropiles, and assuming that the interstitial water in the samples as analyzed with the centrifugation method is negligible. In order to estimate the water uptake of the semolina particles, the respective amount of water for the pore volume of the micropiles was subtracted from the equilibrium water uptake amount. The

pore volume of the samples was calculated through the difference between the initial specific volume of the dry micropiles and the specific volume of the semolina. The results of this estimation are given in Figure 3.15. After this correction, all particle size fractions roughly showed similar water uptake, except the finest granulations which had very low water contents after this estimation. It seems that the water uptake values are overcorrected by the interstitial volume of the dry micropiles. This indicates that the pore volume of the micropiles of the finer granulated semolina particle size fractions decreased during the water uptake, either as a consequence of the wetting of the powder or as a consequence of a more pronounced swelling of the small semolina particles. In contrast, the pore volume of the micropiles of the coarser granulated semolina particle size fractions was not altered during the water uptake process, as the estimated values of the water content correspond well to the water content as determined by the centrifugation method (Figure 3.15). In conclusion, the Enslin technique seems appropriate for the determination of water uptake into semolina as a bulk material and for the determination of the influence of temperature on the water uptake, but unsuitable for the quantitative determination of the water uptake dynamics into semolina material itself.

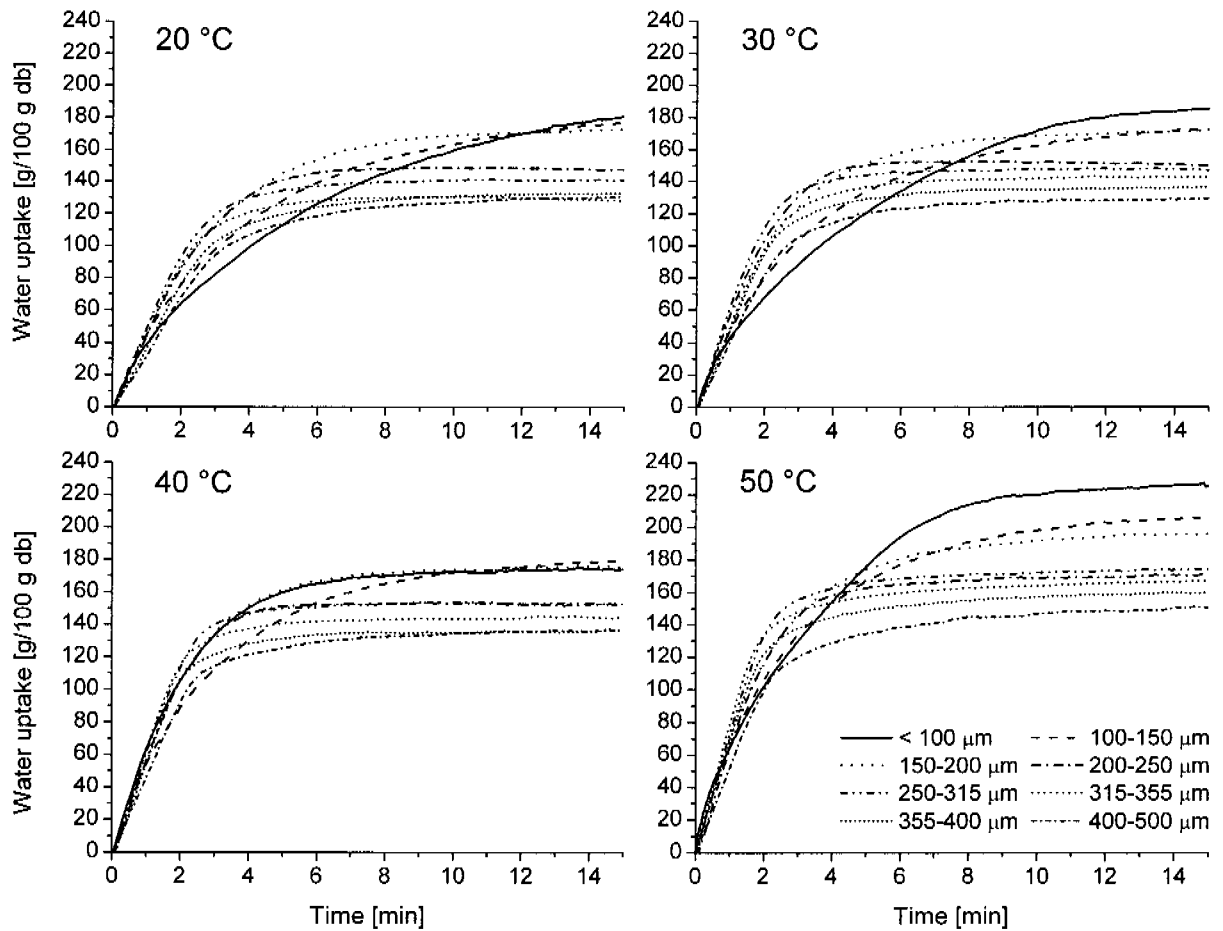


Figure 3.11: Water uptake dynamics of micropiles of particle size fractions of durum wheat semolina at temperatures between 20 and 50 °C.

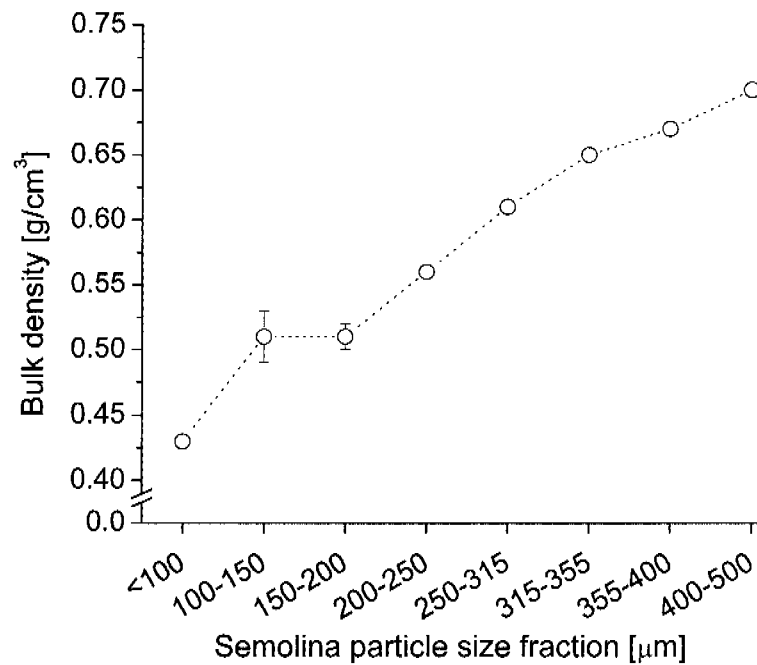


Figure 3.12: Bulk density of durum wheat semolina particle size fractions before water uptake.

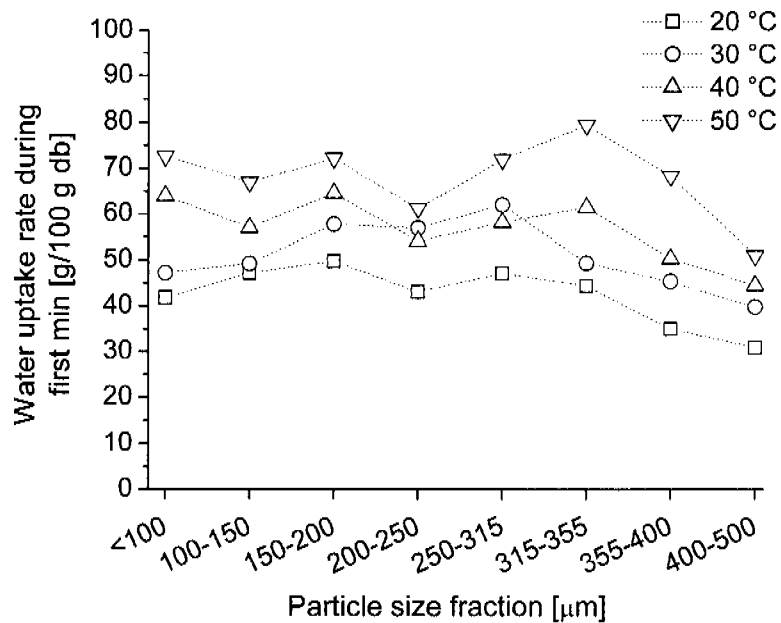


Figure 3.13: Initial water uptake rate of micropiles of durum wheat semolina particle size fractions as calculated from the water uptake during the first minute.

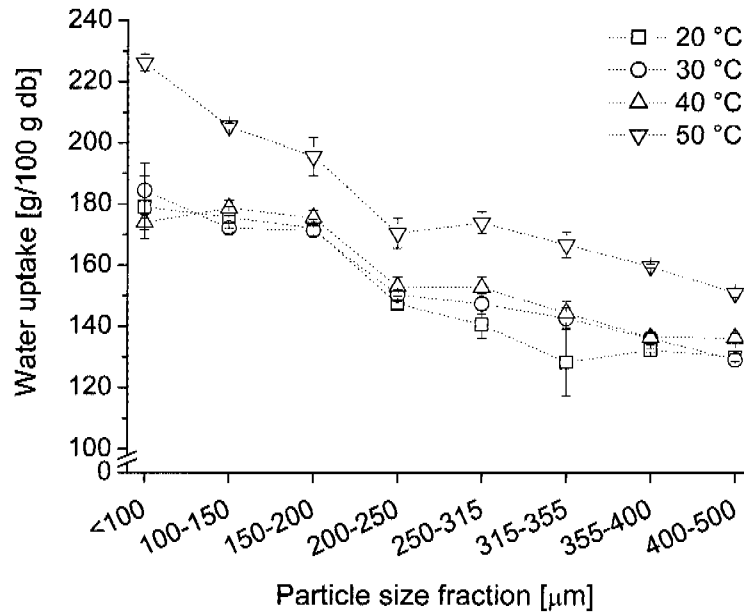


Figure 3.14: Equilibrium water uptake of micropiles of durum wheat semolina particle size fractions at temperatures between 20 and 50 °C.

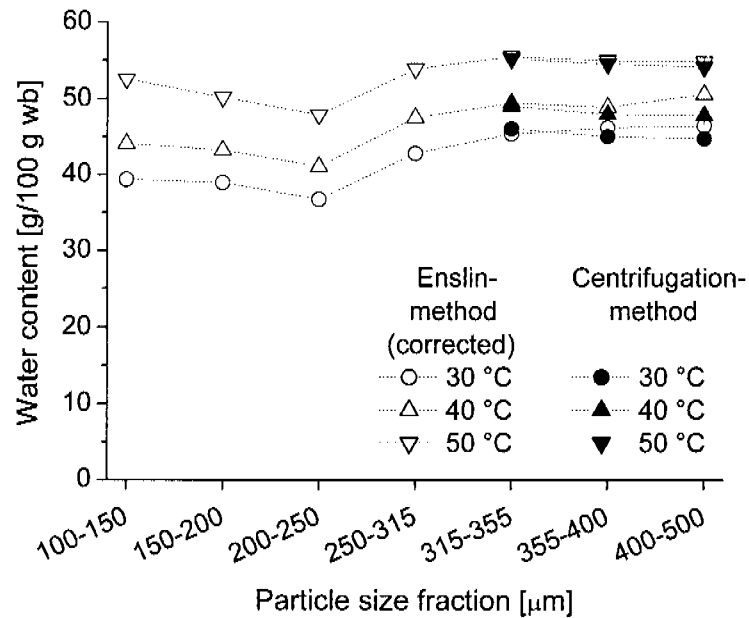


Figure 3.15: Equilibrium water uptake of micropiles of durum wheat particle size fractions at temperatures between 20 and 50 °C, measured by the Enslin method and corrected by the water uptake of the initial pore volume of the micropiles, and measured by the centrifugation method.

3.4 Conclusions

The average equilibrium moisture content of semolina after water vapor sorption at 25 °C was 28.3 g/100 g wb and equilibrium conditions were reached rather slowly (~72 hr at 25 °C). This means that, according to the concept of water activity in food, the water content of common pasta dough (~30-33 g/100 g wb) is sufficient to saturate the semolina with water if a homogenous distribution of water among and within the semolina particles is assumed. On the other hand, the results of the Enslin and the centrifugation method showed that semolina is capable of taking up liquid water very fast (within max. 15 min up to saturation) and in high amounts (~47 g/100 g wb). Consequently, the typical water content of pasta dough is not high enough to meet the liquid water uptake capacity of semolina so that limited water conditions exist for the process of semolina moistening in pasta dough mixing. Therefore, a homogeneous distribution of the added water among all semolina particles during the initial phase of the mixing process is essential to achieve evenly hydrated semolina. This is a challenge due to the limited water condition and the high liquid water uptake capacity of semolina. If the initial distribution of water among all semolina particles is achieved inadequately, an effective distribution of water among the semolina particles may be enabled by long process times of the mixing step. The water is exchanged between the semolina particles in the form of water vapor which has been shown to be a rather slow process at water activity of 1 of the pasta dough. It is conceivable that a faster water distribution could be obtained by mechanically enforced contact between over- and under-moistened semolina particles. From the present results of the Enslin method no conclusions can be drawn regarding the dynamics of liquid water uptake into the semolina particles. For this purpose, dynamic water uptake studies using durum wheat endosperm particles with better defined shape and with larger size than semolina remain to be performed.

4 Hydration dynamics of durum wheat endosperm as studied by magnetic resonance imaging (MRI) and soaking experiments*

The precise knowledge of the kinetics of water transport in durum wheat endosperm is a prerequisite for the optimization of wheat processing techniques like pasta dough mixing on a fundamental basis. Cylindrically cut endosperm pieces were prepared from durum wheat kernels and used to study the water uptake by applying a gravimetric method and magnetic resonance imaging (MRI). The total water uptake of endosperm cylinders at different soaking times was determined by gravimetric soaking experiments and revealed a swelling limit of around 40 g/100 g wb after 60 min. With these results it was possible to estimate an apparent diffusion coefficient of water in durum endosperm by using numerical simulation based on a diffusion model ($D_{25\text{ }^{\circ}\text{C}} \sim 0.76 \times 10^{-10} \text{ m}^2/\text{sec}$). MRI was used to quantify the water distribution in the endosperm cylinders over time at excess and limited water conditions. The calibration of MRI for the quantification of local and time dependent water contents was successful by correlating the spin-spin relaxation time (T_2) with the water content of calibration samples at intermediate moisture levels (19-45 g/100 g wb). Water content maps were generated and showed the kinetics of water distribution inside the endosperm cylinders up to equilibrium conditions. The water uptake of the endosperm cylinders over time as measured by MRI fitted well to the water uptake as determined gravimetrically in soaking tests what validated the applied MRI calibration- and measurement procedure. The results allow to predicting quantitatively the water transport properties of durum wheat endosperm during moistening procedures.

* This chapter has been submitted for publication as:

Kratzer, A., Handschin, S., Lehmann, V., Gross, D., Escher, F., Conde-Petit, B. Hydration dynamics of durum wheat endosperm as studied by magnetic resonance imaging and soaking experiments.

4.1 Introduction

In most cases wheat processing requires a hydration step, since water acts as a very effective plasticizer for biological material. The hydration rate is essentially controlled by the diffusion properties of water in the material. Large wheat particles and short processing times lead to pronounced gradients in water concentration in the material. The precise knowledge of the hydration kinetics of wheat endosperm is of interest for designing and optimizing wheat processing operations. For example, processing of durum wheat into pasta requires the plasticization of durum wheat endosperm particles (semolina) with water, so that the material can be shaped by extrusion or sheeting. Water is added to semolina at a concentration of 30-33 g/100 g wb, and the mixing temperature lays between 25-40 °C (Antognelli 1980, Debbouz and Doetkott 1996, Manser 1981). An inhomogeneous hydration of durum wheat particles is detrimental for the overall appearance of dried pasta and promotes the formation of rough surfaces and some type of white spots and strains (Manser 1985).

So far, the optimization of the semolina moistening and mixing process has been carried out mainly empirically and comparatively little fundamental data on the hydration kinetics of semolina or durum wheat endosperm in general is available. Studies that investigated the interaction of durum wheat semolina and water were either limited to water vapor sorption studies (Erbaş et al. 2005, Hebrard et al. 2003) or based on indirect methods like farinograph experiments (Manser 1981). Kang and Delwiche (1999) studied the water uptake kinetics of pearled durum wheat samples at 22 °C and found an apparent diffusion coefficient of $0.73 \times 10^{-10} \text{ m}^2/\text{sec}$ by numerical modeling of the moisture diffusion using a finite element model. Igathinathane and Chattopadhyay (1997) and Tagawa et al. (2003) followed a similar approach, but used bread wheat for their studies. Generally, a diffusion coefficient would allow the calculation of local and time dependent water concentrations on the basis of diffusion models. However, no experimental data on water concentrations in durum wheat endosperm during hydration are available. Gravimetric methods for such experiments lack precision and practicability due to the small dimension of durum wheat endosperm. In contrast, magnetic resonance

imaging (MRI) is the method of choice for the non-destructive measurement of internal water distributions (McCarthy et al. 1994). MRI allows the detection of water with sufficient spatiotemporal resolution and does not require extensive sample preparation. This technique has been applied for several investigations in the field of cereal science, for instance to study the ingress of water into dried pasta (Duce and Hall 1995, Hills et al. 1996), and to follow the moisture loss during the drying of pasta (Hills et al. 1997) or wheat kernels (Ghosh et al. 2006). The latter studies used the MRI signal just as a semi-quantitative measure for the water distribution, while others calibrated the spin-spin relaxation time with samples of known water content and used this relationship for the determination of moisture gradients in rice during boiling (Takeuchi et al. 1997a, Takeuchi et al. 1997b) and in pasta during boiling and holding (Horigane et al. 2006, Irie et al. 2004).

The aim of the present investigation was the quantitative determination of water distribution in durum wheat endosperm upon hydration. A prerequisite therefore was a precise calibration procedure of the spin-spin relaxation time in a water concentration range that includes low moisture levels. Furthermore, the water contents as assessed by MRI were compared to gravimetrically determined water contents. An additional novelty was the use of cylindrically cut durum wheat endosperm pieces for assessing the diffusion properties of water in the material. Similar cylinders of native wheat endosperm have already been used for the determination of mechanical properties of wheat endosperm (Dobraszczyk et al. 2002, Glenn et al. 1991). The endosperm cylinders were considered as appropriate for the present investigation due to their well defined geometrical shape.

4.2 Experimental

4.2.1 Preparation of durum wheat endosperm cylinders

The raw material for the production of durum wheat endosperm cylinders (DWEC) was integer Canadian western amber durum wheat kernels, obtained from Swissmill (Zurich, Switzerland). For further use, the kernels were hand sorted and only vitreous and faultless kernels were selected. To facilitate this procedure, the kernels were placed on a translucent plane with a light source underneath which allowed the detection of visible cracks in the kernels. The graded wheat kernels were stored in a dark place at ambient conditions until they were machined. For this, the kernels were first cut along the crease in order to obtain the two halves of the wheat endosperm. In a second step, the halves were manually trimmed with the help of a sharp blade until they fitted properly between the chucks of a laboratory lathe (Proxxon PD 230/E, Proxxon GmbH, Niersbach, Germany). Figure 4.1 shows the lathe and the already turned DWEC that was fixed by the help of a rotating chuck that consisted of a brass pipe, equipped with a crown cut and the static chuck in the form of an aluminum cable lug as bearing. For turning at a rotation speed of 6000 1/min, a tapered turning tool was used and the procedure lasted approximately 3 min for one DWEC. Figure 4.2 shows examples of the produced DWEC and after cutting off the endings, geometrically precise DWEC with a diameter of about 1 mm and a length of about 4 mm resulted. For further use, the DWEC were stored in a hermetic container and the exact dimensions (diameter and length) were measured for each cylinder using a micrometer screw (± 0.001 mm). Additionally, the initial water content of DWEC was analyzed gravimetrically by drying approximately ten cylinders for 90 min at 130 °C.

4.2.2 Determination of porosity and surface topography of durum wheat endosperm cylinders

The surface topography of the turned cylinders was examined by using scanning electron microscopy (SEM). Therfor, samples of the turned cylinders were fixed on double-sided tape and sputter-coated in a planar magnetron sputtering device MED 010 (Bal-Tec, Balzers, Liechtenstein) with 5 nm platinum. The samples were observed in a SEM (Zeiss Gemini 1530 FEG, Oberkochen, Germany) and secondary electron images were recorded at an accelerating voltage of 5 kV.

Mercury intrusion porosimetry was performed on a porosimeter (Pascal 440, Thermo Fisher Scientific Inc., Waltham, USA) consisting of a micro- and a macropore-unit. A sample of approximately 20 durum wheat endosperm cylinders without their clamping edges was placed in the dilatometer and mercury pressure was increased from 1 to 400 MPa. The mercury contact angle was estimated to be 140°. The porosity of glassy durum wheat kernels (approximately 20 pieces) which were cut into halves orthogonally to the kernel crease was also detected with the same method. Porosity was expressed as cumulative specific pore volume (mm³/g) and pore radius was estimated by using the Washburn-equation (equation 4.1).

$$P = \frac{-2\sigma_{\text{Hg}} \cdot \cos\theta_{\text{Hg}}}{r} \quad (\text{equation 4.1})$$

where P is the mercury pressure [Pa], σ_{Hg} the surface tension of mercury (0.5 N/m), θ_{Hg} the contact angle of mercury (140°) and r the capillary radius [m].

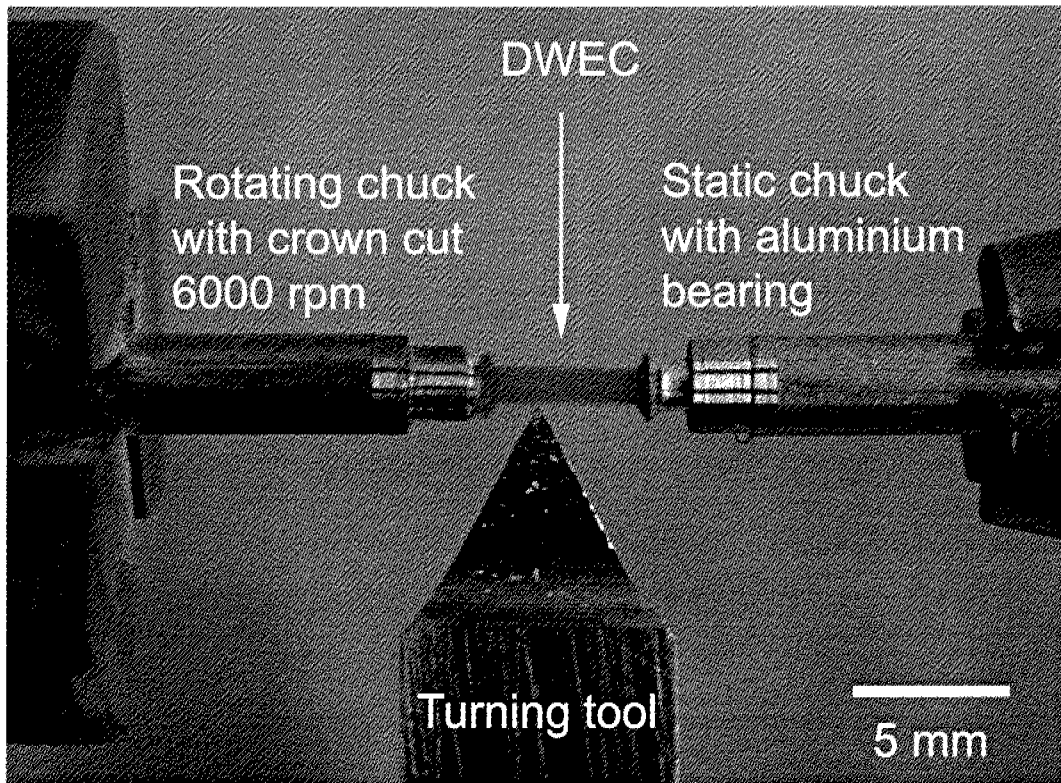


Figure 4.1: Set up for the preparation of DWEC on the laboratory lathe.

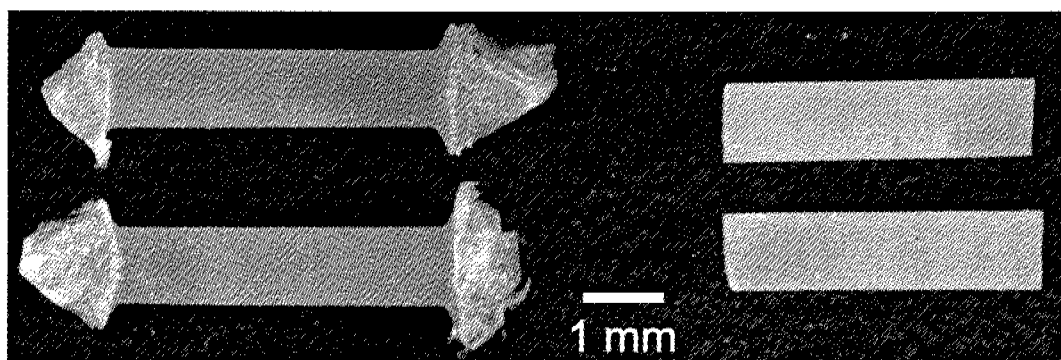


Figure 4.2: DWEC after lathing; left: Examples with clamping edges and right: After cutting off the clamping edges.

4.2.3 MRI experiments for following the hydration of durum wheat endosperm

Magnetic resonance imaging (MRI) was performed at 25 °C in a nuclear magnetic resonance spectrometer operating at 500 MHz (AVANCE500WB, Bruker-Biospin GmbH, Rheinstetten, Germany) using the Bruker MRI accessory equipment. The spectrometer operated at a magnetic field of 11.7 Tesla. A multi-slice multi-echo (MSME) sequence was used and the repetition time was 300 msec, the echo time was 2.6 msec and the number of echoes was 32. Spin-spin relaxation time (T_2) maps were generated from a sequence of 32 images and eight averages using the equation 4.2.

$$M = M_0 \cdot e^{\frac{-t}{T_2}} \quad (\text{equation 4.2})$$

where M is the signal intensity at echo time t and M_0 the signal intensity at echo time zero. The decay of the signal intensity was fitted to an exponential decay curve and it was assured that all the experimental parameters were equivalent for the calibration as well as for the dynamic tests.

4.2.4 Calibration of the T_2 relaxation time as function of water concentration

A calibration curve for the calculation of absolute water contents from T_2 -maps was prepared by using endosperm material with defined moisture concentrations as reference. Endosperm material in a water content range between 19 and 45 g/100 g wb was prepared by moistening endosperm cylinders or by moistening and pelletizing granular durum wheat endosperm. The moistened endosperm cylinders (DWECS) were prepared by placing a DWECS and a droplet of distilled water of known mass inside a 2 mm (o.d.) NMR capillary (Figure 4.3). The capillary was sealed with vacuum grease to prevent moisture loss during the equilibration period of approximately 24 hr at room temperature. The moisture content of the samples prepared by this procedure ranged between 19 and 40 g/100 g wb and was calculated from the initial mass and water content of the DWECS and the mass of the added water. The equilibrated samples were

placed in a solenoid type coil (2 mm, i.d.) and were subjected to the MRI measurement as described above. The imaging matrix size was 128 x 64 pixels and the slice thickness was 1 mm. Hence, the spatial resolution of the experiment was 17 x 31 x 1000 μm and T_2 -maps for DWEC cross sections at different water contents were obtained. Calibration samples which based on granular durum wheat endosperm were prepared by compacting approximately 500 mg of moistened durum wheat semolina (HWG-M, Swissmill, Zurich, Switzerland) into uniform pellets in a hydraulic pellet press at a pressure of approximately 5.9×10^8 Pa which was applied during 10 sec. The semolina was moistened to water contents between 25 and 45 g/100 g wb by mixing it with water in a classical pasta dough batch mixer. The compacted pellets of the moistened semolina were placed into 5 mm (o.d.) NMR capillaries and the equilibrated samples were analyzed with the above-mentioned MRI-method.

4.2.5 In-situ determination of durum wheat endosperm hydration at excess water conditions by MRI

For these measurements, a DWEC was fixed inside a 5 mm (o.d.) NMR capillary that was equipped with water inlet and outlet tubes (Figure 4.4). Upon positioning the sample in the spectrometer by employing a standard radiofrequency coil (5 mm, i.d.), the NMR capillary was filled with distilled water through the attached tubes. The time of the initial contact between the DWEC and water was defined as time zero. The MRI measuring procedure was started exactly 1 min after the first contact of the DWEC with water. The first minute was needed to adjust the MRI device and to adapt the MRI scanning area to the examined DWEC. T_2 -maps across the central region of the cylinder were obtained with an imaging matrix size of 128 x 64 pixels and at a slice thickness of 2 mm, what resulted in a spatial resolution of 78 x 39 x 2000 μm . The scan time for one T_2 -map was 3.05 min and consecutive maps were generated during the continuous water uptake of the DWEC for times up to 90 min.

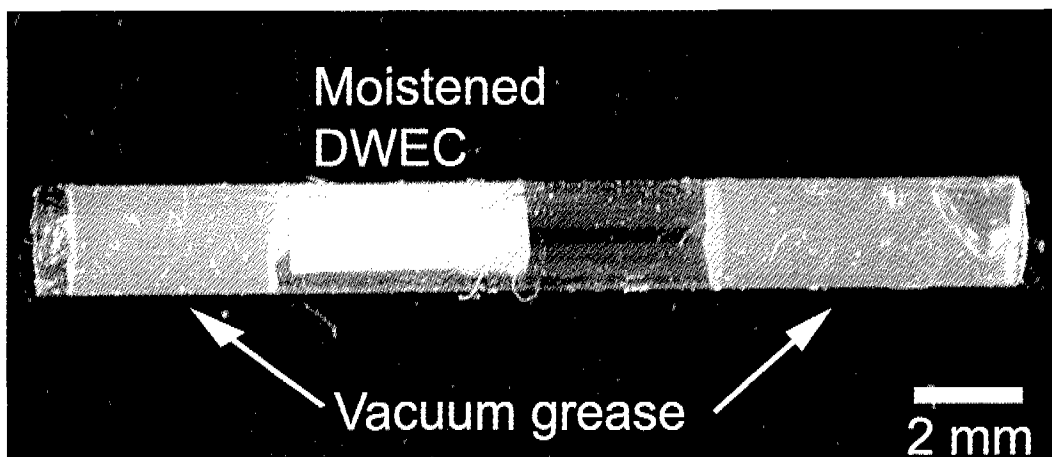


Figure 4.3: Set up for the MRI calibration experiments: moistened DWEC in a 2 mm NMR capillary that was sealed with vacuum grease to prevent moisture loss during equilibration.

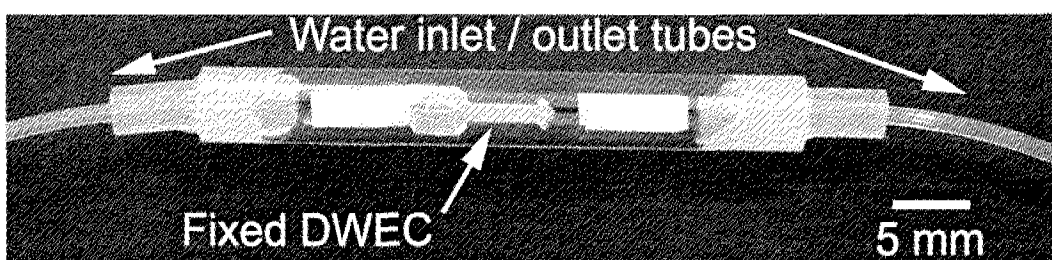


Figure 4.4: Fixed DWEC in a 5 mm NMR capillary for the in-situ monitoring of the hydration of a DWEC with MRI. The water inlet and outlet tubes permitted rapid water addition inside the spectrometer.

4.2.6 In-situ determination of durum wheat endosperm hydration at limited water conditions by MRI

The water transport in durum wheat endosperm after limited contact with water was also assessed. For this purpose, a DWEC was soaked for exactly 3 min in distilled water at 25 °C and after removing excess surface water by blotting on filter paper, it was placed inside a 5 mm (o.d.) NMR capillary. To prevent water evaporation from the sample, the capillary was previously filled with a water droplet which did not come into direct contact with the DWEC. The MRI scanning procedure was started exactly 9.8 min after the DWEC had the first contact with water. The same MRI procedure as described above for the experiments at excess water conditions was used.

4.2.7 Gravimetric determination of water uptake upon hydration at excess water conditions

The experiments were carried out with single DWEC of known mass (± 0.002 mg) and known initial water content. The DWEC were immersed individually in distilled water at 25 °C for various soaking times (5, 10, 15, 35, 60 and 90 min), and for each soaking time at least five cylinders were tested. The DWEC were removed from the soaking bath with the help of tweezers and were quickly blotted on filter paper to remove excess surface water. Thereafter, the DWEC were immediately weighed on the microbalance and the detected increase in mass was considered as the water uptake.

The following correction procedure was necessary to be able to compare the results of the gravimetric water uptake experiments to the data obtained by MRI. The radial water uptake through the circumferential surface of the cylinder after soaking was calculated considering the dry matter loss of the DWEC during the soaking procedure (equation 4.3). Finally, the water content of the DWEC cross section as a result of water uptake through the circumferential surface of the cylinder was calculated by considering the initial water content of the DWEC (equation 4.4) by using equation 4.5.

$$\text{Water uptake through the circumferential surface [mg]} = l \cdot \frac{M_a - M_i + \text{DML}}{l + r} \quad (4.3)$$

$$\text{Initially incorporated water of the DWEC [mg]} = \frac{X_i}{100} \cdot \left[M_i - \left(\frac{\text{DML}}{100} \cdot \frac{X_i}{100 - X_i} \right) \right] \quad (4.4)$$

$$\text{Water cont. of DWEC cross section [g/100 g wb]} = \frac{\text{water uptake} + \text{initial water}}{M_a} \cdot 100 \quad (4.5)$$

where M_i and M_a are the masses of the DWEC before and after the soaking test [mg], r and l are the radius and the length of the DWEC [mm], X_i is the water content of the DWEC before the soaking test [g/100 g wb], and DML is the dry matter loss of the DWEC during the soaking procedure [mg]. In order to determine this dry matter loss, some of the soaked samples were analyzed gravimetrically for their dry matter after drying at 105 °C for 14 hr.

4.2.8 Determination of an apparent diffusion coefficient of water in durum wheat endosperm by numerical modeling

With the geometrical information of the DWEC (length, diameter) and the water uptake data as assessed by the gravimetric soaking tests, a n model for cylinders based on Fick's second law of diffusion was solved numerically for the apparent diffusion coefficient by using the Visual Basic and Excel software packages (Microsoft Corp.). The boundary conditions and theoretical considerations made for the numeric model were that:

- (1) The water transfer in the endosperm material is a diffusion process and can be described by Fick's second law of diffusion.
- (2) There is no change of the cylinder dimensions during the water uptake.
- (3) At the outer layer of the cylinder, the concentration of water is the constant saturation moisture content (M_{∞}) of the endosperm material throughout the whole water uptake process.

As saturation moisture content, the water holding capacity of durum wheat semolina as determined by a centrifugation method was used (see 3.3.2). The value for M_{∞} was 47 g/100 g wb at temperatures between 20-30 °C. This value is in good agreement with the saturation moisture content reported by Igathinathane and Chattopadhyay (1997), who also found M_{∞} to be 47 g/100 g wb after soaking pearled wheat kernels for 15 hr at 30 °C.

4.3 Results and discussion

4.3.1 Porosity and surface topography of durum wheat endosperm cylinders

Micrographs of the surface topography of the turned cylinders are shown in Figure 4.6. The surface appears rather homogeneous and as a consequence of the turning process, the surface is evenly corrugated at a scale of approximately 50 μm . In addition, the surface shows micro-cracks that most probably are a result of the turning process but also cracking due to the preparation and the high vacuum in the electron microscope can be responsible for the observed cracks. The results of the mercury intrusion porosimetry are presented in Figure 4.5 and indicate rather low porosity for the cylinders. In comparison to durum wheat kernels, the cylinders even exhibited lower porosity as expressed by the cumulative pore volume (37 and 47 mm^3/g , respectively). Therefore, the observed cracks are on the one hand not contributing to the porosity as they are only at the surface of the cylinders or on the other hand, cracks are also present in unturned durum wheat endosperm to the same extent.

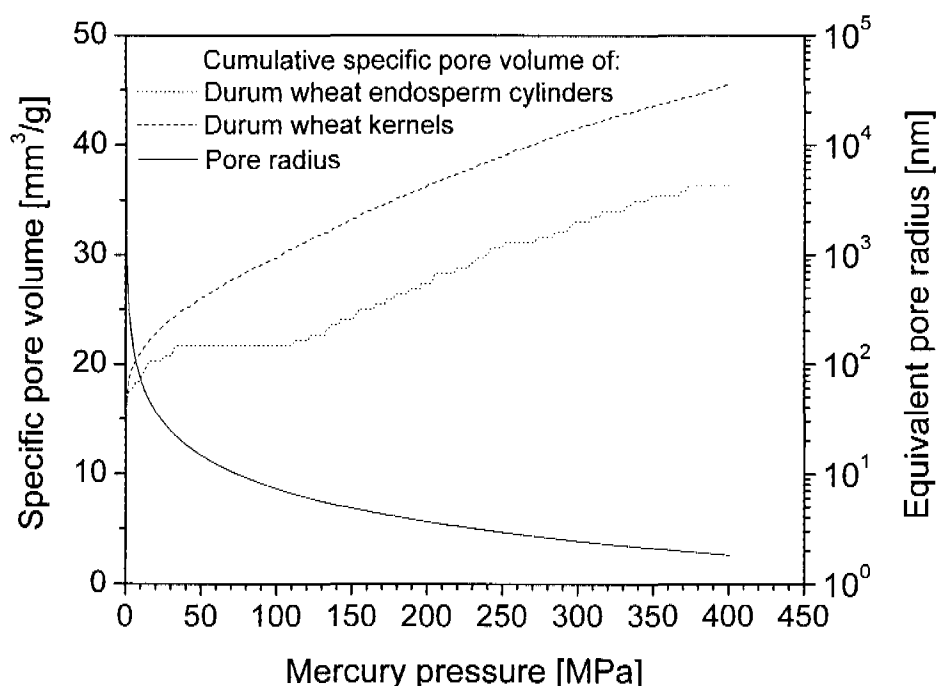


Figure 4.5: Porosity (cumulative specific pore volume) of DWEC compared to durum wheat endosperm kernels as assessed by mercury intrusion.

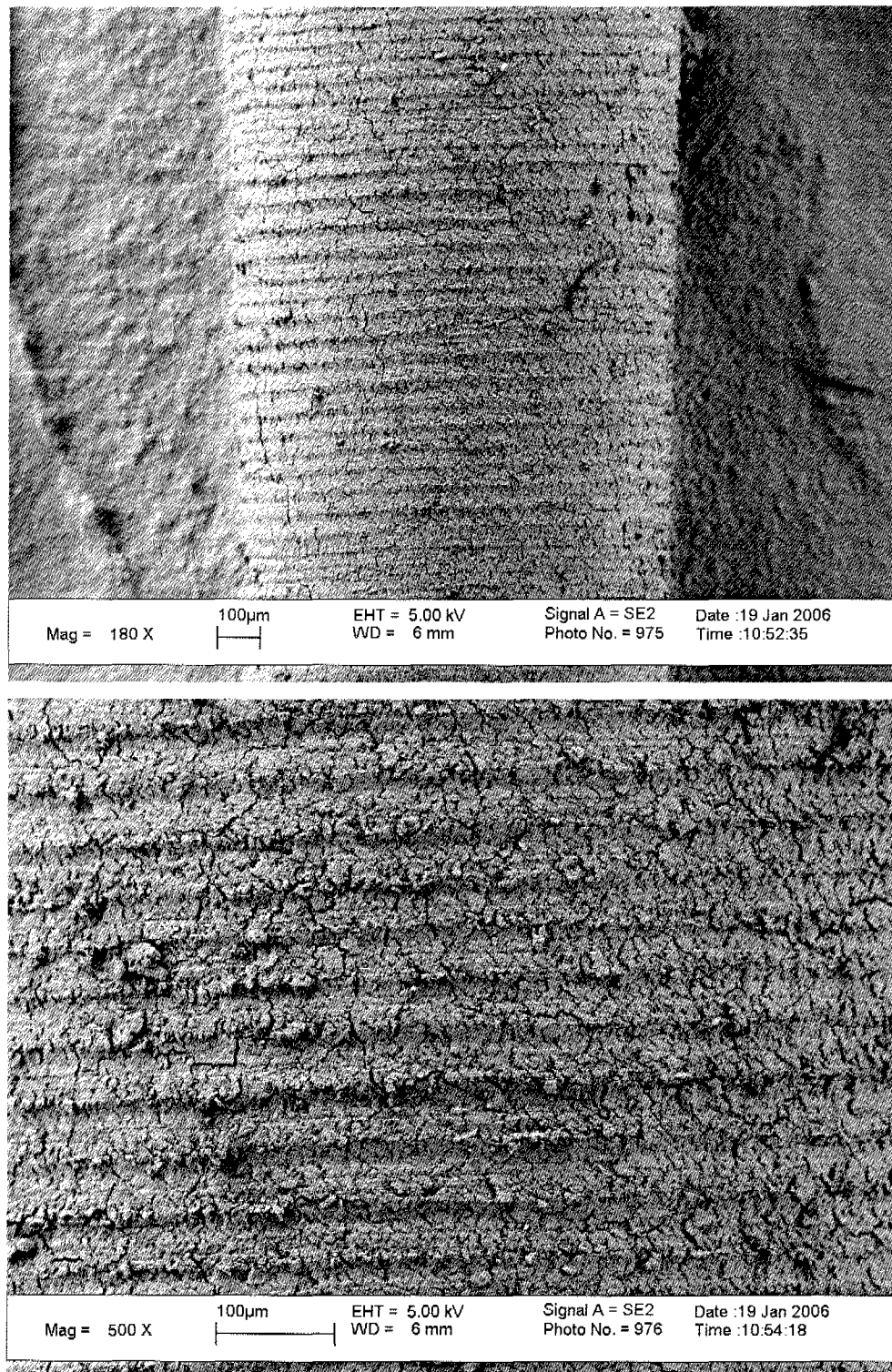


Figure 4.6: SEM-micrographs of the surface topography of turned durum wheat endosperm cylinders at different magnification.

4.3.2 Calibration curve for the calculation of water contents from T_2 relaxation time

Wheat endosperm samples with defined water content were equilibrated for 24 hr and thereafter used as reference for calibration. All voxels of the cross section of the moistened DWEC showed T_2 values in a very narrow range, so that it can be assumed that a homogeneous water distribution was reached. Figure 4.7 shows a plot of the average T_2 values against the respective water content of the DWEC. A linear correlation between T_2 and the water content of the DWEC was found ($R^2 = 0.9$) for a water content range between 20 and 40 g/100 g wb. The same linear relationship was found for moistened and pelletized durum wheat semolina up to water contents of 45 g/100 g wb. Higher moisture levels can be achieved in the semolina pellets since more water can be included in the pellets than in the native endosperm tissue. Furthermore, the congruence of the calibration with DWEC and pellets reveals on one side that the DWEC were hydrated as evenly as the pellets and, on the other hand that the determined calibration curve is valid for durum wheat endosperm material in general, irrespective of its particle size. Irie et al. (2004) found a similar relation between T_2 and water content for durum wheat semolina, pulverized durum wheat semolina and spaghetti, although in the high water content range (50-85 g/100 g wb). In contrast, our calibration data covers the intermediate moisture range and can be considered as complementary to data from Irie et al. (2004). However, samples having a water content lower than 20 g/100 g wb resulted in very low signal to noise ratios reflecting the detection limit of the present MRI procedure. Interestingly, a water content of 20.2 g/100 g wb and 25 °C correspond to the glass-to-rubber transition point of durum wheat endosperm as reported by Cuq and Icard-Vernière (2001). Nevertheless, the glass to rubber transition of durum wheat endosperm just refers to the increased mobility of the polymers in the system due to the plasticizing effect of water and not to the mobility of the water molecule itself. Moreover, especially the state of the water molecules (free or bound) plays an important role for the water mobility and therefore sufficient signal to noise ratios of water. The found correlation between the glass to rubber transition of the system and the concurrently improved signal/noise ratio of the water molecules indicates that the amount of free water

increased significantly at the glass to rubber transition of durum wheat endosperm. Hence, it can be assumed that the water mobility is too low at water contents that are associated with the glassy state of the durum wheat endosperm. This leads to the hypothesis that a successful determination of water contents in durum wheat endosperm using the T_2 value is limited by the mobility of the water in the system and would either demand highly sensitive MRI devices or rather long scanning times for measurements in the glassy state.

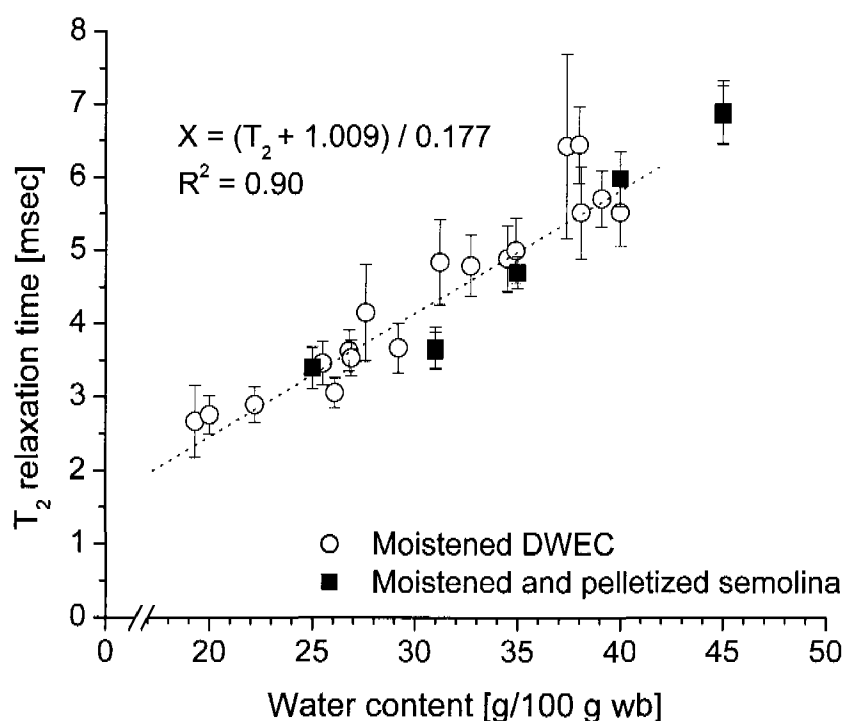
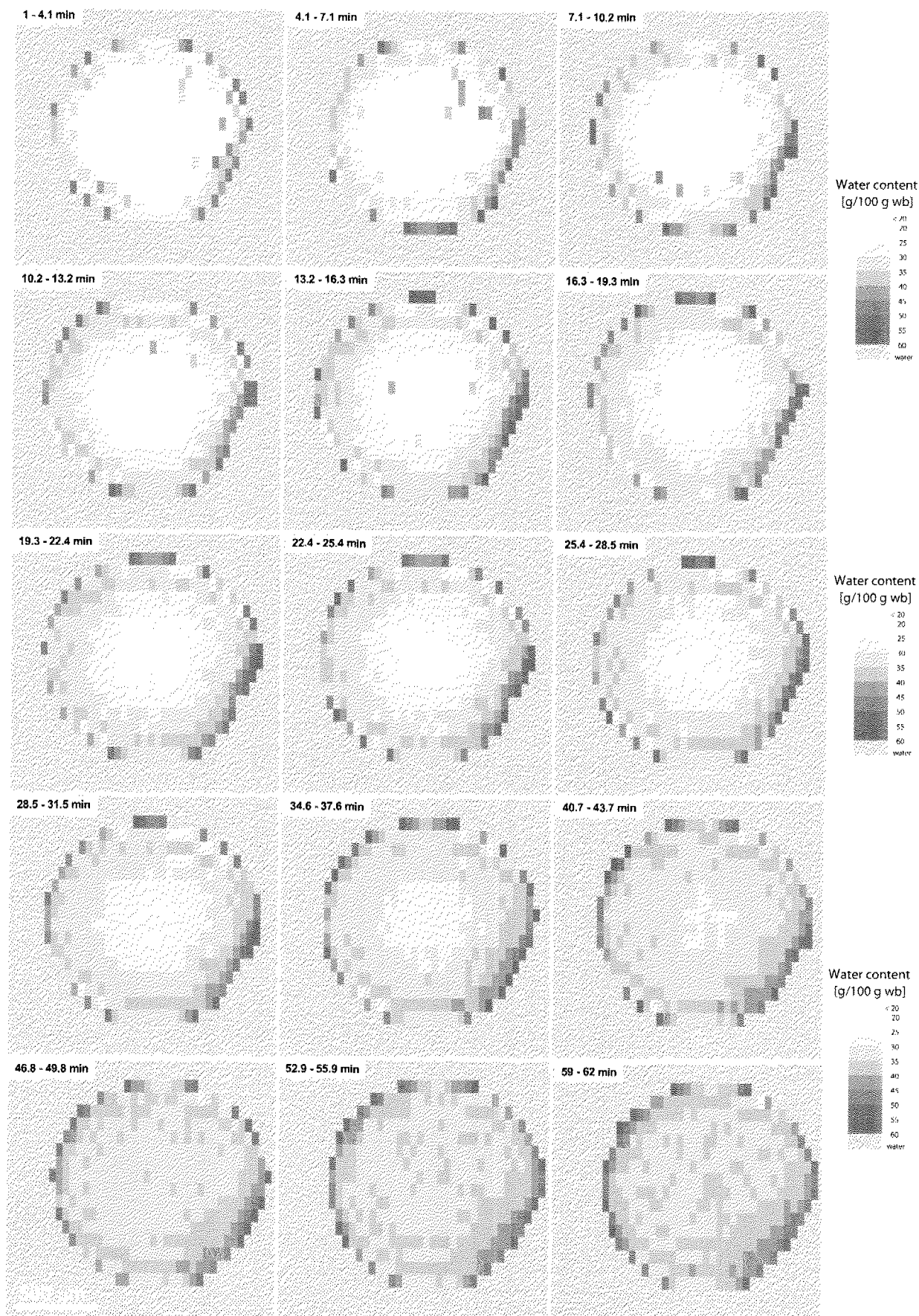


Figure 4.7: Correlation between the water content of durum wheat endosperm and the spin-spin relaxation time (T_2). Error bars indicate the standard deviation of the measured T_2 values along the cross section of one DWEC or semolina pellet.

4.3.3 Water distribution in durum wheat endosperm during hydration at excess water conditions

The evolution of the water distribution along the cross section of a DWEC during hydration was followed with MRI. Figure 4.8 shows the water content maps that were generated every 3.05 min by converting the T_2 values according to the relationship between T_2 and water content as presented in Figure 4.7. The first water content map is based on the T_2 -map scanned between 1 and 4.1 min after the initial contact of the DWEC with water. The water gradually penetrated the DWEC and after approximately 30 min of water uptake, water contents higher than 20 g/100 g wb were also detectable in the center of the DWEC. After approximately 60 min, the DWEC reached an equilibrium water content and no further distinctive change in the water distribution was observed between 60 and 90 min. In the center of the DWEC, an equilibrium water content of approximately 36 g/100 g wb was found whereas in the outermost layer of the DWEC of approximately 150 μm , water contents were higher. With the resolution given by the MRI experiment (78 x 39 x 2000 μm), the voxels at the edge of the cylinder were influenced by the bulk water phase surrounding the DWEC. Therefore voxels with water contents higher than 60 g/100 g wb were regarded as invalid. From the water content maps (Figure 4.8) of two individual MRI experiments, mean water contents were calculated and plotted versus the distance of the respective voxel from the center using concentric layers with a thickness of 50 μm . The radial water content profiles are shown in Figure 4.9 and quantitatively give the water contents at radial DWEC positions at increasing hydration time.

Figure 4.8: Water content maps of a DWEC cross section during hydration at excess water conditions (25 °C). Time interval between maps: 3.05 min between 1 and 31.5 min and 6.1 min between 31.5 and 62 min after the initial contact of the DWEC with water.



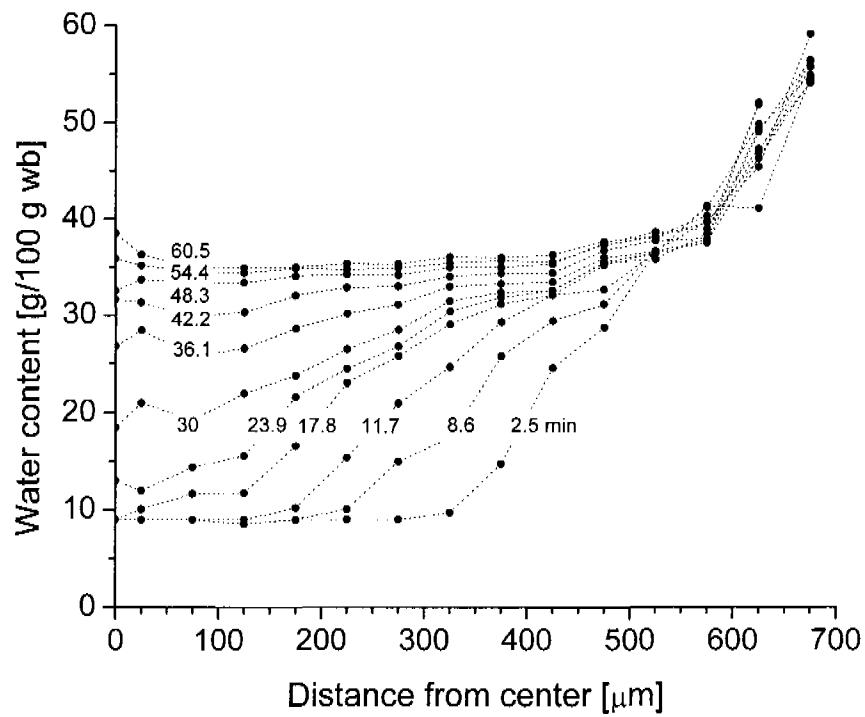


Figure 4.9: Evolution of the radial water content profiles of DWEC during hydration at excess water conditions. Mean values of two individual experiments. Numbers indicate the median hydration time.

4.3.4 Water uptake of durum wheat endosperm cylinders upon hydration at excess water conditions

The initial moisture content of the DWEC before soaking was 8.5 ± 0.8 g/100 g wb. The water content gradually increased during soaking in water as determined by gravimetric experiments (Figure 4.10). It should be noted that these results just reflect the water content as a consequence of the water penetration through the circumferential surface of the DWEC and furthermore the values are corrected by the dry matter loss of the DWEC during soaking which turned out to be up to 9 g/100g db for the longest soaking time. The water content was followed for times up to 90 min but the DWEC reached an equilibrium water content of 39.4 ± 1.4 g/100 g wb after approximately 60 min of soaking.

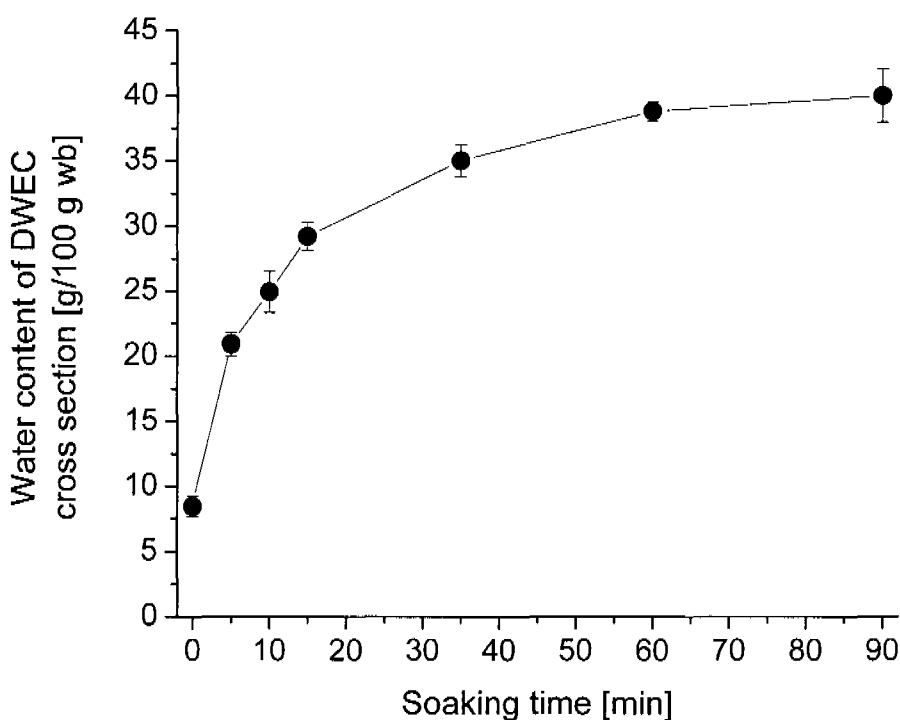


Figure 4.10: Calculated water content of the DWEC after soaking in water at 25 °C as a result of the radial water uptake through circumferential surface of the cylinder.

4.3.5 Water contents of durum wheat endosperm during hydration at excess water conditions: comparison of MRI and gravimetric experiments

From the radial water content profiles as described by MRI (Figure 4.9), integral water contents of the DWEC cross sections were calculated by summing the radial water contents multiplied with their volume fractions at the respective radial cylinder position. The calculated total water content of the DWEC slice was directly comparable to the gravimetrically determined water contents of the DWEC after soaking. Figure 4.11 shows the total water content of DWEC at different hydration time as assessed gravimetrically or by MRI. In general, a good agreement was found between the two methods what validated the used MRI calibration and measurement procedures.

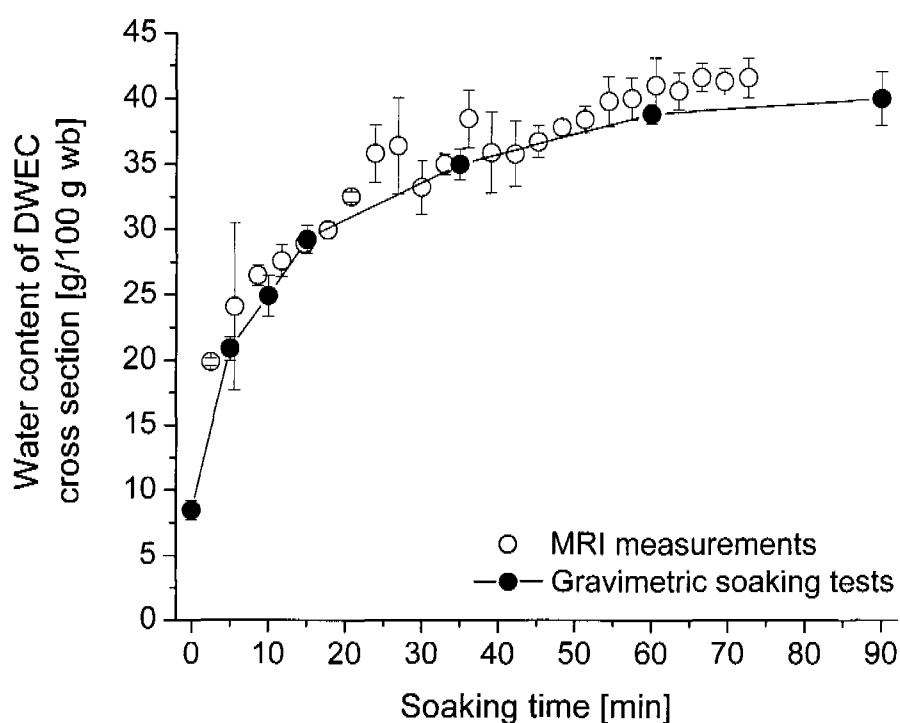
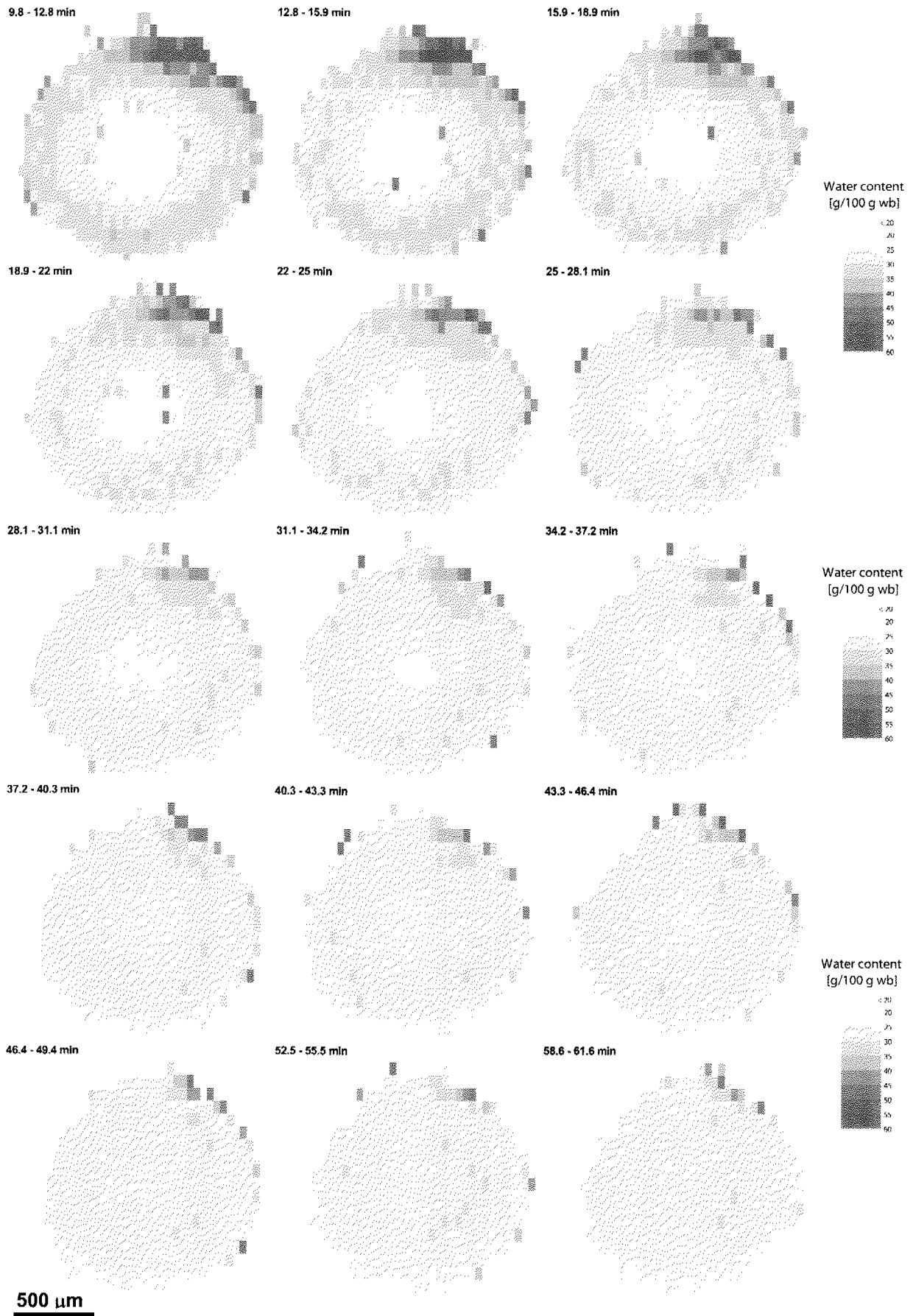


Figure 4.11: Comparison of the water contents of DWEC as assessed by calculation from MRI data or as determined gravimetrically after soaking (both at 25 °C).

4.3.6 Water distribution in durum wheat endosperm after hydration at limited water conditions

After a soaking time of 3 min, a DWEC was removed from the water and changes in the distribution of the soaked water along the cross section of the DWEC were monitored with MRI. Figure 4.12 shows the water content maps of this experiment. The first water content map was generated between 9.8 and 12.8 min after the DWEC had initial contact with water, since placing the sample in the spectrometer required a certain time. At this time, the DWEC was already penetrated with water to a large extent but the center part, approximately one third of the radius, still presented water contents lower than 20 g/100 g wb. With increasing holding time, the water gradually diffused towards the center of the DWEC, and consequently the water content in the outer regions decreased. The calculated integral water content along the cross section of the DWEC was the same at all holding times (25.3 ± 0.8 g/100 g wb) and after approximately 60 min, the water distribution reached an equilibrium condition. The radial water content profiles, presented in Figure 4.13, point out the water transport from the exterior parts towards the center which is accompanied by a decrease in the slope of the radial water content profiles with increasing holding time. Horigane et al. (2006) performed similar MRI experiments and found a leveling-off of the moisture gradient in cooked spaghetti with increasing holding time. However, even after 15 hr, the cooked pasta did not present a homogeneous water distribution along its cross section which might be due to differences in the water diffusion properties in gelatinized starch, compared to the native starch in the DWEC.

Figure 4.12: Water content maps of a DWEC cross section during equilibration after hydration at limited water conditions (both at 25 °C). Time interval between maps: 3.05 min between 9.8 and 49.4 min and 6.1 min between 49.4 and 61.6 min after the initial contact of the DWEC with water.



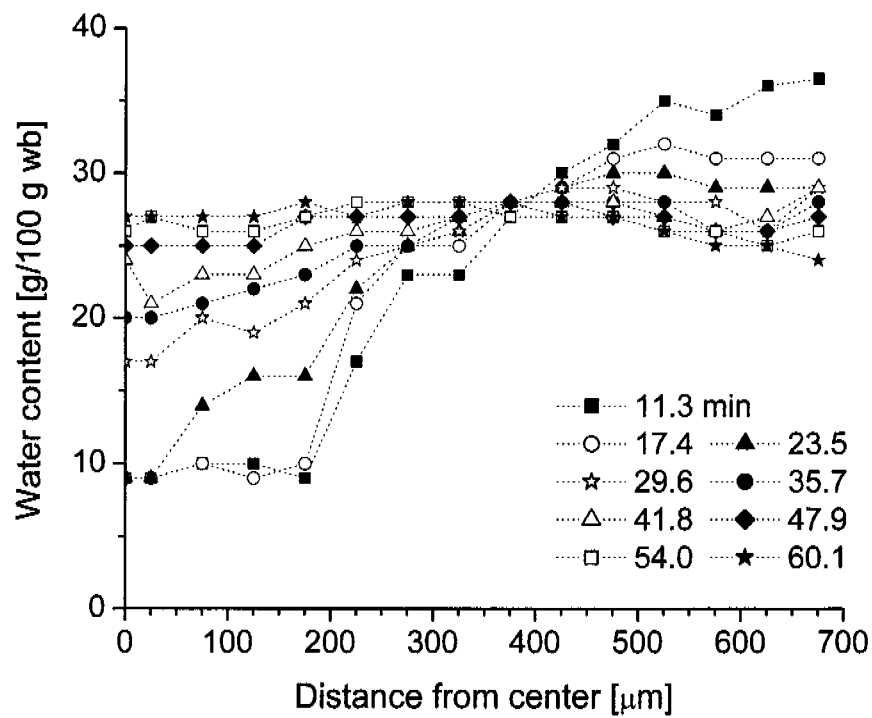


Figure 4.13: Evolution of the radial water content profiles of a DWEC after hydration at limited water conditions. The time labels refer to the median time after the initial contact of the DWEC with water.

4.3.7 Numerically modeled apparent diffusion coefficient of water in durum wheat endosperm

The results for the numeric calculation of the apparent diffusion coefficient (D) of water in DWEC were between 0.43×10^{-10} and 1.0×10^{-10} m²/sec, with an overall mean of 0.76×10^{-10} m²/sec (Figure 4.14). As expected, D did not exhibit a distinct dependence on soaking time. The average apparent diffusion coefficient agrees well with results from Kang and Delwiche (1999) who reported an apparent diffusion coefficient of 0.73×10^{-10} m²/sec at 22 °C for water in durum wheat endosperm as calculated from soaking experiments too. In contrast, Igathinathane and Chattopadhyay (1997) determined a higher value of 1.9×10^{-10} m²/sec at 30 °C for pearled soft wheat. The higher temperature of 30 °C, the use of soft wheat and differences in the used diffusion model, based on a spherical geometry of the kernel, might explain this difference of the latter study to the value presented in this study.

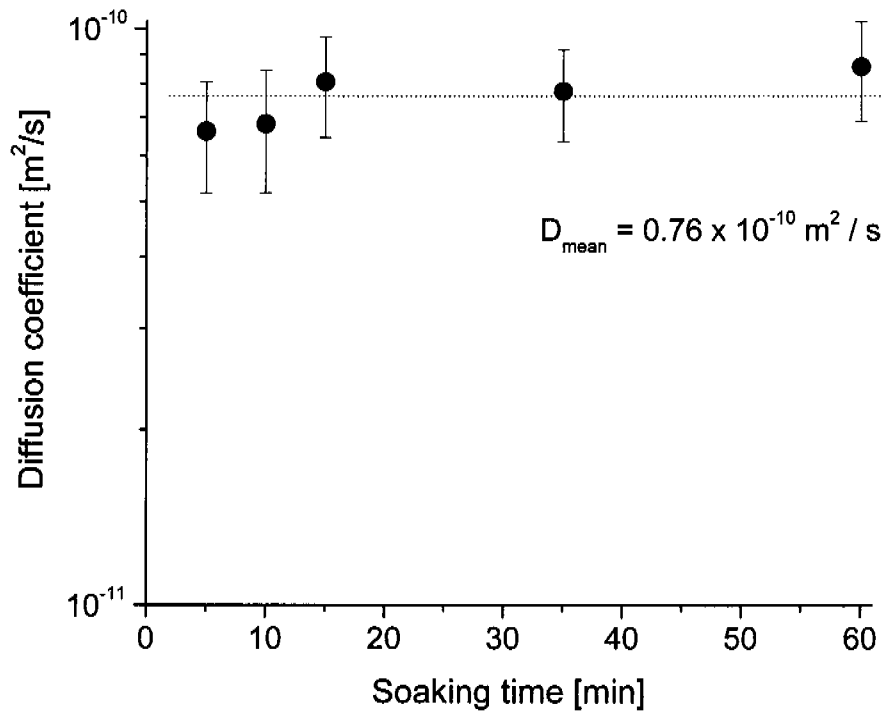


Figure 4.14: Numerically modeled apparent diffusion coefficient of water in durum wheat endosperm after soaking in water at 25 °C. The dotted line reflects the mean apparent diffusion coefficient over all soaking times.

4.4 Conclusions

Based on our investigation we can conclude that durum wheat endosperm cylinders in the millimeter range can be produced conserving the native structure of the cellular tissue with the help of a turning tool. These cylinders possess excellent suitability for studying fundamental material properties, such as the hydration dynamics, due to their well defined geometrical shape. The study of endosperm hydration by gravimetric soaking experiments is suitable for determining the total water uptake in a given time, while MRI has the advantage of giving information on the water distribution, in the case of endosperm cylinders, as radial water content maps. The prerequisite for a quantitative assessment of water distribution is the calibration of the T_2 relaxation time in the relevant moisture range, which in the present study was between 20 and 45 g/100 g wb. Overall, a good congruence between the results of gravimetric water determination and MRI was obtained, validating the calibration procedure. Hydration experiments at excess water conditions show that the native endosperm tissue can absorb around 40 g of water per 100 g in one hour. During pasta dough production water is added far below the swelling limit of the material so that limited water conditions apply. Based on the present results it is conceivable that short processing times result in considerable gradients in water distribution within semolina particles in pasta dough. Further numerical simulations of the water penetration in durum wheat endosperm are necessary for quantifying the dynamics of water transport and polymer swelling in durum wheat semolina particles at limited water availability.

5 General discussion – hydration and dough formation at intermediate water concentrations

5.1 Overall view on hydration of wheat endosperm

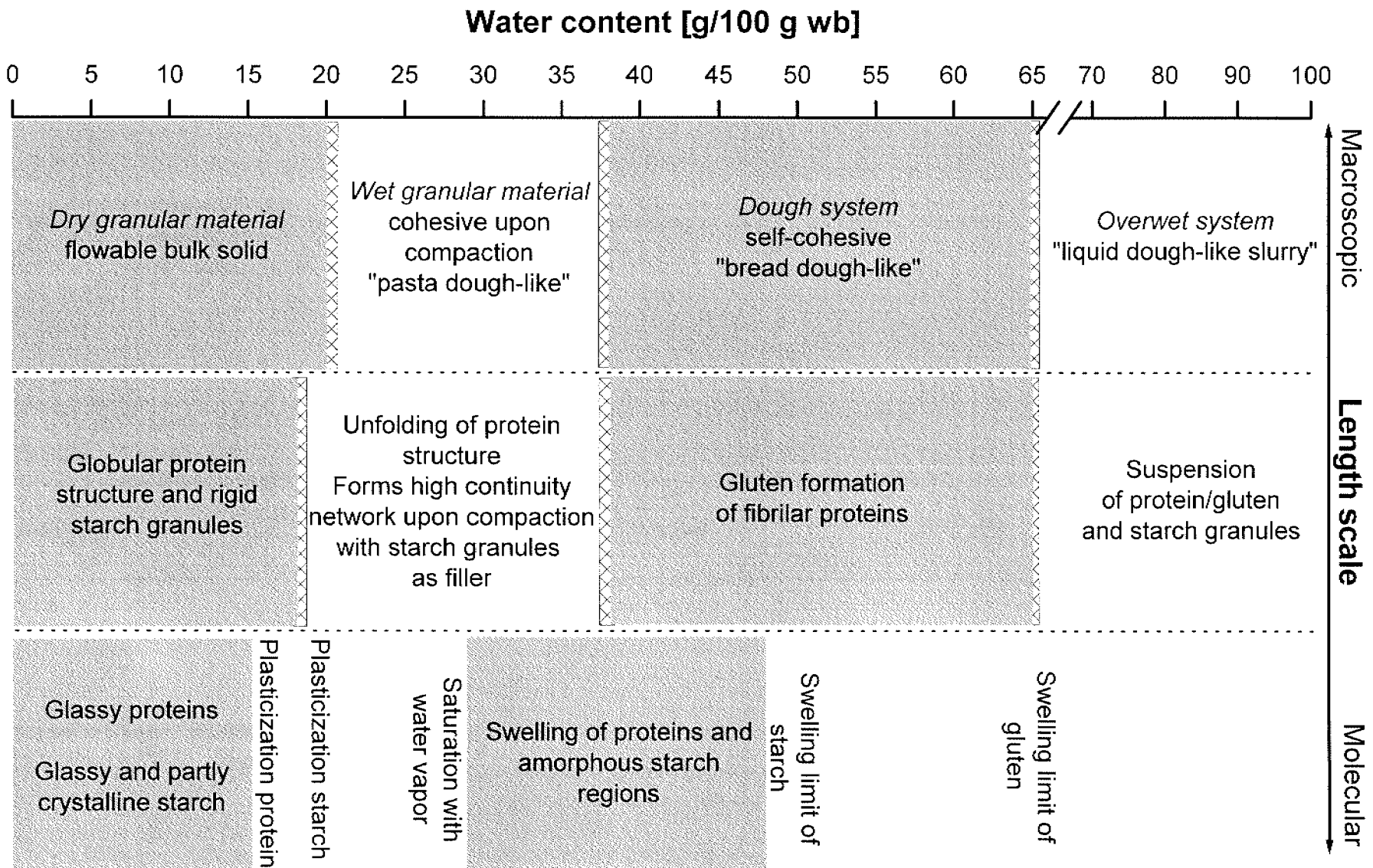
In the present investigation the focus was put on the interactions of the material wheat endosperm, e.g. in the shape of semolina, with water. For that reason, the behavior of semolina at different water concentrations is discussed in the following at different levels of organization (Figure 5.1). According to the concepts of materials physics (Mitarai and Nori 2006) semolina can be seen at the macroscopic scale as a *dry granular material* which exhibits the flowable behavior of a bulk solid. Interparticular binding is hampered by the low water level in the bulk solid. At the molecular and supramolecular level, this condition is characterized by the glassy state of semolina and in turn starch and protein as its major constituents. The proteins are organized in a native, globular conformation while the starch is packed densely in granules of bimodal distribution. The starch granules have ordered structures, primarily in the partly crystalline regions formed of amylopectin. At increased water concentration, the glassy immobile fractions of starch and protein become plasticized at the glass to rubber transition water content (16-20 g/100 g wb).

At water concentrations above the glass to rubber transition, plasticized semolina material can be regarded as *wet granular material* at the macroscopic level. In this state, semolina becomes susceptible to intergranular and irreversible cohesion when compression in the form of mechanical stress and/or shear is exerted on the system. However, in contrast to the classical concept for wet granular material, where the granules are inert, and cohesion only depends on liquid bridges, the constituents of

semolina particles also show swelling effects, starting at water concentrations corresponding to the saturation point of semolina with water vapor (~28 g/100 g wb). The increased mobility at higher water concentrations in combination with swelling effects induce the unfolding of the globular protein structure to a fibrillar conformation while the starch fraction still keeps its native granular organization due to the partly crystalline structure (Amend et al. 1991). When the wet granular material semolina is compressed the proteins have the ability to form a network of high continuity which acts as a binder for the system and eliminates the granular nature of semolina.

By further increasing the water concentration, the swelling of starch proceeds up to a water concentration of approximately 48 g/100 g wb whereas the proteins are capable to swell up to a water concentration of 65-70 g/100 g wb. At the macroscopic level, the material is now characterized as *self-cohesive dough* without any granular behavior left, even when no compressive forces are exerted on the system. This state concurs with the formation of gluten from the unfolded and fibrillar proteins. The water concentrations which are linked to bread dough-like behavior may range up to approximately 65-70 g/100 g wb. At even higher water concentrations, the system becomes *overwet* and presents a slurry of semolina particles or liquid dough, depending on the hydration rate and depending on whether dough formation has taken place or not.

Figure 5.1: Changes of durum wheat semolina and its main constituents starch and protein in the binary system semolina/water at different levels of organization as a function of water content at ambient temperature.



5.2 Hydration of wheat endosperm at intermediate water concentrations

Intermediate water concentrations correspond to the state in which wheat endosperm in the shape of semolina can be seen as wet granular material as pointed out in detail in the preceding section. The properties of semolina at this moisture level are of particular relevance for the subsequent dough formation.

Figure 5.2 presents the state diagram of semolina, wheat starch and gluten with the glass transition temperature and the onset temperature of starch melting. In addition, the diagram contains equilibrium data on the hydration of durum wheat endosperm as assessed in the present investigation, i.e. the water vapor sorption capacity at 25 °C and the swelling and imbibition capacity at temperatures between 20 and 60 °C.

Prior to any hydration, semolina commonly contains between 10 and 15 g water/100 g wb which renders the material to be in a glassy state at room temperature. Upon mixing to an integral water content of 31 g/100 g wb the effective water concentration inside and among the semolina particles and in the mixture as such may vary over a large range between the initial water content and the water imbibition capacity of semolina, i.e. between 10 and 60 g/100 g wb.

The water distribution depends significantly on the particle size distribution of the semolina and on exterior process parameters like mixing technique, temperature and time. In other words, at non-equilibrium conditions upon mixing there exist semolina particles, or at least inner parts of them, in which water concentrations are below the plasticization water content of the material (~20 g/100 g wb). However, as the plasticization of the material is a prerequisite for the molecular mobility enabling the formation of homogeneous pasta dough, an optimal mixing process should aim at least at conditions which allow all the material to become plasticized. Two approaches are commonly chosen to reach this goal: (1) mixing techniques capable to wet semolina

surfaces homogeneously, provided that semolina particle size distribution is as small as possible, and (2) prolonged equilibration time. As the diffusion driven transport of water in durum wheat endosperm is a dynamic process, the kinetics of water transport inside the semolina particles will control the duration of the equilibration period. The quantification of the water transport in the durum wheat endosperm at intermediate water conditions showed that it took approximately 20-30 min to increase the water content at a 200 μm remote endosperm position, corresponding to the maximum water diffusion path in a large semolina particle, to the plasticization water content of approximately 20 g/100 g wb (see section 4.3.6, Figure 4.13). Considering these results, common pasta dough mixing times in the range of 15-20 min for semolina containing particles up to $\sim 500 \mu\text{m}$ seem to match the physical limit of the water transport capacity of durum wheat endosperm. If shorter processing times for the mixing step were of interest, either smaller semolina particles or higher temperatures up to the onset of starch melting ($\sim 47.5^\circ\text{C}$) would be a key to the solution.

Additionally, it should be noted that the times mentioned above for the water transport only refer to the transport inside the material of durum wheat endosperm. If water distribution between under- and overwet semolina particles also has to be accomplished during mixing, mixing times might be significantly longer, as the water will have to be exchanged through the water vapor saturated air volume surrounding the semolina particles. The kinetics of water vapor sorption have shown that this is a slow process which takes place in the range of hours. However, in industrial pasta mixing systems water transport may be enhanced by motion or compression of the moistened semolina which enforce the contact and therefore the water transport between under- and overwet particles.

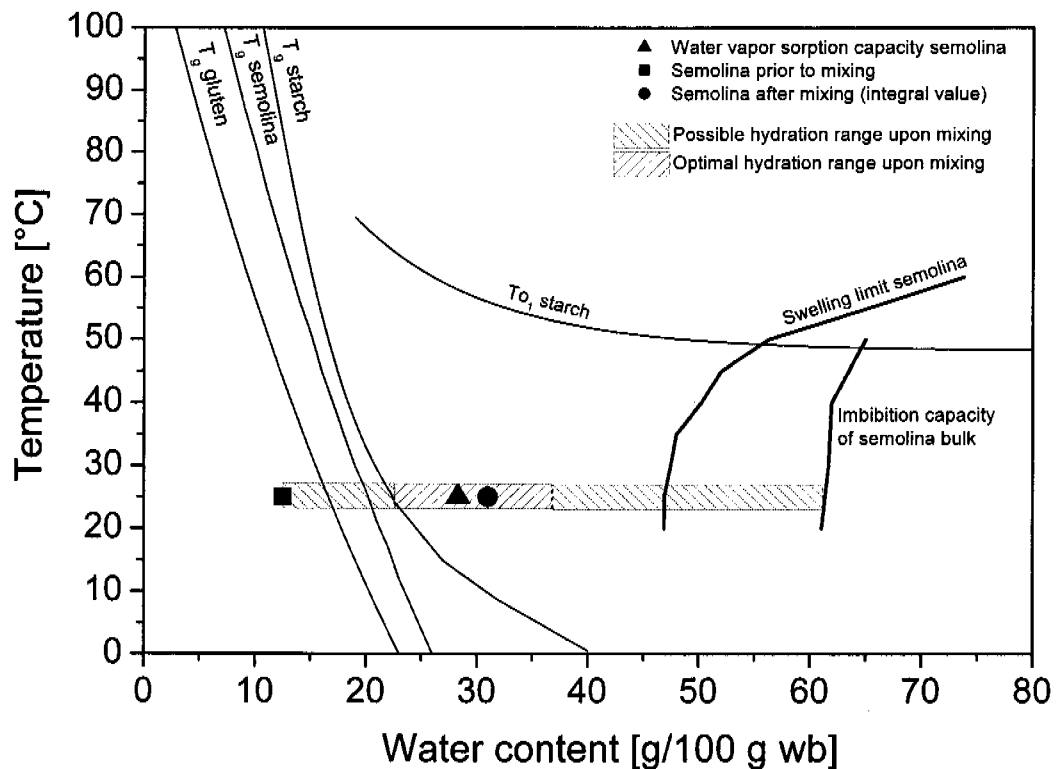


Figure 5.2: Moisture conditions of durum wheat semolina during the mixing process in relation to glass transition temperature, water vapor sorption capacity, swelling limit and imbibition capacity of semolina. Additionally, the onset temperature of starch melting and the glass transitions of starch and gluten are shown.

Data sources:

T_g gluten: DSC-measurements of own laboratory (results not shown)

T_g wheat starch: Zeleznak and Hoseney (1987)

T_g durum wheat semolina: Cuq and Icard-Vernière (2001)

To_1 wheat starch: see section 3.3.3 and Zweifel (2001)

Water vapor sorption capacity: see section 3.3.1

Swelling limit semolina: see section 3.3.2

Imbibition capacity of semolina bulk solid: see section 3.3.4

5.3 Dough formation of wheat endosperm at intermediate water concentrations

The dough formation is induced by the compression of the wet granular material semolina to cohesive pasta dough by means of extrusion or sheeting. As discussed in section 5.1, the forces for the cohesion of pasta dough arise from the plasticization of semolina and the start of swelling of the protein phase at intermediate water content.

Provided that the optimal hydration of wheat endosperm (e.g. semolina during the mixing step) was effective in fully plasticizing the material, Figure 5.3 indicates optimal process conditions for a compressing step (e.g. extrusion) of semolina in relation to the material temperature and water content. Optimal in this context refers to the generation of a cohesive and microscopically homogeneous pasta dough structure, possessing a protein network of high continuity. Generally, as a result of the mechanical energy input during the compression step, temperatures will rise to some extent. But for an optimal process, the mechanically induced temperature increase of the dough should be kept below the denaturation temperature of the proteins. As mechanical and thermal energy input on the material depend on the type of compressing device used (extruder, rollers) and the extent of the applied shear or stress on the dough, no absolute denaturation temperature can be recorded. However, considering the results of the present investigation and relevant literature data on pasta extrusion (Abecassis et al. 1994, Debbouz and Doetkott 1996, Manser 1981), a hypothetical denaturation temperature will be in the range of 55-60 °C at the intermediate water concentration of pasta dough. Moreover, the onset temperature of starch melting was observed to be in a similar temperature range. If the transformations of starch are undesirable, material temperatures should be kept below 55-60 °C.

Results of the present investigation showed on the one hand that the formation of a finely structured protein network depends on the extent of mechanical and thermal energy exerted on the system during pasta dough extrusion. Beyond critical energy input, phase separation of protein and starch result in a protein network of less continuity. On the other hand, it was also concluded that minimal energy input has to be applied on the hydrated semolina in order to obtain a homogeneous pasta dough matrix in which the native cellular structure of wheat endosperm is lost. This is particularly relevant when pasta products must exhibit only low levels of roughness and little inhomogeneities like white spots and strains.

Temperature also determines the viscosity of pasta dough and the flow properties of dough in the processing equipment. Since industrial pasta processing involves dies of large dimensions to shape the dough, homogeneous and smooth-running flow is preferred. This also contributes to low energy consumption of the equipment. Therefore, elevated dough temperatures just below the critical temperatures are of importance also in this respect.

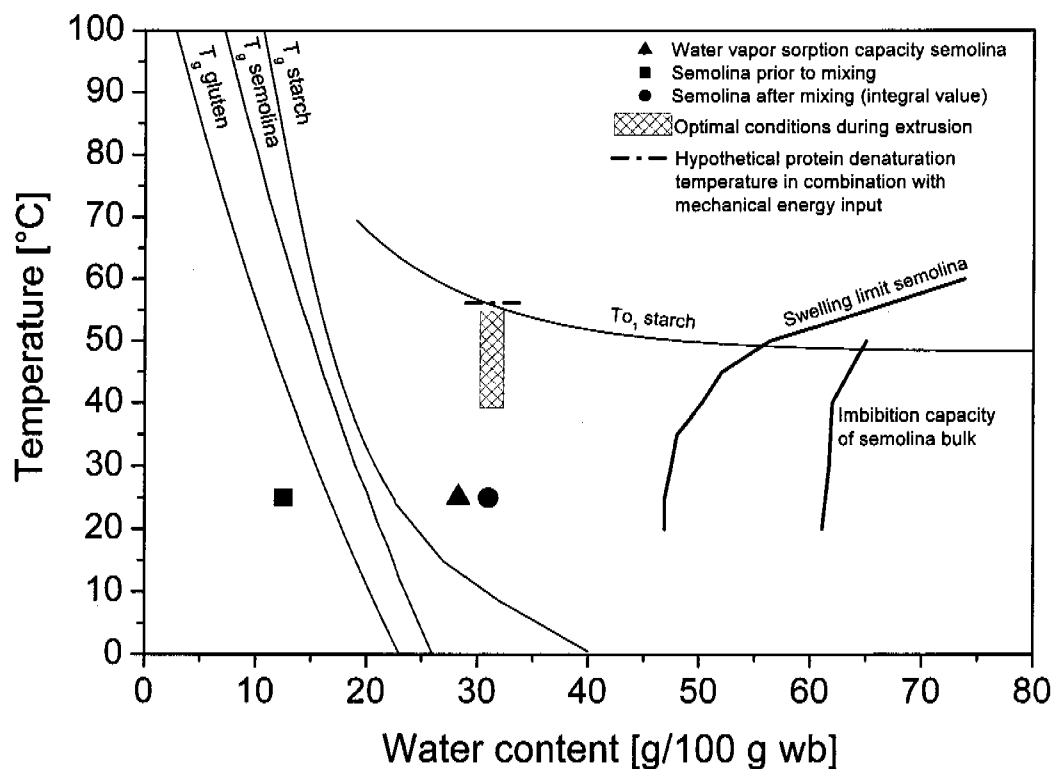


Figure 5.3: Temperature conditions during the extrusion process in relation to the onset temperature of starch melting and the hypothetical protein denaturation temperature. Additionally, glass transition temperature (T_g), water vapor sorption capacity, swelling limit and imbibition capacity of semolina are shown.

Data sources:

T_g gluten: DSC-measurements of own laboratory (results not shown)

T_g wheat starch: Zeleznak and Hoseney (1987)

T_g durum wheat semolina: Cuq and Icard-Vernière (2001)

T_o wheat starch: see section 3.3.3 and Zweifel (2001)

Water vapor sorption capacity: see section 3.3.1

Swelling limit semolina: see section 3.3.2

Imbibition capacity of semolina bulk solid: see section 3.3.4

Hypothetical protein denaturation temperature: see section 2.3

6 References

- Abecassis, J., Abbou, R., Chaurand, M., Morel, M. H. and Vernoux, P. 1994.** Influence of Extrusion Conditions on Extrusion Speed, Temperature, and Pressure in the Extruder and on Pasta Quality. *Cereal Chemistry* 71:247-253.
- Aktan, B. and Khan, K. 1992.** Effect of High-Temperature Drying of Pasta on Quality Parameters and on Solubility, Gel-Electrophoresis, and Reversed-Phase High-Performance Liquid-Chromatography of Protein-Components. *Cereal Chemistry* 69:288-295.
- Amend, T., Belitz, H. D., Moss, R. and Resmini, P. 1991.** Microstructural Studies of Gluten and a Hypothesis on Dough Formation. *Food Structure* 10:277-288.
- Antognelli, C. 1980.** The manufacture and applications of pasta as a food and as a food ingredient - a review. *Journal of Food Technology* 15:125-145.
- Arrigoni, E., Caprez, A., Neukom, H. and Amadò, R. 1987.** Determination of water uptake by an automated method. *Lebensmittel-Wissenschaft und -Technologie - Food Science and Technology* 20:263-264.
- Bushuk, W. and Winkler, C. A. 1957.** Sorption of water vapor on wheat flour, starch, and gluten. *Cereal Chemistry* 34:73-86.
- Cuq, B. and Icard-Verniere, C. 2001.** Characterisation of glass transition of durum wheat semolina using modulated differential scanning calorimetry. *Journal of Cereal Science* 33:213-221.

- Debbouz, A. and Doetkott, C. 1996.** Effect of process variables on spaghetti quality. *Cereal Chemistry* 73:672-676.
- Dexter, J. E. and Matsuo, R. R. 1977.** Changes in Semolina Proteins During Spaghetti Processing. *Cereal Chemistry* 54:882-894.
- Dexter, J. E. and Matsuo, R. R. 1978.** Effect of Gluten Protein-Fractions on Pasta Dough Rheology and Spaghetti-Making Quality. *Cereal Chemistry* 55:44-57.
- Dexter, J. E. and Matsuo, R. R. 1979.** Effect of Water-Content on Changes in Semolina Proteins During Dough-Mixing. *Cereal Chemistry* 56:15-19.
- Dobraszczyk, B. J., Whitworth, M. B., Vincent, J. F. V. and Khan, A. A. 2002.** Single kernel wheat hardness and fracture properties in relation to density and the modelling of fracture in wheat endosperm. *Journal of Cereal Science* 35:245-263.
- Don, C., Lichtendonk, W., Plijter, J. J. and Hamer, R. J. 2003a.** Glutenin macropolymer: a gel formed by glutenin particles. *Journal of Cereal Science* 37:1-7.
- Don, C., Lichtendonk, W. J., Plijter, J. J. and Hamer, R. J. 2003b.** Understanding the link between GMP and dough: from glutenin particles in flour towards developed dough. *Journal of Cereal Science* 38:157-165.
- Duce, S. L. and Hall, L. D. 1995.** Visualization of the hydration of food by Nuclear-Magnetic-Resonance imaging. *Journal of Food Engineering* 26:251-257.
- Dürr, P. and Neukom, H. 1973.** Konsistenzmessung an gekochten Teigwaren mit dem Instrongerät. *Lebensmittel-Wissenschaft und -Technologie - Food Science and Technology* 6:23-25.
- Edwards, N. M., Mulvaney, S. J., Scanlon, M. G. and Dexter, J. E. 2003.** Role of gluten and its components in determining durum semolina dough viscoelastic properties. *Cereal Chemistry* 80:755-763.

- Edwards, N. M., Peressini, D., Dexter, J. E. and Mulvaney, S. J. 2001.** Viscoelastic properties of durum wheat and common wheat dough of different strengths. *Rheologica Acta* 40:142-153.
- Elizalde, B. E., Pilosof, A. M. R. and Bartholomai, G. B. 1996.** Empirical model for water uptake and hydration rate of food powders by sorption and Baumann methods. *Journal of Food Science* 61:407-409.
- Enslin, O. 1933.** Über einen Apparat zur Messung der Flüssigkeitsaufnahme an quellbaren und porösen Stoffen. *Chemische Fabrik* 6:147.
- Erbas, M., Ertugay, M. F. and Certel, M. 2005.** Moisture adsorption behaviour of semolina and farina. *Journal of Food Engineering* 69:191-198.
- Freundlich, H., Schmidt, O. and Lindau, G. 1931.** Über die Thixotropie von Bentonitsuspensionen. *Zeitschrift für physikalische Chemie. Bodenstein-Festband*: 333-340.
- Frey, A. and Neukom, H. 1967.** Eine moderne Versuchsanlage zur Herstellung von Teigwaren in: *Getreidechemiker Tagung*. Granum Verlag Detmold.
- Ghosh, P. K., Jayas, D. S., Gruwel, M. L. H. and White, N. D. G. 2006.** Magnetic resonance image analysis to explain moisture movement during wheat drying. *Transactions of the Asabe* 49:1181-1191.
- Glenn, G. M., Younce, F. L. and Pitts, M. J. 1991.** Fundamental physical properties characterizing the hardness of wheat endosperm. *Journal of Cereal Science* 13:179-194.
- Hebrard, A., Oulahna, D., Galet, L., Cuq, B., Abecassis, J. and Fages, J. 2003.** Hydration properties of durum wheat semolina: influence of particle size and temperature. *Powder Technology* 130:211-218.

- Hills, B. P., Babonneau, F., Quantin, V. M., Gaudet, F. and Belton, P. S. 1996.** Radial NMR microimaging studies of the rehydration of extruded pasta. *Journal of Food Engineering* 27:71-86.
- Hills, B. P., Godward, J. and Wright, K. M. 1997.** Fast radial NMR microimaging studies of pasta drying. *Journal of Food Engineering* 33:321-335.
- Horigane, A. K., Naito, S., Kurimoto, M., Irie, K., Yamada, M., Motoi, H. and Yoshida, M. 2006.** Moisture distribution and diffusion in cooked spaghetti studied by NMR imaging and diffusion model. *Cereal Chemistry* 83:235-242.
- Icard-Verniere, C. and Feillet, P. 1999.** Effects of mixing conditions on pasta dough development and biochemical changes. *Cereal Chemistry* 76:558-565.
- Igathinathane, C. and Chattopadhyay, P. K. 1997.** Mathematical prediction of moisture profile in layers of grain during pre-conditioning. *Journal of Food Engineering* 31:185-197.
- Irie, K., Horigane, A. K., Naito, S., Motoi, H. and Yoshida, M. 2004.** Moisture distribution and texture of various types of cooked spaghetti. *Cereal Chemistry* 81:350-355.
- Kang, S. and Delwiche, S. R. 1999.** Moisture diffusion modeling of wheat kernels during soaking. *Transactions of the Asae* 42:1359-1365.
- LeRoux, D., Vergnes, B., Chaurand, M. and Abecassis, J. 1995.** A Thermomechanical Approach to Pasta Extrusion. *Journal of Food Engineering* 26:351-368.
- Manser, J. 1981.** Optimale Parameter für die Teigwarenherstellung am Beispiel von Langwaren. *Getreide Mehl und Brot* 35:75-83.
- Manser, J. 1985.** Feinheitgrad von Durum-Mahlerzeugnissen aus der Sicht der Teigwarenindustrie. *Getreide Mehl und Brot* 39:117-123.

- Matsuo, R. R., Dexter, J. E. and Dronzek, B. L. 1978.** Scanning Electron-Microscopy Study of Spaghetti Processing. *Cereal Chemistry* 55:744-753.
- McCarthy, M. J., Lasseux, D. and Maneval, J. E. 1994.** NMR imaging in the study of diffusion of water in foods. *Journal of Food Engineering* 22:211-224.
- Mestres, C., Matencio, F. and Faure, J. 1990.** Optimizing process for making pasta from maize in admixture with durum-wheat. *Journal of the Science of Food and Agriculture* 51:355-368.
- Mitarai, N. and Nori, F. 2006.** Wet granular materials. *Advances in Physics* 55:1-45.
- Novaro, P., Degidio, M. G., Mariani, B. M. and Nardi, S. 1993.** Combined Effect of Protein-Content and High-Temperature Drying Systems on Pasta Cooking Quality. *Cereal Chemistry* 70:716-719.
- Pagani, M. A., Resmini, P. and Dalbon, G. 1989.** Influence of the Extrusion Process on Characteristics and Structure of Pasta. *Food Microstructure* 8:173-182.
- Peighambardoust, S. H., van der Goot, A. J., Hamer, R. J. and Boom, R. M. 2005.** Effect of simple shear on the physical properties of glutenin macro polymer (GMP). *Journal of Cereal Science* 42:59-68.
- Peressini, D., Degidio, M. G., Galterion, G., Pollini, C. M. and Sensidoni, A. 2000.** Characterisation of durum wheat doughs based on fundamental rheological measurements. Pages 125-128 in: *Durum wheat, semolina and pasta quality*. J. Abecassis, J. C. Autran and P. Feillet, eds. INRA, Montpellier.
- Resmini, P. and Pagani, M. A. 1983.** Ultrastructure Studies of Pasta - a Review. *Food Microstructure* 2:1-12.
- Roman-Gutierrez, A. D., Guilbert, S. and Cuq, B. 2002.** Distribution of water between wheat flour components: A dynamic water vapour adsorption study. *Journal of Cereal Science* 36:347-355.

- Shotton, E. and Harb, N. 1965.** The effect of humidity and temperature on the equilibrium moisture content of powders. *Journal of Pharmacology* 17:504.
- Sissons, M. J., Egan, N. E. and Gianibelli, M. C. 2005.** New insights into the role of gluten on durum pasta quality using reconstitution method. *Cereal Chemistry* 82:601-608.
- Spiess, W. E. L. and Wolf, W. 1987.** Critical evaluation of methods to determine moisture sorption isotherms. Pages 215-233 in: *Water Activity: Theory and Applications to Food*. L. B. Rockland and L. R. Beuchat, eds. Marcel Dekker Inc., New York and Basel.
- Tagawa, A., Muramatsu, Y., Nagasuna, T., Yano, A., Iimoto, M. and Murata, S. 2003.** Water absorption characteristics of wheat and barley during soaking. *Transactions of the ASAE* 46:361-366.
- Takeuchi, S., Fukuoka, M., Gomi, Y., Maeda, M. and Watanabe, H. 1997a.** An application of magnetic resonance imaging to the real time measurement of the change of moisture profile in a rice grain during boiling. *Journal of Food Engineering* 33:181-192.
- Takeuchi, S., Maeda, M., Gomi, Y., Fukuoka, M. and Watanabe, H. 1997b.** The change of moisture distribution in a rice grain during boiling as observed by NMR imaging. *Journal of Food Engineering* 33:281-297.
- Ummadi, P., Chenoweth, W. L. and Ng, P. K. W. 1995.** Changes in Solubility and Distribution of Semolina Proteins Due to Extrusion Processing. *Cereal Chemistry* 72:564-567.
- Weegels, P. L., Degroot, A. M. G., Verhoek, J. A. and Hamer, R. J. 1994.** Effects on Gluten of Heating at Different Moisture Contents .2. Changes in Physicochemical Properties and Secondary Structure. *Journal of Cereal Science* 19:39-47.

Zelevnak, K. J. and Hosney, R. C. 1987. The glass-transition in starch. *Cereal Chemistry* 64:121-124.

Zweifel, C. 2001. Influence of high-temperature drying on the structural and textural properties of durum wheat pasta. Dissertation No. 14073, Swiss Federal Institute of Technology (ETH), Zurich, Switzerland.

Zweifel, C., Conde-Petit, B. and Escher, F. 2000. Thermal modifications of starch during high-temperature drying of pasta. *Cereal Chemistry* 77:645-651.

Zweifel, C., Handschin, S., Escher, F. and Conde-Petit, B. 2003. Influence of high-temperature drying on structural and textural properties of durum wheat pasta. *Cereal Chemistry* 80:159-167.

DANK

Herrn Prof. Dr. Felix Escher möchte ich einen grossen Dank für die Übernahme des Referates und die Leitung der vorliegenden Dissertation aussprechen. Seine Begeisterung und sein Engagement für diese Forschungsarbeit habe ich von der ersten Besprechung an sehr geschätzt und zudem war Prof. Escher für alle Anliegen seines Doktoranden über die gesamte Dauer des Projektes immer offen. Herzlichen Dank!

Für die vielen fachlichen Besprechungen und Anregungen bedanke ich mich bei Frau PD Dr. Béatrice Conde-Petit. Sie stand mir während meiner Dissertation immerzu hilfsbereit und vor allem äusserst fachkompetent zur Seite. Nicht zuletzt bedanke ich mich bei ihr auch für die Übernahme des Korreferates.

Für die Übernahme des externen Korreferates und für die kritische Durchsicht meiner Dissertation bedanke ich mich bei Herrn Dr. Bernard Cuq vom INRA in Montpellier.

Ein spezieller Dank geht an den mitinjizierenden Projektpartner meiner Doktorarbeit, die Firma Bühler AG in Uzwil. Die Möglichkeit eine praxisnahe Dissertation zu absolvieren und während der wissenschaftlichen Arbeit an der ETH immer auch Kontakt zu erfahrenen Spezialisten zu pflegen, motivierte mich sehr. Insbesondere werde ich die effektive und gute Zusammenarbeit mit den Herren Arturo Bohm, Klaus-Jochen Lisner, Dres. Raphael Geiger und Riccardo Cattaneo, Thomas Lang, Gabriel Stösser und Andreas Müller in besonders guter Erinnerung behalten und teilweise auch in Zukunft geniessen dürfen! Der Firma Bühler und nicht zuletzt auch dem Projektpartner KTI, der Förderagentur für Innovation des Eidgenössischen Volkswirtschaftsdepartementes, danke ich zudem für die Finanzierung des Forschungsprojektes.

Herrn Dr. Dieter Gross und seinem Team von Bruker GmbH in Karlsruhe danke ich sehr für die bereitwillige Zusammenarbeit und die fachliche und praktische Unterstützung bei den Messungen der Wasseraufnahme mittels MRI.

Ohne die Einsatzbereitschaft der vielen motivierten Studentinnen und Studenten, die im Rahmen ihrer Diplom-, Bachelor- und Semesterarbeiten massgeblich zu dem Gelingen der vielen Experimente in diesem Projekt beigetragen haben, wäre diese Arbeit nicht zu Stande gekommen. In besonderer Weise danke ich deshalb: Sabine Mattmann, Sofie Harder, Marco Pfändler, Catrina Niklaus, Tamara Eisele, Lucie Ecoffey, Yvonne Amacher, Lukas Bernhard, Bastian Zuberbühler, Tanja Zürcher, Mascha Hug und Daniela Hediger.

Innerhalb der Gruppe Lebensmitteltechnologie am Institut für Lebensmittelwissenschaften der ETH erhielt ich durch die grossartige Unterstützung von allen Kolleginnen und Kollegen nicht nur ein Umfeld in dem es sich perfekt forschen liess, sondern wo auch durch den sehr kollegialen Umgang meine Disszeit einen grossen Teil ihrer Unvergesslichkeit bekommen hat. Dafür danke ich allen herzlich! Insbesondere danke ich aber Horst Adelman, der mir bei allen praktischen Fragen mit vollster Unterstützung immer zur Seite stand und auch Stephan Handschin, der nicht nur massgeblich zum Gelingen aller mikroskopischer Arbeiten im Projekt beigetragen hat, sondern zudem in den vielen fachlichen Diskussionen und nicht zuletzt bei der Gestaltung des Layouts meiner Doktorarbeit unverzichtbar war. An Horst Adelman, Jürg Baggenstoss und Thomas Amrein geht natürlich noch ein ganz spezieller Dank, denn sie waren nicht nur tolle Kollegen, sondern gemeinsam injizierten wir auch zahlreiche und unvergessliche Weindegustationen in den Gruppen Lebensmittelchemie und -technologie.

Zu besonderem Dank bin ich auch meinen Eltern verpflichtet. Sie und mein privates Umfeld der letzten Jahre machten mir das Studium, die Doktoratszeit und das Leben in der Schweiz zu einer der angenehmsten Erfahrungen meines Lebens.

CURRICULUM VITAE

Andreas Markus Kratzer

born April 2, 1979

from Austria

2003-2007 Doctoral student and research assistant in the group of Prof. Dr. Felix Escher and PD Dr. Béatrice Conde-Petit, Laboratory of Food Chemistry and Technology, Institute of Food Science and Nutrition, Swiss Federal Institute of Technology (ETH), Zurich.

2003 Diploma degree in Food Science and Technology (Dipl. Lm.-Ing. ETH)

1998-2003 Studies in Food Science and Technology at the Swiss Federal Institute of Technology (ETH), Zurich, including practical training at:

- Bühler AG, Uzwil
- Tetra Pak (Schweiz) AG, Kloten
- Weinkellerei Zweifel & Co. AG, Zürich

1997-1998 Military service (compulsory national service)

1989-1997 High School at the Kollegium Aloisianum in Linz, Austria.

1985-1989 Primary School in Leonding, Austria.